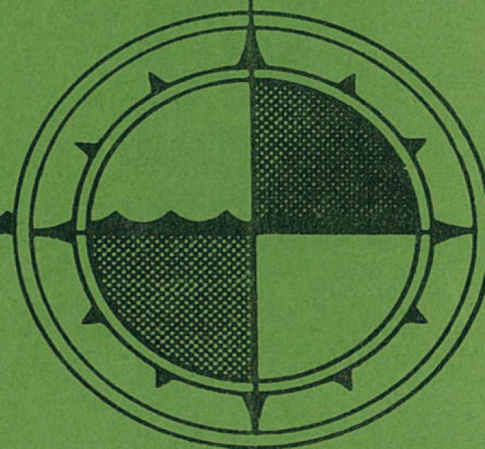


**SUBSURFACE CURRENT MEASUREMENTS
IN EASTERN LANCASTER SOUND,
N.W.T. - SUMMER 1977**

by

**D.B. Fissel and G.R. Wilton
Arctic Sciences Ltd.**

**For
INSTITUTE OF OCEAN SCIENCES, PATRICIA BAY
Sidney, B.C.**



Contractor Report Series 78-3

SUBSURFACE CURRENT MEASUREMENTS IN EASTERN
LANCASTER SOUND, N.W.T. - SUMMER 1977

by

D.B. Fissel and G.R. Wilton
Arctic Sciences Ltd.

For

Institute of Ocean Sciences, Patricia Bay
Sidney, B.C.

1978

1957

Abstract

Two month time series records of current speed and direction, temperature and salinity were obtained at three locations in eastern Lancaster Sound, N.W.T. in the summer of 1977. At each location three Aanderaa RCM-4 current meters were used at levels near the surface (35-51 m), approximately 200 m and 550 m depth. At the near surface and 200 m levels, strong southerly flows were measured in the centre of the Sound with a net easterly flow on the southern side. The near surface currents reached speeds up to 112 cm/s with an average magnitude of 30 cm/s. The temporal variations of the currents were characterised by a great deal of low frequency activity, particularly for the north-south component in the centre of Lancaster Sound. In comparison with these low frequency variations, the diurnal and semi-diurnal tidal currents, with typical amplitudes of 7 to 10 cm/s, were insignificant at the near surface level, becoming more important at 200 m and 550 m depth. The correlation between currents at different positions are described, for both horizontal and vertical displacements. On the basis of concurrent wind measurements at a shore station on the south coast of Lancaster Sound, the estimated surface movements due to the large scale circulation pattern were generally larger than those estimated movements due directly to wind driven currents generated by the local wind.

Acknowledgements

In this study, many people provide assistance of various forms without which the project would have been less successful than it was. We thank the officers and crew of the Canadian Coast Guard Ship Labrador and in particular, Capt. P.W. Tooke and his Chief Officer, Don MacKay for their unfailing cooperation and assistance in deploying and recovering the equipment. The Canadian Hydrographic Service of the Bedford Institute of Oceanography, Dartmouth, N.S. allowed us to use a portion of their ship time, and their personnel provided helpful advice onboard the ship for which we are grateful. At the Bedford Institute of Oceanography, the Atlantic Oceanographic Laboratory made available the use of workspace and facilities for assembling the equipment; we especially wish to acknowledge the assistance of Dr. J. Elliott and Messrs. Bert Hartling and Richard Russell. At the Institute of Ocean Sciences, Patricia Bay Al Stickland and Reg Bigham of Coastal Zone Oceanography provided a great deal of valuable advice on the design and assembly of the equipment. We benefited greatly from the assistance of Mr. W.S. Huggett, Tidal and Current Survey in the mooring design and in planning shipboard operations. Gordon Fleming, Steven Hill and Robert Shepard all participated in the shipboard work and in preparing for the cruises. We are deeply grateful to Mr. R.H. Herlinveaux of the Arctic Marine Science Group for his assistance and advice through all phases of this study. Finally, we thank Mr. A.R. Milne of the Arctic Marine Science Group and Dr. A. Rutgers of Norlands Petroleum Ltd. for providing the necessary financial support to carry out this project.

Table of Contents

Abstract	i
Acknowledgements	iii
1. Introduction	1
2. Review	1
2.1 Lancaster Sound Bathymetry and Ice Conditions	1
2.2 Oceanographic features of Lancaster Sound	3
2.2.1 The circulation of eastern Lancaster Sound	3
2.2.2 Previous direct current measurements in eastern Lancaster Sound	4
3. Data Collection and Processing	9
3.1 Station Locations and Logistics	9
3.2 Instrument Description	13
3.2.1 Aanderaa current meters	13
3.2.2 Weather data	16
3.3 Data Processing	16
3.3.1 Current Meter Data	16
3.3.2 Weather Station Data	20
4. Results	21
4.1 Current Meter Depth	21
4.2 Current Speed, Direction and Components	21
4.2.1 Time series plots, histograms and basic statistics	21
4.2.2 Spectral and harmonic analysis	37
4.2.3 Correlation and cross-spectral analysis of currents	51
4.3 Temperatures and Salinities	53
4.4 The Local Wind and Near Surface Currents	66
5. Summary and Conclusions	69
6. References	71

LIST OF FIGURES

<u>Figure</u>		<u>Page</u>
1	A map of Eastern Parry Channel and adjacent water bodies.	2
2	The sites of direct current measurements made in previous oceanographic studies of eastern Lancaster Sound.	5
3	Time series plots of current measurements at 10m depth off Cape Crauford made in 1974 by the Canadian Hydrographic Service.	8
4	Progressive vector diagram of the current meter data of the Canadian Hydrographic Service taken in 1974.	8
5	Location of the current meter moorings and weather station in Lancaster Sound, summer 1977.	10
6	Current meter mooring.	11
7	A schematic representation of the data recovered from each current meter at stations 1,3 and 4.	12
8	The horizontal components of the geomagnetic field in Resolute for the months of July, August and September 1977.	15
9	The data processing system used on the current meter data.	17
10a	Time series plots of the speed measurements at station 1.	22
10b	Time series plots of the speed measurements at station 3.	23
10c	Time series plot of the speed measurements at station 4.	24
11a	Time series plots of the direction measurements at station 1.	25
11b	Time series plots of the direction measurements at station 3.	26
11c	Time series plots of the direction measurements at station 4.	27
12a	Time series plots of the easterly and northerly current components at station 1.	28
12b	Time series plots of the easterly and northerly current components at station 3.	29
12c	Time series plots of the easterly and northerly current components at station 4.	30
13	Histograms of the current speeds.	35
14	Histograms of the current direction.	36
15a	Progressive vector diagrams of the currents at station 1.	38
15b	Progressive vector diagrams of the currents at station 3.	39
15c	Progressive vector diagram of the current at station 4 - 549m depth.	40
16a	Power spectral densities of the easterly and northerly current components at station 1.	41

<u>Figure</u>		<u>Page</u>
16b	Power spectral densities of the easterly and northerly current components at station 3.	42
17	Power spectral densities of the current speeds.	43
18a	Time series plots of temperature recorded at the upper current meter level on each mooring.	54
18b	Time series plots of temperature recorded at 200m level on each mooring.	55
18c	Time series plots of temperature recorded at the 550m level on each mooring.	56
19a	Time series plots of salinity recorded at the upper current meter level on each mooring.	57
19b	Time series plots of salinity recorded at the 200m level on each mooring.	58
19c	Time series plots of salinity recorded at the 550m level on each mooring.	59
20	Temperature and salinity profiles taken from the files of the Marine Environmental Data Service, Ottawa together with the average and range of temperatures and salinities observed at stations 1, 3 and 4.	60
21a	Histograms of the temperatures.	61
21b	Histograms of the salinities.	62
22	Power spectral densities of the temperature data.	64
23	Power spectral densities of the salinity data.	65
24a	The air pressure, air temperature, wind speed and direction measured at Cape Charles Yorke.	67
24b	The wind components, speed and direction.	68

TABLES

<u>Table</u>		<u>Page</u>
1	The speed (knots) and direction (degrees true) of the residual current at four stations in Lancaster Sound from a survey aboard M.V. <u>Theta</u> in 1960.	6
2	The accuracy and resolution of Aanderaa current meter and weather station measurements, as supplied by the manufacturer.	14
3	Criteria used to eliminate erroneous current meter data.	18
4	Summary of rejected Current Meter Data.	19
5a	The basic data statistics for station 1.	32
5b	The basic data statistics for station 3.	33
5c	The basic data statistics for station 4.	34
6	Harmonic analysis results for currents at station 1 - 39m depth over the period 0300 July 29th to 1500 Sept 25 GMT.	44
7	Harmonic analysis results for currents at station 1 - 203m depth over the period 1500 July 29 to 0300 Sept. 29 GMT.	45
8	Harmonic analysis results for currents at station 3 - 51m depth over the period 1500 July 29 to 0300 Sept. 29 GMT.	46
9	Harmonic analysis results for currents at station 3 - 216m depth over the period 1500 July 29 to 0300 Sept. 29 GMT.	47
10	Harmonic analysis results for currents at station 4 - 549m depth over the period 1500 July 29 to 0300 Sept. 29 GMT.	48
11	Results of the linear regression analysis between time series of currents of the form: $x_1 = a + b \cdot x_2$	52

1. Introduction

In late July of 1977, four subsurface current meter moorings were installed in eastern Lancaster Sound, N.W.T. by Arctic Sciences Ltd. under contract to the Institute of Ocean Sciences, Patricia Bay, Arctic Marine Science Group. This report provides a data summary and preliminary analysis of the oceanographic information obtained from three of the subsurface moorings recovered September 29 to October 1, 1977.

The basic objective of the current metering program was to obtain long term measurements of the water movements of eastern Lancaster Sound. The information obtained was used in an environmental assessment of proposed deep water oil-well drilling in the area (Milne and Smiley, 1978). As well, the data adds to our basic knowledge of the circulation of Lancaster Sound, a region where direct measurements of water movements are very limited.

2. Review

2.1 Lancaster Sound Bathymetry and Ice Conditions

Lancaster Sound forms the easternmost segment of Parry Channel, the major east-west connection between Baffin Bay and the Arctic Ocean (see Figure 1). In the eastern end of Lancaster Sound adjoining Baffin Bay, the water depths are largest, in excess of 800 m. As one progresses westward, the depths decrease to approximately 140 m, in the vicinity of the Barrow Strait sill. On its southern boundary, Lancaster Sound is connected to the Prince Regent Inlet-Gulf of Boothia Waterway and to Admiralty Inlet. The latter is an enclosed water body, while the former has two additional openings, Fury and Hecla Strait (limiting sill depth of 50 m) and Bellot Strait (limiting sill depth of 40 m). In transverse cross-section, Lancaster Sound is roughly 'U' shaped with steeply rising sides.

Lancaster Sound is normally completely ice covered in winter and early spring, although the ice cover usually remains unconsolidated and in motion as far west as N.E. Somerset Island (Marko, 1977), where a landfast ice edge often forms in late winter. Ice to the east of this tends to drift eastward through the Sound, with ice formation apparently occurring in the vicinity of the ice edge. By May, ice growth stops and clearing begins from the eastern end of the Sound (Milne and Smiley, 1978). Ice then begins drifting into the Sound as the various water bodies to the south and the west empty. Based on 17 years of data, Milne and Smiley (1978) report that the period of relatively open water (one to three tenths ice cover in which the floes are not in contact) extends from early July to late September. However, during the summer, intrusions of multi-year ice with concentrations of three tenths or more are quite common in the eastern end of Lancaster Sound.

Icebergs are frequently seen in the eastern end of the Sound with diminishing frequencies as one moves westwards. Like the late summer intrusion of multi-year ice, the icebergs move into Lancaster Sound from northern Baffin Bay. They are carried to the south along the east coast of Devon Island and then swept westward into the Sound. Once into the Sound, it is thought that icebergs tend to move southward across the sound and then often exit to the east (Fenco, 1974).

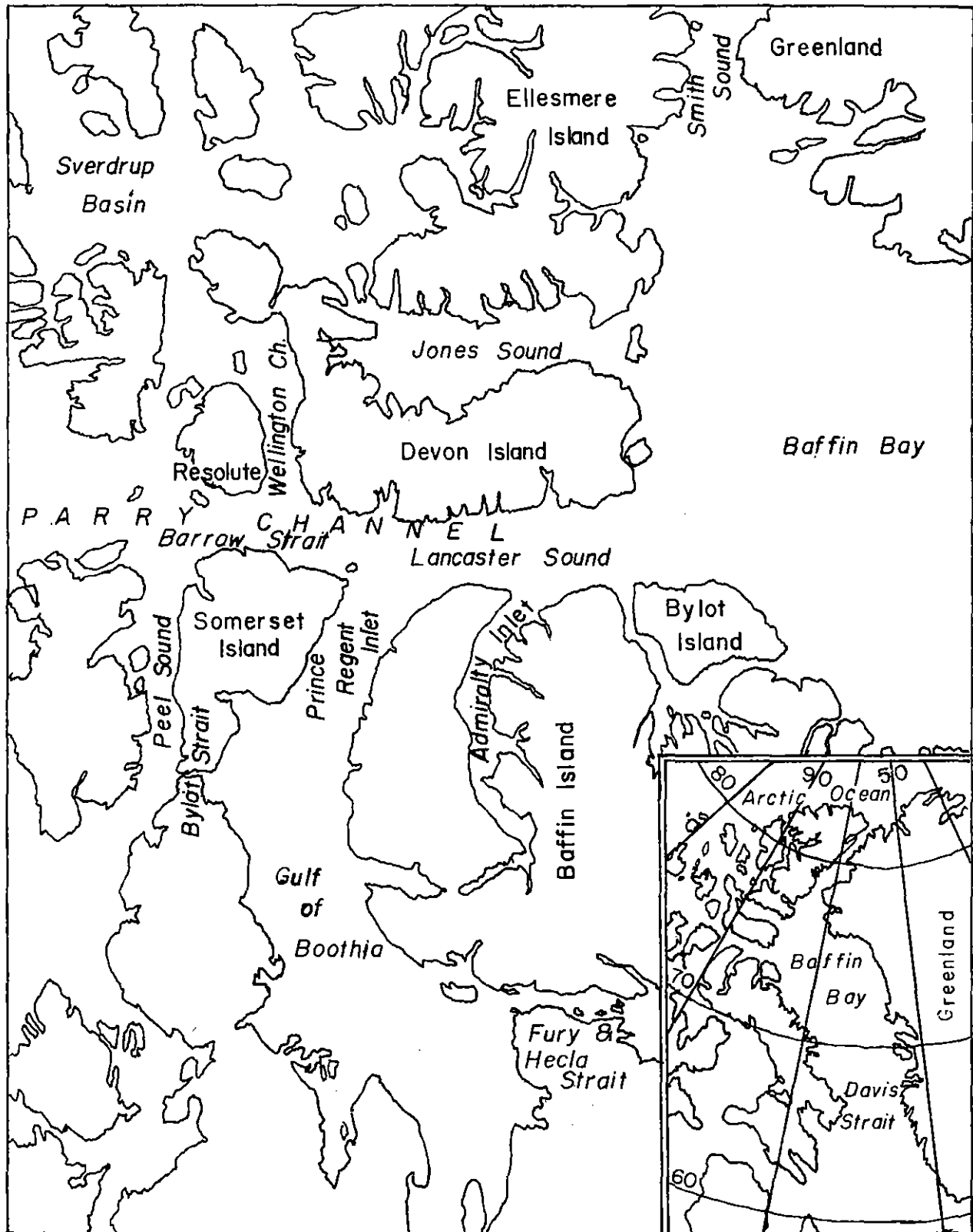


Figure 1: A map of Eastern Parry Channel and adjacent water bodies. The inset map illustrates the location of Parry Channel in relation to Baffin Bay and the Arctic Ocean.

2.2 Oceanographic features of Lancaster Sound.

Beginning as early as the mid-nineteenth century, many oceanographic observations have been gathered in Lancaster Sound (e.g. Kane, 1857); however, analyses of such observations are much fewer in number. These include the studies of Kiilerich (1939) based on the Godthaab expedition of 1928, and the studies of Bailey (1957), Collin (1962), and Barber (1977) all using data collected aboard the CCGS Labrador in various summer cruises between 1954 and 1960. Muench (1971), in a comprehensive review of the physical oceanography of the northern Baffin Bay region, discusses the water masses and circulation of eastern Lancaster Sound.

2.2.1 The circulation of eastern Lancaster Sound

In this section, we shall describe the main features of the circulation of eastern Lancaster Sound based on previous studies. In most studies, currents are inferred from the internal water mass distribution through geostrophic computations. This indirect method of current determination has deficiencies; these include the assumed vanishing of water currents at the depth of no motion and the question of the response time of the mass distribution field to changes in the currents. Muench (1971) explains the "lack of volume continuity implied by the existing transports for Smith, Jones and Lancaster Sounds and northern Baffin Bay" as a result of deficiencies in the geostrophic method of computing volume transports. In the following section we shall examine the direct current measurements which have been made in eastern Lancaster Sound, prior to this study. Unfortunately, these are so few in number that they add little to our knowledge of the overall circulation of the Sound.

The waters of Lancaster Sound can be divided into two types; Arctic water in the upper 250 m characterised by low temperatures (-1.8°C to 0.0°C) and low salinities ($<31\text{‰}$ to 34.4‰) and below this, water that is markedly warmer (0.0°C to 2.0°C) and more saline (34.2‰ to 34.5‰). Based on the similarity between the latter water mass and the Atlantic Intermediate water mass of Baffin Bay, the deeper water of Lancaster Sound is believed to result from an intrusion of Baffin Bay water (Collin, 1962). The Arctic water of Lancaster Sound could be transported either eastward from the western Parry Channel region or southward via Smith Sound and northern Baffin Bay; Muench (1971) suggests that a combination of both of these sources can account for the water properties of the upper 250 m of eastern Lancaster Sound. { For a detailed description of the water masses of Lancaster Sound see Collin (1963) or Muench (1971) }.

From the computed baroclinic currents determined in several different years, two persistent features emerge. One of these is a permanent anticlockwise circulation in eastern Lancaster Sound resulting in westward currents along the northern side of the Sound and eastward currents along the southern side together with southward currents in central Lancaster Sound. Such a circulation accounts for the intrusion of Baffin Bay water in Lancaster Sound as well as observed ice movements noted in the previous section. Muench (1971) suggests that "the circulation of Baffin Bay water westward into northern Lancaster Sound appears to be due to conservation

of potential vorticity; the southward current impinges on Lancaster Sound from the relatively shallow shelf area off Devon Island --- and hence exhibits a tendency to turn west."

The other persistent feature to emerge from computed baroclinic currents is the net eastward volume transport through Lancaster Sound. According to Muench (1971) approximately one-half of the net computed baroclinic transport through northern Baffin Bay (of $2.0 \pm 0.7 \times 10^6 \text{ m}^3/\text{sec}$ southward) originates in Lancaster Sound with the remainder of the flow coming from Smith and Jones Sounds.

The presence of the anti-clockwise circulation at the mouth of Lancaster Sound suggests that much of the net eastward transport may be concentrated on the southern side of eastern Lancaster Sound. This contention is supported by observed ship and ice drifts (Canadian Hydrographic Service, 1968) and the movement of a satellite tracked drifting buoy in early October 1977 (Fissel and Marko, 1978) which indicated intense currents of up to 100 cm/s near the southern boundary of the Sound. The westward current on the northern side of the Sound also is limited in extent; Bailey (1957) observed that it was confined to within 11 km of the Devon Island coast while Collin (1958) found no evidence of the current at 15 km off the northern coast.

Based on the estimation that conservation of potential vorticity through changes in the bottom topography appears to control the westward current entering Lancaster Sound from Baffin Bay together with the uniformity of the temperatures distribution in the deeper Atlantic water, Muench (1971) argues that the currents extend nearly to the bottom.

The previous oceanographic studies suggest considerable temporal variations in the circulation of Lancaster Sound from year to year. The estimated net baroclinic volume transport varies from 0.3 to $1.0 \times 10^6 \text{ m}^3/\text{sec}$, using data from cruises in different years (Muench, 1971). Similarly, the extent and depth of the deeper water mass varies from one year to another (Collin, 1962). Furthermore, the dynamic height distribution over eastern Lancaster Sound indicate the presence of eddies and gyres which differ in size, position and direction of rotation (Muench, 1971, p.89). Clearly, direct observations through a combination of moored current meters and drifting surface drogues, are required to delineate these features.

2.2.2 Previous Direct Current Measurements in Eastern Lancaster Sound

In 1960, current measurements were taken at four locations across Lancaster Sound (see figure 2) between Aug. 25 and Sept. 27. The measurements were made with a variety of instruments suspended from the side of the anchored M.V. Theta. The results of these measurements were never published and much of the original data is missing (Barber, 1977). However, some computed residuals (see table) over periods of either 24 or 48 hours together with a brief written summary were located at the Bedford Institute of Oceanography Dartmouth, N.S. The largest residual current of 38 cm/s (0.71 knots) was found at the northernmost station at depths of 10m.

The summary reads, in part:

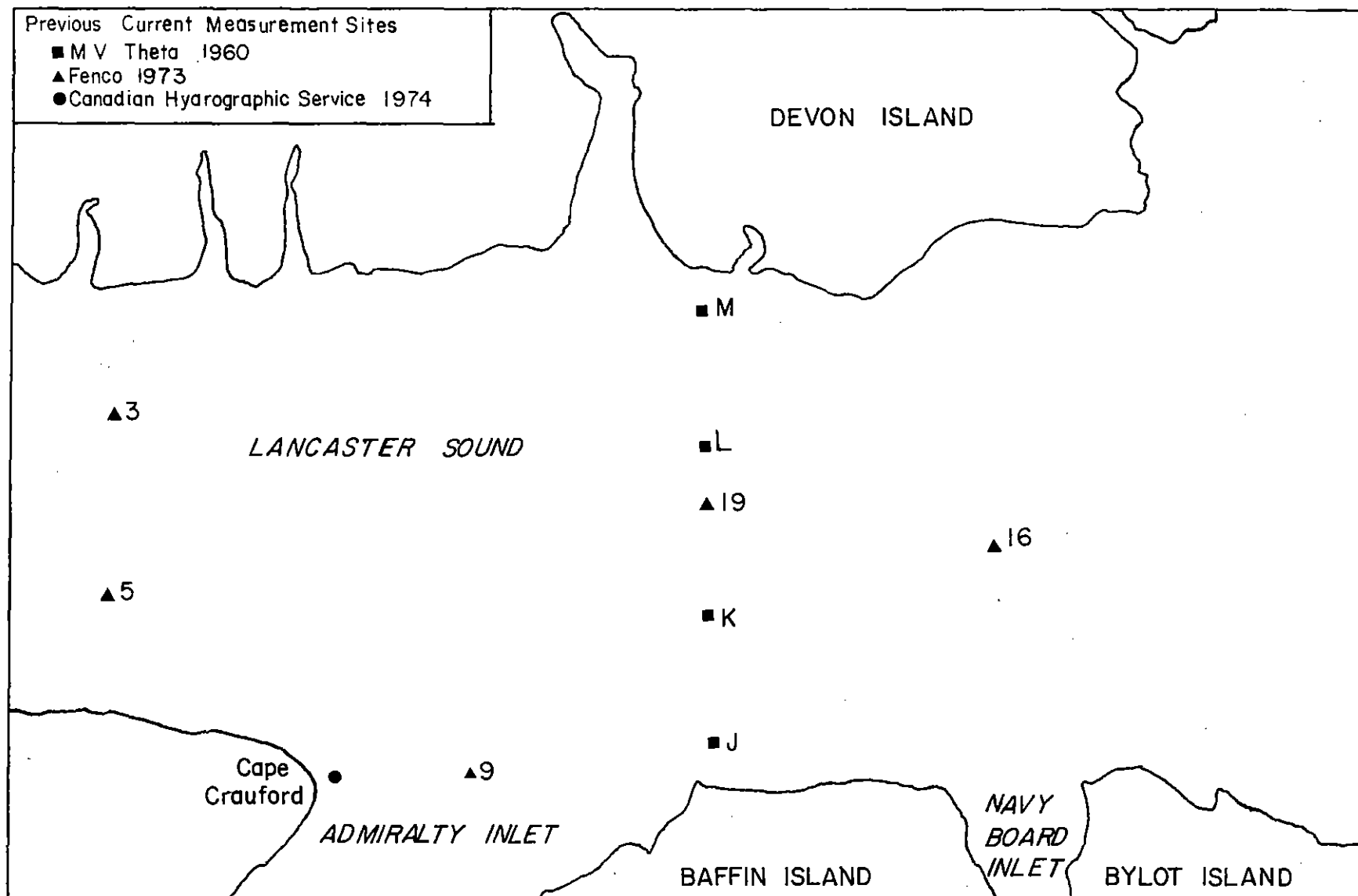


Figure 2: The sites of direct current measurements made in previous oceanographic studies of eastern Lancaster Sound.

"No tidal movement apparent anywhere across Lancaster Sound, stream weak and indefinite for the most part, slightly stronger on the north side and decreasing with depth. Due to the close proximity of the magnetic pole and relatively weak directive power of small compasses directions observed can be considered approximate only. These directions, coupled with ice observations, indicated a predominately easterly flow with meteorological conditions the most deciding factor. Indications of a counter flow in a westerly direction, at a depth of 300 m on the south side and 600 m on the north may possibly be verified when the oceanographic results are completed."

Table 1

The speed (knots) and direction (degrees true) of the residual current at four stations in Lancaster Sound from a survey aboard the M.V. Theta in 1960 (1 knot = 51.5 cm/s).

Station	J				K			L			M		
	Averaging				Averaging			Averaging			Averaging		
Depth	Period	Spd.	Dir.		Period	Spd.	Dir.	Period	Spd.	Dir.	Period	Spd.	Dir.
(M)	(hrs)				(hrs)			(hrs)			(hrs)		
7	48	.63	83°		48	.31	7°	48	.14	8°	48	.71	76°
	48	.59	80°		24	.57	40°	48	.19	101°			
40	48	.46	61°		48	.33	133°	24	.35	162°			
	48	.40	97°		48	.46	152°	24	.35	200°			
	24	.33	8°		24	.24	144°	24	.35	150°			
	24	.50	35°		24	.41	150°	24	.35	120°			
	24	.44	90°		24	.51	152°						
	24	.40	84°		24	.52	156°	24	.35	74°			
100	48	.22	130°		48	.17	128°	48	.07	315°	24	.66	128°
	48	.16	132°										
300	48	.13	292°		48	.18	277°	48	.17	15°			
	48	.13	278°										
	24	.12	279°										
400	48	.11	80°										
	24	.27	74°										
600					48	.04	124°	48	.15	30°	48	.26	260°
								48	.19	333°			

It is also interesting to note the tendency of the currents to flow south easterly at depths of 40 and 100 m, especially at the two centre stations. This southeasterly flow may reflect the presence of the ant-clockwise gyre at the mouth of the Sound forcing the generally easterly flow across the Sound towards the southern side. The evidence of a westerly "counter flow" in the deeper water with speeds of 6.1 to 13.3 cm/s may represent the intrusion of Baffin Bay water into the Sound.

Fenco (1974) reports current profiles made with a current meter lowered from the M.V. Orion Arctic in the summer of 1973 at locations shown in Figure 2. While no direction measurements were made, the recorded speeds range from 5 to 33 cm/s. in agreement with the 1960 data. At two stations, relatively large vertical current shears (a change of 20 cm/s in speed over 20 m depth) were measured over the upper 30 m while little change was observed with depth below 250 m. As the current profiles were not repeated at any one location, this data set yields no information as to the magnitude of tidal currents.

In the summer of 1974, the Canadian Hydrographic Service installed and recovered a Hydrowerstaten current meter at 10m depth on a sub-surface mooring at $73^{\circ} 45' \text{ N}$, $84^{\circ} 84.6' \text{ W}$, about 7.4 km off Cape Crauford on the northern side of Baffin Island. The 26 days of current observations, recorded at 5 minute sampling intervals, represents the longest continuous set of current measurements taken in Lancaster Sound prior to this study. However as the current meter was moored in 140 m of water at the entrance to Admiralty Inlet where the bathymetry runs north-south, the currents may not be indicative of those in the major portion of eastern Lancaster Sound with an east-west orientation of bathymetry and water depths of 500 to 800 m.

The time series plot of the current record, shown in Figure 3, indicates a maximum speed of 90.5 cm/s with a mean speed of 27.7 cm/s. That the north-south component indicates considerable diurnal and semi-diurnal tidal variations, is borne out by a harmonic analysis of the data. This analysis (Godin 1972) reveals that the M_2 semi-diurnal tidal constituent is largest, which together with the K_1 , S_2 and O_1 constituents, accounts for the more than one-half of the total variance of the current time series. For all four of these major constituents, the tidal ellipses are orientated within 5 degrees of the true north-south direction, parallel to the local bathymetry. Thus, contrary to the 1960 data, tidal currents are significant at this coastal location.

The mean current, over 26 days, set southeasterly with most of this net flow taking place over the last 15 days of the record, as shown by the progressive vector diagram in Figure 4. This indicates a flow from southern Lancaster Sound into Admiralty Inlet around Cape Crauford.

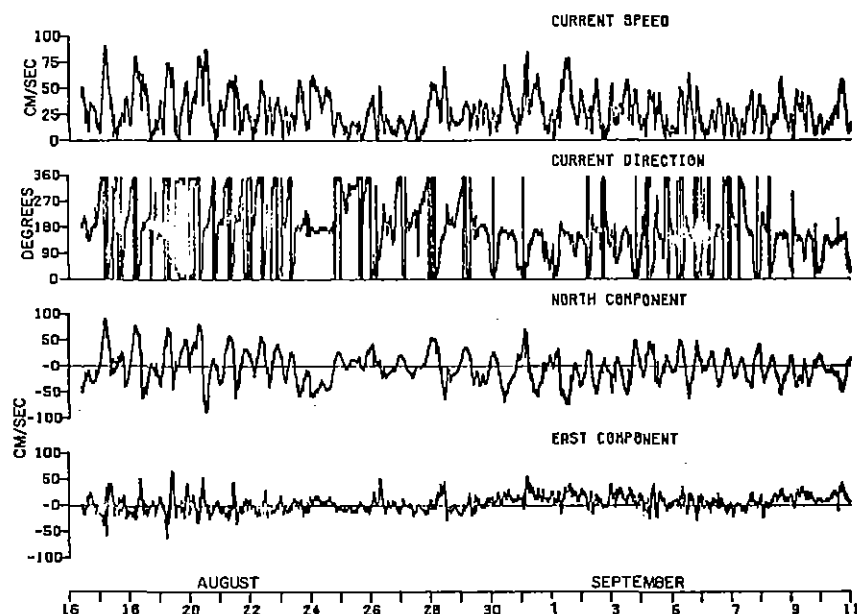


Figure 3: Time series plots of current measurements at 10m depth off Cape Crauford made in 1974 by the Canadian Hydrographic Service.

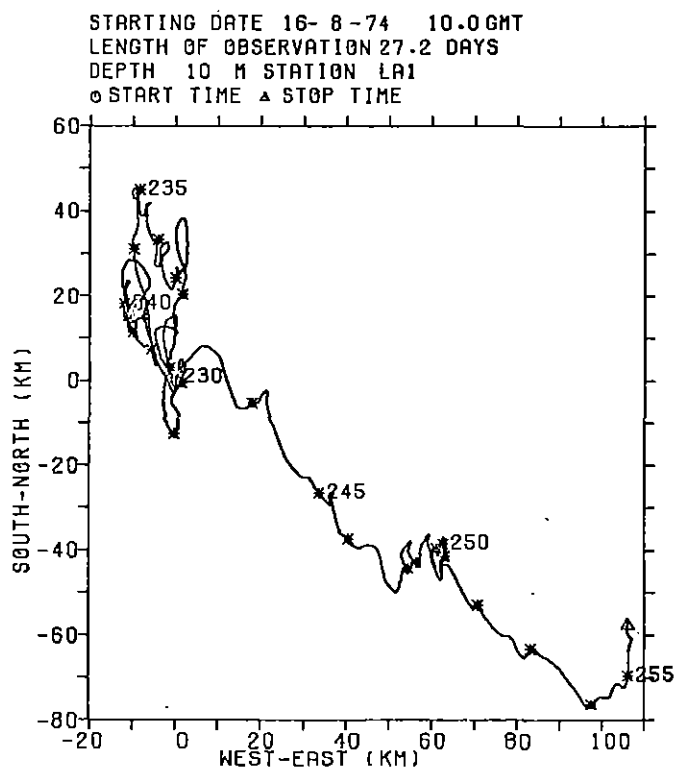


Figure 4: Progressive vector diagram of the current meter data of the Canadian Hydrographic Service taken in 1974.

3. Data Collection and Processing

3.1 Station Locations and Logistics

Four current meter moorings were deployed in eastern Lancaster Sound July 28-29, 1977 off the CCGS Labrador at locations shown in Figure 5. Each mooring used three Aanderaa RCM-4 current meters at nominal depths of 35 m, 200 m and 550 m respectively (see Figure 6). The moorings were assembled on the port foredeck of the ship, and when the ship was on station the mooring was layed off the ship beginning with the upper end. When all but the anchor weights (three railway wheels) were off the deck and in the water, the weights were cut free and fell to the bottom pulling the remainder of the mooring down with it.

The positions of the stations were located using three radar fixes on prominent coastal features. The accuracy of these positions are estimated as ± 1 nautical mile (± 1.8 km) with better accuracy at stations 2 and 4, located near the northern and southern sides of the Sound, respectively.

During the deployment cruise, a flux gate magnetometer was installed at Dundas Harbour, Devon Island using an abandoned building to shelter the recording system. Also, two COSRAM * satellite tracked surface drifting buoys were released. The results of the drifting buoy measurements are presented in Fissel and Marko (1978)

The oceanographic party disembarked from the Labrador at Resolute Bay on July 29 and rejoined the ship on Sept. 27. The moorings at stations 1,3 and 4 were recovered from Sept. 29 to Oct. 1. The mooring at station 2 was not recovered; we were able to locate the mooring through interrogation of the acoustic release but repeated attempts to activate the release and raise the mooring to the surface failed. This could be a result of any number of causes; our best guess is that either the floatation was torn off by a passing iceberg or that a piece of the wire rope of the mooring wrapped around the release as it was lowered into the water when deployed. If the latter is the case, it maybe possible to raise the mooring by grappling for it in the forthcoming navigation season, assuming the release is still functioning so that the mooring can be precisely located.

After servicing the current meters, the three recovered moorings were redeployed at stations 2,3 and 4. These will operate through the winter with recovery planned for the summer of 1978.

Of the data recorded by the nine recovered current meters, the number of valid time series recorded was seven for current speed, six for current direction, nine for temperature and six for conductivity, as illustrated schematically in Figure 7. Problems during deployment of the equipment resulted in the missing speed and direction data. Apparently, as the moorings were layed off the side of the ship, mooring wire caught the direction vane, wrapping around it so it was unable to turn; this

* Continental Shelf Random Access Measurement

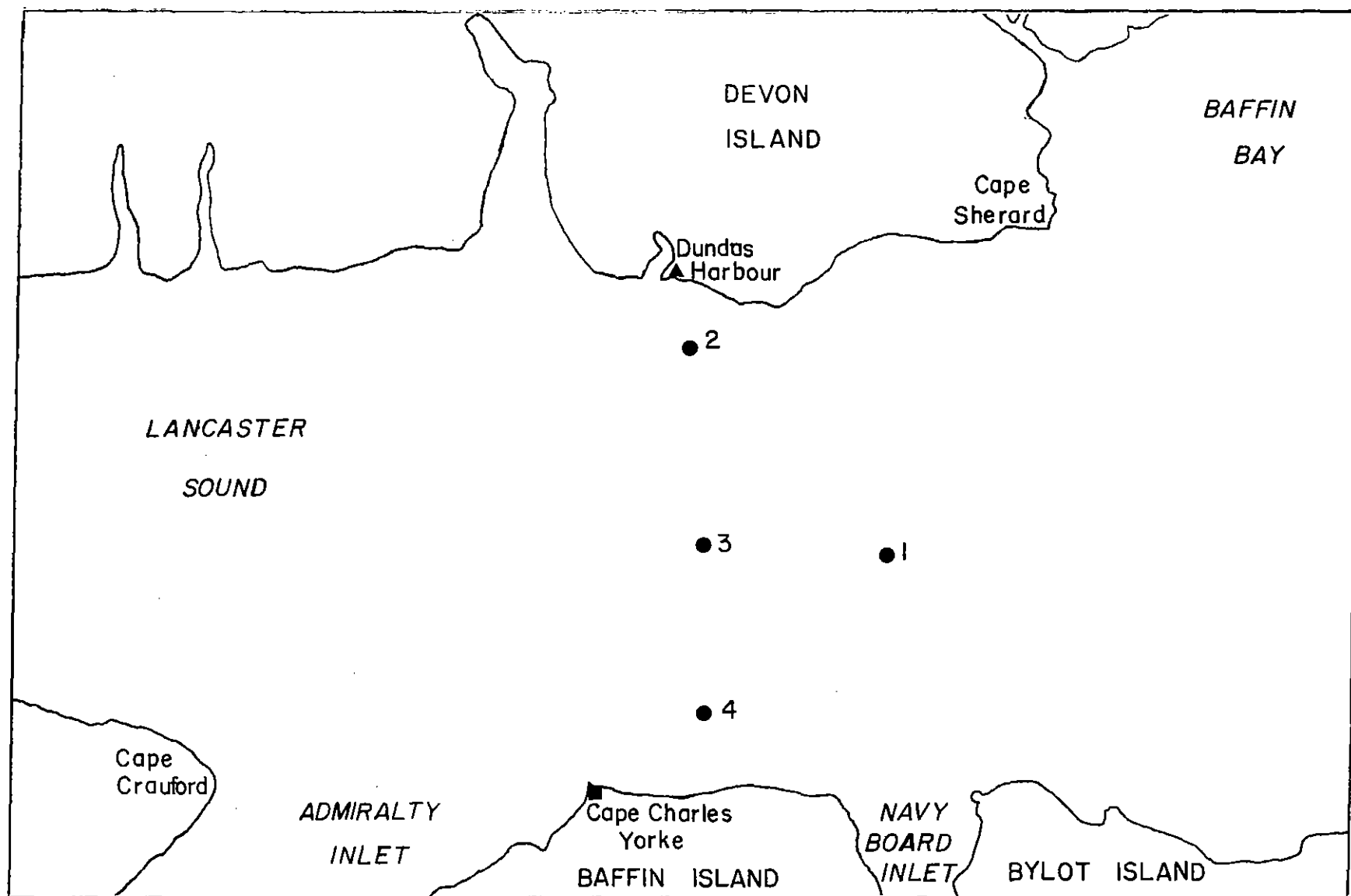
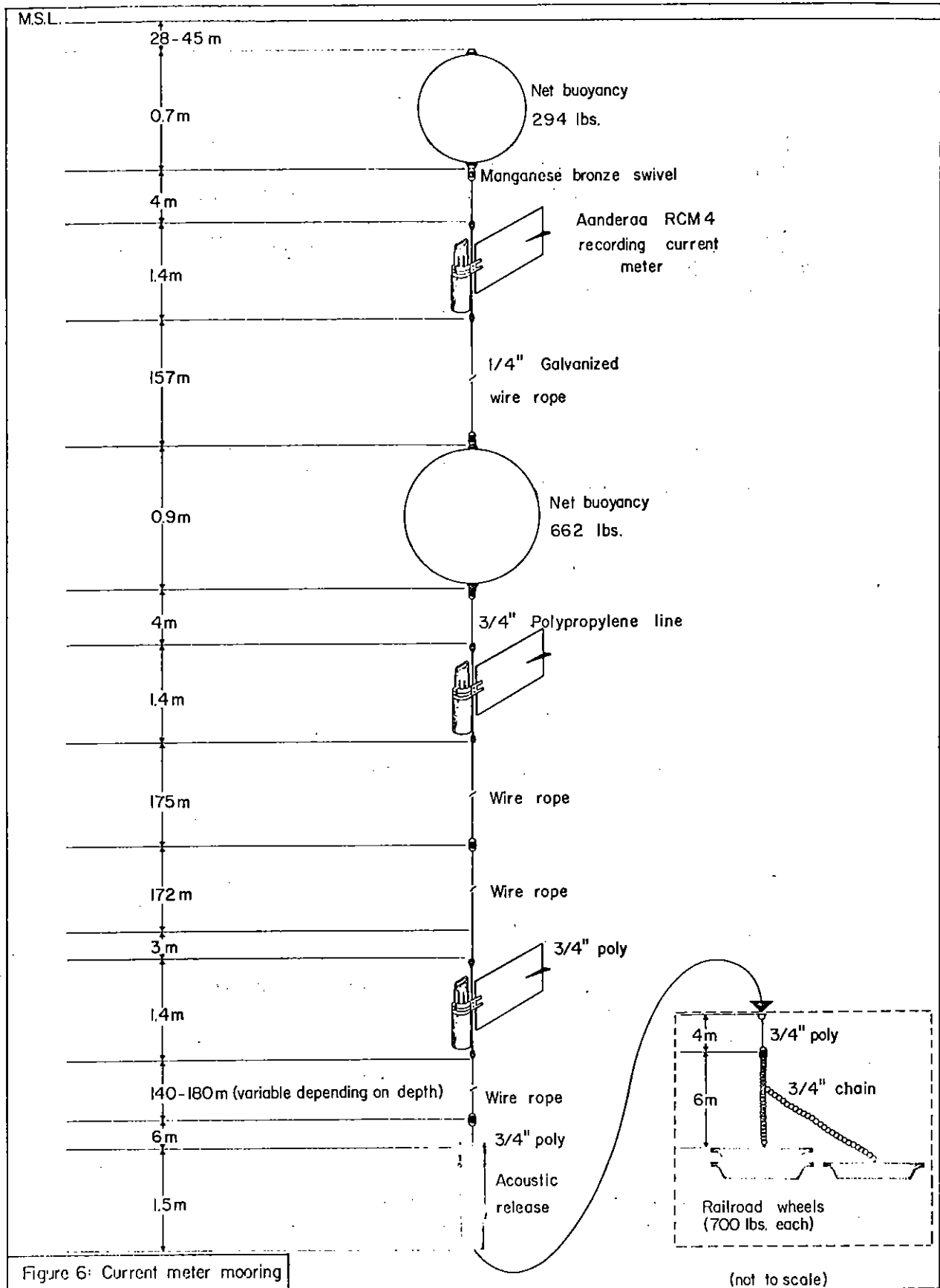


Figure 5: Location of the current meter moorings and weather station in Lancaster Sound, summer 1977.



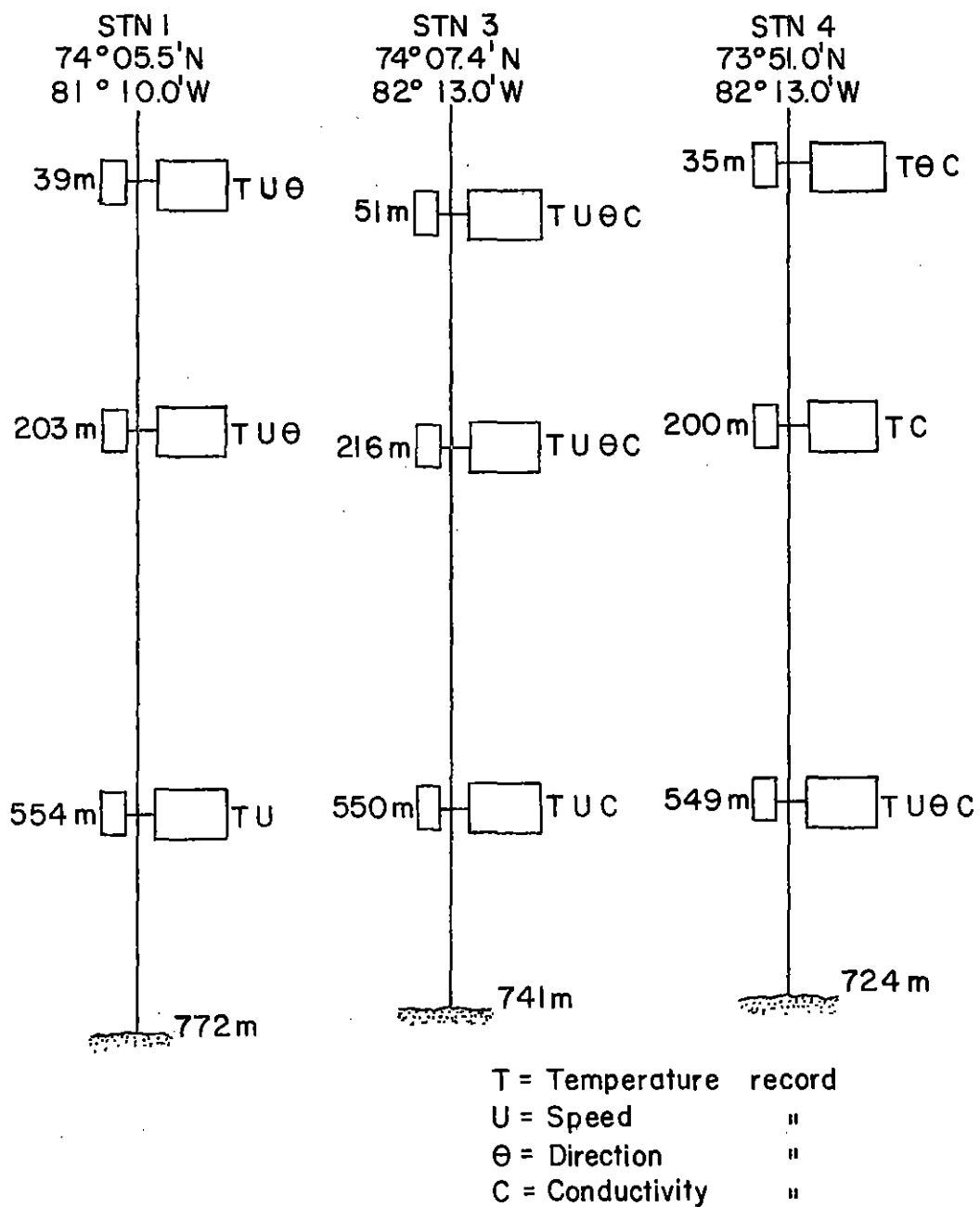


Figure 7: A schematic representation of the data recovered from each current meter at stations 1,3 and 4.

occurred with three current meters resulting in no direction information. While the moorings were layed off the ship two Savonious rotors were broken off with the result that no speed data were obtained for these two meters. These difficulties were due in large part to the necessity of working off the foredeck which is 20 feet above the waterline. At this height, managing the instruments as they enter the water and visually checking for snags is complicated by the distance off the water. At station 1 the current meters used were not equipped with conductivity sensors so that a total of six conductivity time series only were recorded.

A self recording weather station was established at Cape Charles Yorke on Aug. 5, 1977 and recovered Sept. 16, 1977 by Dobrocky Seatech Ltd., (see Figure 5). The weather station produced measurements of wind speed and direction, air pressure and air temperature. In this report, the recorded weather data is presented and employed in the examination of the correlation between the near surface currents and winds.

Weather and sea surface temperature data were also obtained from the weather observer aboard the CCGS Labrador during the deployment and recovery operations.

3.2 Instrument Description

3.2.1 Aanderaa Current Meters

The Aanderaa RCM-4 current meters recorded speed, direction, temperature and conductivity at 10 minute sampling intervals. While the measured speed is a 10 minute average, the other quantities are instantaneous samples. No pressure data was recorded as use of this channel can result in errors to direction measurements (Keenan, 1976). The specifications as to accuracy and resolution of the recorded signal are given in Table 2 based on the manufacturers values.

The temperature, conductivity and direction sensors of each current meter were calibrated at the Northwest Regional Calibration Center, Bellevue, Washington in May 1977. As for the speed, standard speed calibration values, supplied by the manufacturer, were used.

Since eastern Lancaster Sound is within 700 km of the north magnetic pole, the accuracy of the direction measurements require special attention. The horizontal component of the geomagnetic field in the study area is 3000 gamma; by comparison, the horizontal component is 19000 gamma in Victoria, B.C. and 17000 gamma in Halifax N.S. Laboratory tests carried out on one of the Aanderaa current meters used in this project (serial no. 2703) indicated that the current meter reading is repeatable on average to 5 degrees, ranging from 1.4 to 8.4 degrees, at 3000 gamma field strength (Fissel, 1978). However, Barfoot (1972) found an average error of about 10 degrees ranging from 3.5 to 15.1 degrees at 3000 gamma for another Aanderaa current meter. Neither of these tests include errors due to temporal variations in the geomagnetic field direction, the presence of magnetic fields from mooring materials such as steel wire rope

Table 2

The accuracy and resolution of Aanderaa current meter and weather station measurements, as supplied by the manufacturer.

a) Current Meters (S/N 2696-2704)

Sensor	Temperature	Conductivity	Speed
Accuracy	0.15°C		1cm/s or 2% of speed, whichever greater.
Resolution	0.02°C	0.07 mmho/cm	0.28 cm/s

Current Meters (S/N 340,360,361)

Sensor	Temperature	Speed
Accuracy	0.15°C	1 cm/s or 2% of speed, whichever is greater
Resolution	0.02°C	0.41 cm/s

b) Weather Stations

Sensor	Temperature	Speed	Direction	Pressure
Accuracy		2%	5°	0.1 mbar
Resolution		1.7 cm/sec	0.35°	0.01 mbar

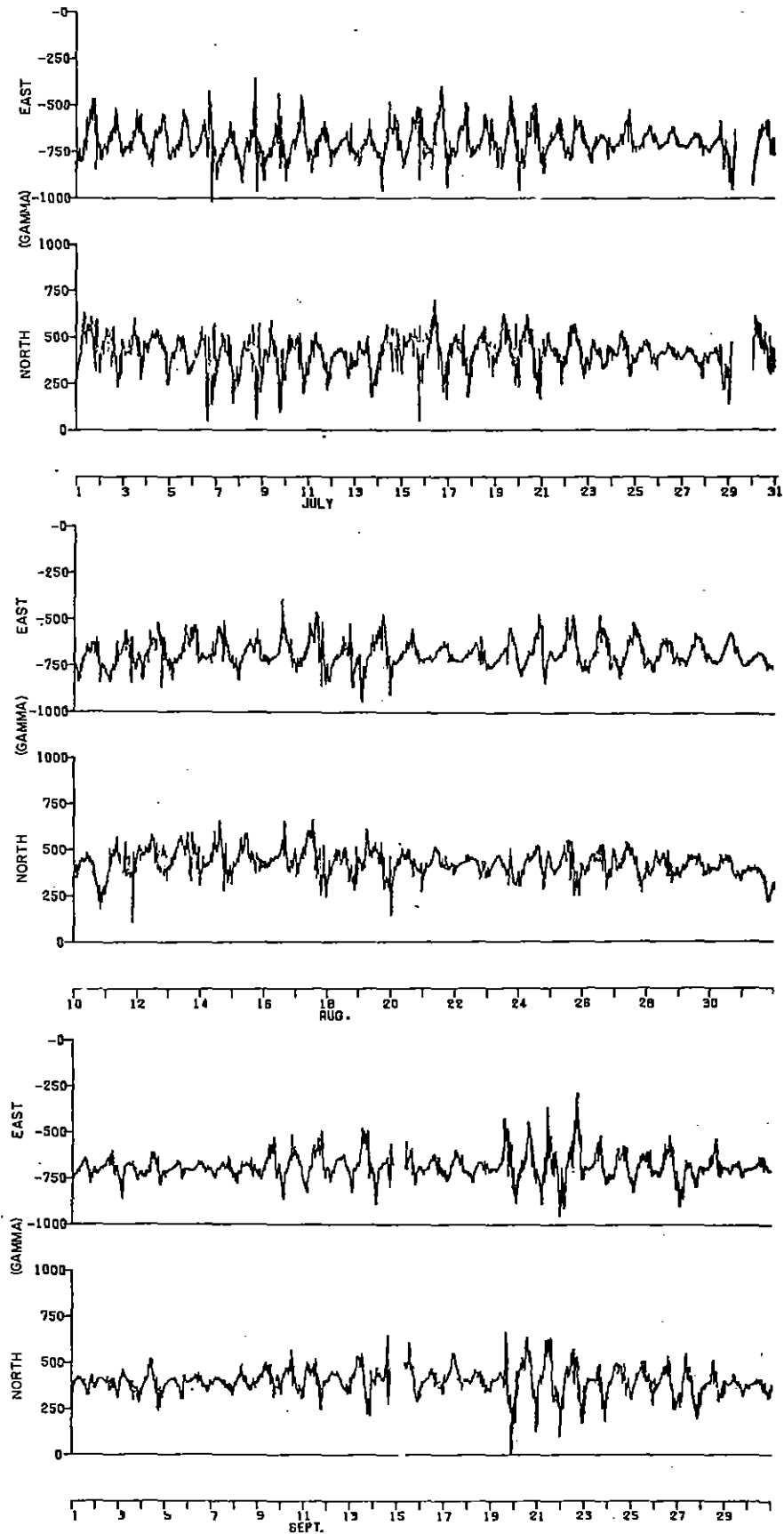


Figure 8: The horizontal components of the geomagnetic field in Resolute for the months of July, August and September 1977.

and errors due to linear or angular accelerations of the compass due to mooring motion.

As previously mentioned, a flux gate magnetometer was installed at Dundas Harbour with the data recorded on an Aanderaa data logger. Unfortunately, after about 9 hours of operation, the data logger failed and no further data were obtained. The geomagnetic data recorded at Resolute Bay, N.W.T. the closest magnetic observatory, were obtained from the Earth Physics Branch, Division of Geomagnetism, Department of Energy, Mines and Resources. The times series shown in Figure 8 indicate a strong diurnal variation with typical peak to peak amplitudes of 300 gamma with a maximum peak to peak change of 750 gamma recorded on Sept. 19, 1977. We assume that temporal variations in the geomagnetic field at Resolute Bay are representative of those in eastern Lancaster Sound which is not unreasonable in view of the good agreement between Resolute Thule and Godhavn in Greenland (Witham and Anderson, 1962). Therefore, over the measurement period, the typical changes in the geomagnetic field direction is estimated at ± 3 degrees with a maximum value of ± 7 degrees. Combining the errors of the compass itself according to Fissel (1978) with the errors due to variations of the geomagnetic field results in a typical error of ± 6 degrees with a maximum value of ± 16 degrees. In these error estimates errors associated with magnetic mooring materials and accelerations of the compass have not been included as no numerical values are available. However we feel that the current directions should be accurate to 10 degrees typically with maximum errors of ± 20 degrees.

No corrections were made to the current direction due to changes in the geomagnetic field direction since these errors are not significantly greater than uncertainties due to other causes. However when interpreting the results reference can be made to Figure 8 to determine those days on which this error is particularly large.

3.2.2 Weather Data

The self recording weather station located at Cape Charles Yorke used Aanderaa wind speed, wind direction and air temperature sensors together with an Aanderaa TGI-A water level gauge to measure atmospheric pressure. See Table 2 for accuracy specifications. The site "was on large flat gravel bar to the east of the large river at the end of the Cape. The elevation above sea level was estimated using a hand level as 20 meters. The site was clear of all obstructions and was relatively flat for 500 meters in all direction" (Lea, 1977). The wind speed and direction sensors were mounted on a guyed mast 4 meters above the ground.

3.3 Data Processing

3.3.1 Current Meter Data

The processing scheme for current meter data, illustrated in Figure 9, begins with translating the raw data on $\frac{1}{4}$ " reel to reel tapes to a 9 track computer tape. The number of translated records are checked to see that it agrees with the total number expected based on the start and stop times and the sampling intervals. Of the nine current meter tapes, one was.

CURRENT METER DATA PROCESSING SYSTEM

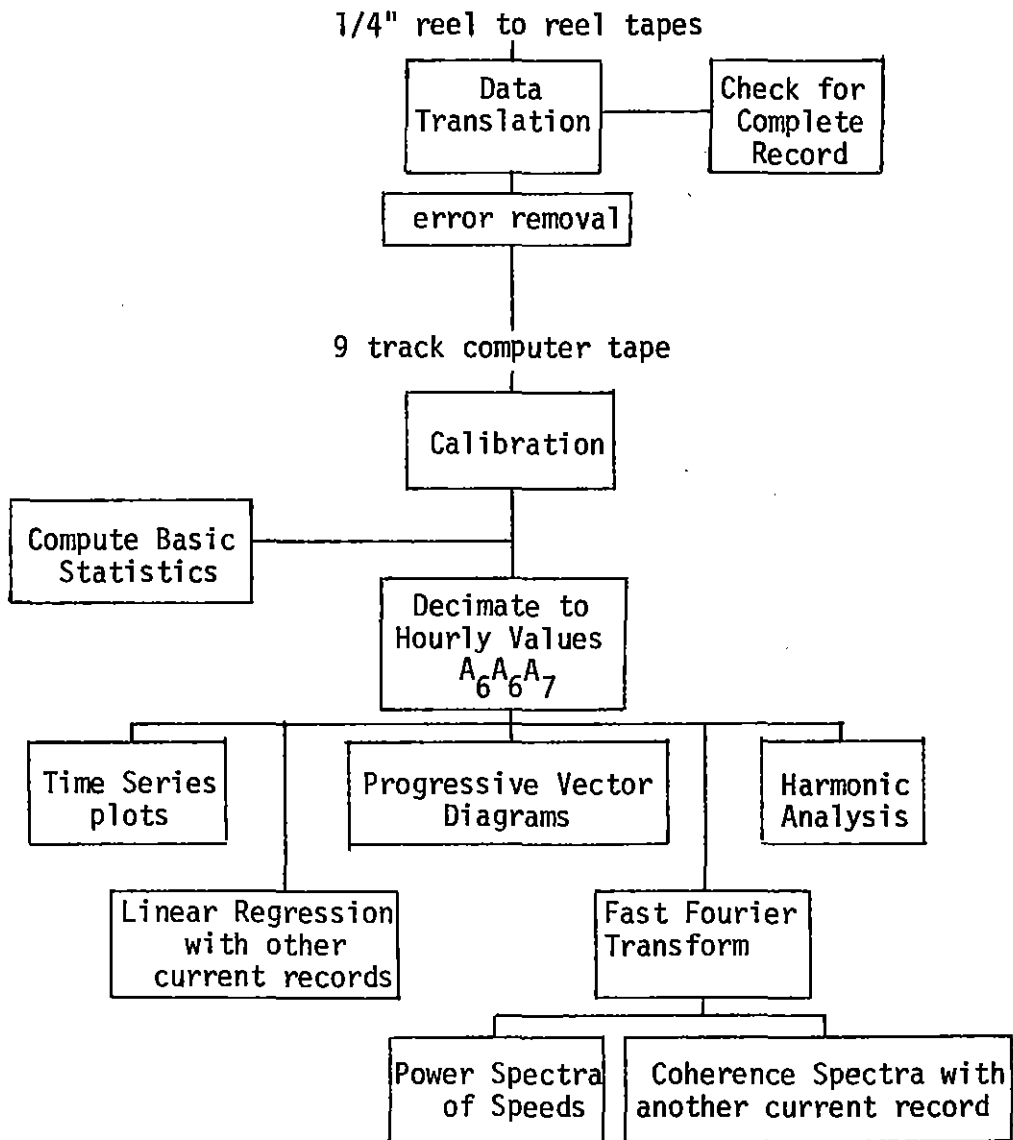


Figure 9: The data processing system used on the current meter data.

missing data; for station 1, 39 m depth, the record was short by 556 readings. Furthermore, the end of the recorded data for this current meter had many missing bits. As the most likely explanation for this performance is a weak battery, we assumed that the current meter functioned correctly until the latter part of the record. At some point, the battery output became sufficiently low that the recorded data no longer could be trusted. On the basis of the number of bits recorded in each word, we chose to delete data recorded after 1300 Sept. 26 GMT so that the last 128 readings on the translated tape were rejected. The data were then examined for errors using the following criteria:

Table 3

Criteria used to eliminate erroneous current meter data.

Quantity	Temperature	Conductivity	Speed
1) exceeds maximum allowable value of	6.5° C	46 mmho/cm	163*cm/s
2) below minimum allowable value of	-2.0° C	0 mmho/cm	0 cm/s
3) absolute value of first difference of successive measurements exceeds	2.0° C	3.0mmho/cm	50 cm/s

* for depths of 200 m or more, a maximum allowable speed of 80 cm/s was used.

Erroneous values that exceeded a maximum value or were less than the specified minimum value were replaced by the previous data point. If the data value was rejected because the absolute value of the first difference is too large, it is replaced by interpolating between the previous value and the next good value. The number of erroneous values was very small, being 0.4% or less as summarised in Table 4.

From the temperature and conductivity measurements together with the nominal depths, the salinity in parts per thousand and sigma-t were computed using the algorithms of Bennett (1967) and Knudsen as quoted by Fofonoff (1962), respectively. Also, the east-west and north-south components of the currents in cm/s were computed taking a current flowing to the east and flowing to the north as positive, respectively.

Following error removal and calibration, and computation of the basic statistics for each measured quantity (mean, standard deviation, minimum and maximum), the time series data were decimated to hourly values using a three pass moving average filter, described as A₆A₆A₇ following Godin (1972) and then subsampling on the hour. This low pass filter effectively removes variations with periods less than 2 hours. From this reduced number of data points, time series plots and progressive vector diagrams were produced.

Table 4

Summary of Rejected Current Meter Data

Station	Depth (m)	Serial No.	No. of Readings	T	C	U
1	39	340	8606	32	N	34
1	203	360	9353	1	N	4
1	554	361	9353	0	N	26
3	51	2697	9019	6	0	0
3	216	2700	9019	0	0	1
3	550	2703	9019	0	0	0
4	35	2698	9076	15	1	N
4	200	2701	9076	2	3	N
4	549	2704	9075	0	0	0

N - not recorded

T - temperature

C - Conductivity

U - Speed

The tidal energy of each available vector time series was examined using the harmonic analysis method described by Godin (1972) as adapted to the Institute of Ocean Sciences computer by Foreman (1978).

A spectral analysis of the currents was carried out to examine the relative amount of variance over the inherent frequency range resolved by the analysis. The fast Fourier transform algorithm of Singleton (1968) was used to compute raw transform values. From these values, power spectral densities, coherence and phase spectral estimates were computed over frequency bands with 10 degrees of freedom each. The definitions of the computed spectral values are found in Fissel (1976).

To examine the overall correlation among pairs of current time series at two different locations, a linear regression analysis was used following the method of Panofsky and Brier (1958).

3.3.2 Weather Station Data

Translation, error removal and calibration of the weather station data uses the same procedures as for current meter data processing. In this report, the analysis of the weather data is limited to time series plots and examination of the correlation of the wind with the currents recorded at the top of each mooring. A more complete analysis of the weather station data together with similar measurements at various sites in Barrow Strait is presented in Hill et.al. (1978).

4. Results

In this section, the features and character of each set of measured physical quantities are described: current meter depth (in section 4.1), current speed, direction and components (section 4.2), temperature and salinities recorded by current meters (4.3) and the weather data (4.4). We then examine the relatedness of different types of physical quantities. The correlation of the currents temperature and salinity provide information on the horizontal heat and salt transports (section 4.4) while the role of the wind in driving currents at the level of the upper current meter is studied in section 4.5.

4.1 Current Meter Depth

The drag on the subsurface moorings due to the water currents results in the mooring to be pulled away from the vertical with the result that the actual depth of the current meters increase when the currents are strong. The depths used in this report are nominal values based on the lengths of wire used in constructing the mooring and the total water depth at the time of deployment corrected to mean sea level using tide tables. While these nominal depths are correct for weak or nonexistent currents, the actual depth deviates from the nominal depth as the current speed increases. Using a static analysis numerical model of a single point mooring (Bell, 1977), the vertical excursions beyond the nominal depths were computed. The results indicate that for the maximum current profile recorded (on Sept. 10 at station 3) the depth of the upper current meter increased by 23m while the mid-depth current meter was pulled down 12m. The increase in the depth of the deepest meter was only 4m. For a current profile using average speeds (37cm/s at 51m, 20cm/s at 216m and 7.4 cm/s at 550m), the vertical excursion was only 0.7m for the upper current meter and less for the other two meters.

Even for the maximum speed profile, the tilt of the mooring never exceeds 16 degrees, well below the maximum 23 degrees of line tilt at which the Aanderaa current meter can remain upright through the gimbals on which it is mounted. Therefore, the speed and direction measurements will not be directly affected by mooring tilt. However, if there are large vertical gradients in any of the quantities measured by the current meters, the vertical excursions will result in significant differences from what the instrument would have measured at its nominal depth. Such large vertical gradients seem most likely to occur in salinity and temperature at the level of the near surface current meters.

4.2 Current Speed, Direction and Components

4.2.1 Time series Plots, Histograms and Basic Statistics.

Figures 10 to 12 show the time series plots of the speed, direction, north-south and east-west components of the currents while the basic statistics (mean, standard deviation, minimum and maximum)

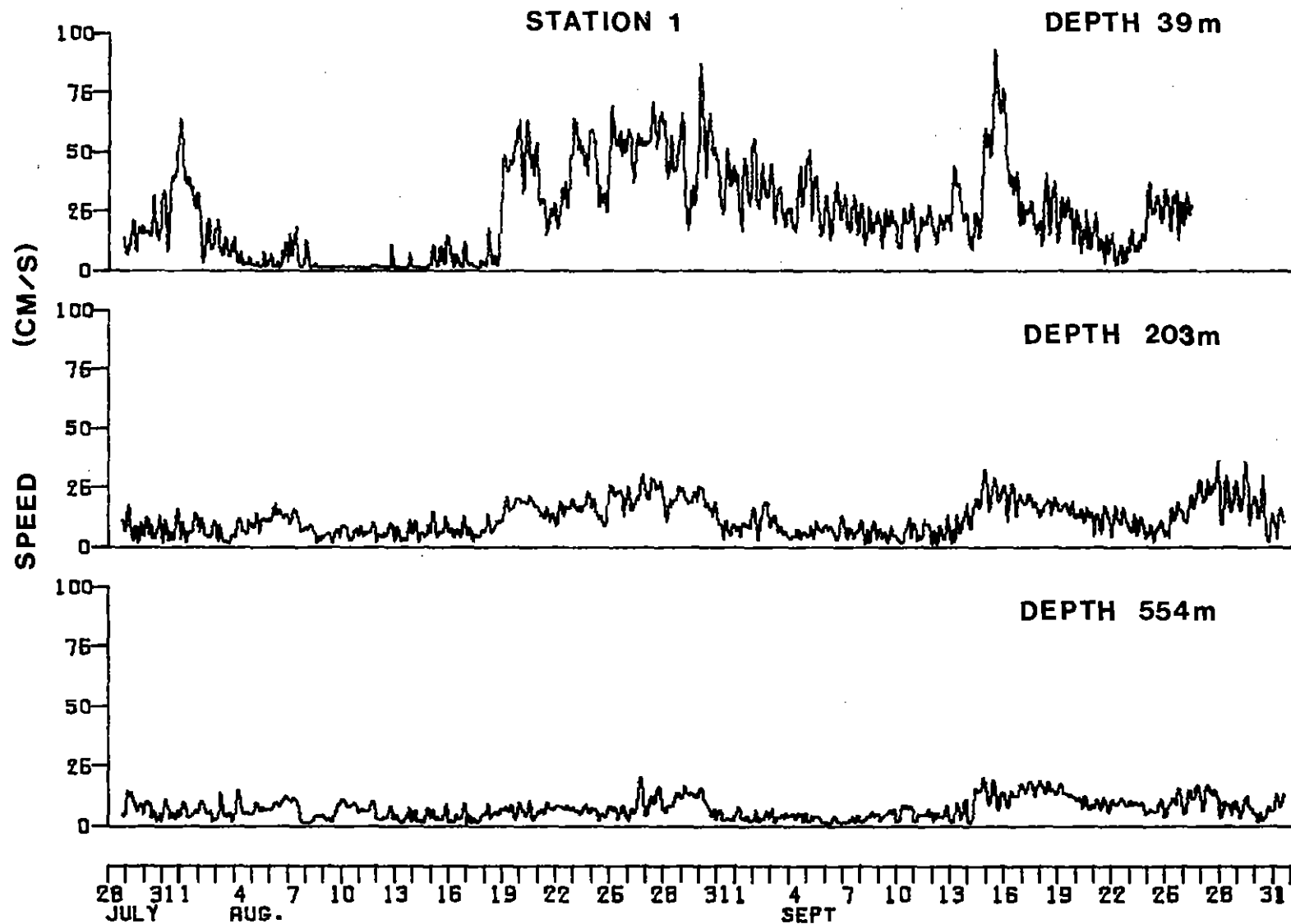


Figure 10a: Time series plots of the speed measurements at station 1.

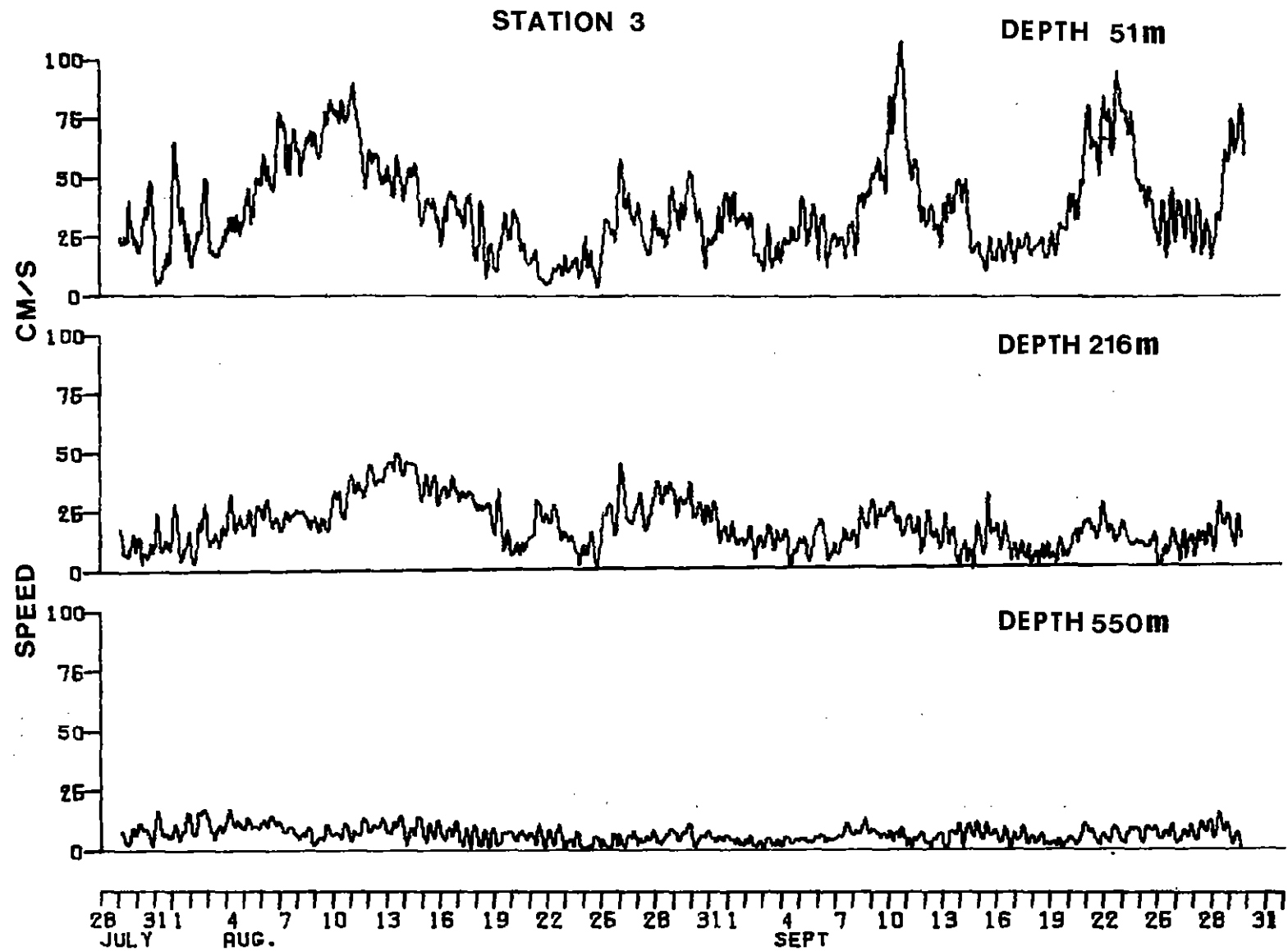


Figure 10b: Time series plots of the speed measurements at station 3.

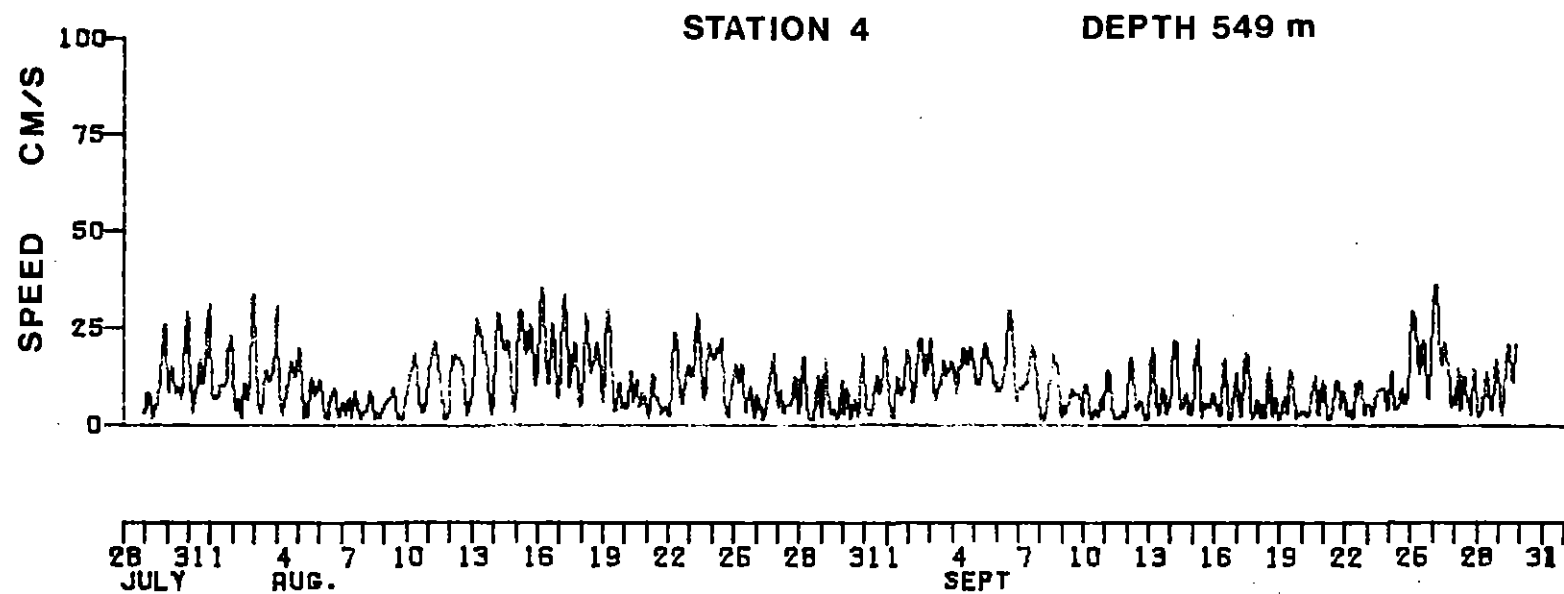


Figure 10c: Time series plot of the speed measurements at station 4.

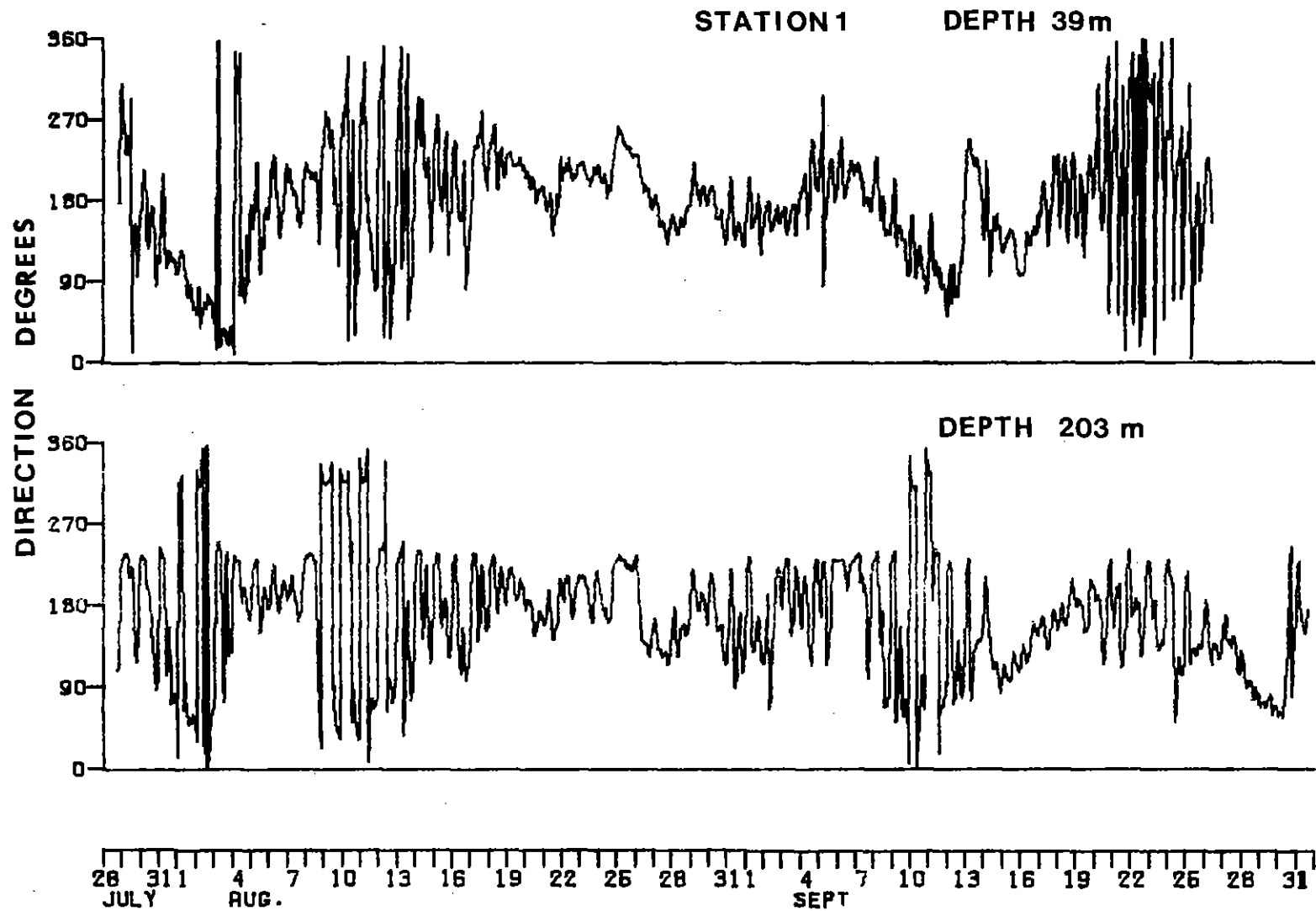


Figure 11a: Time series plots of the direction measurements at station 1.

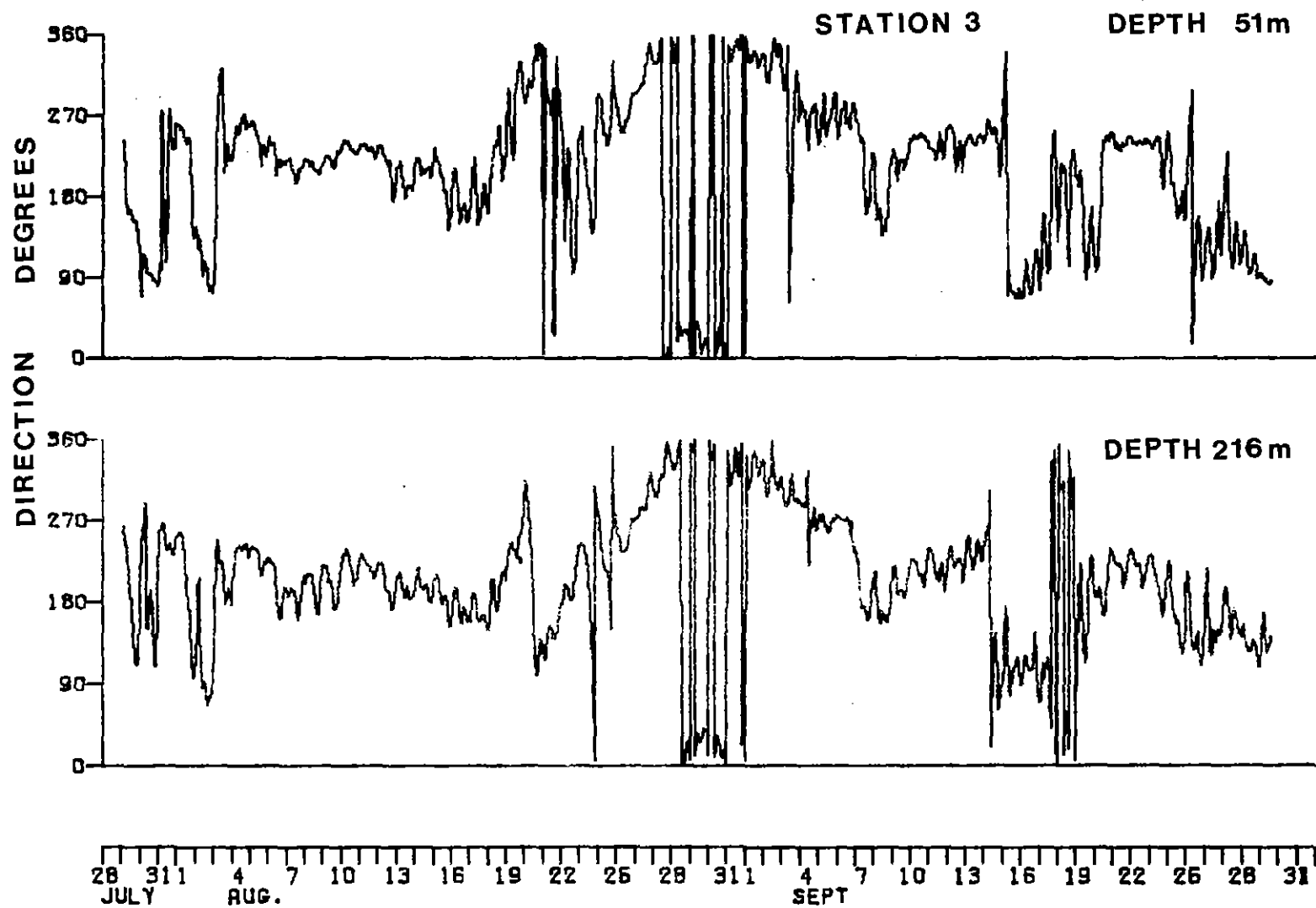


Figure 11b: Time series plots of the direction measurements at station 3.

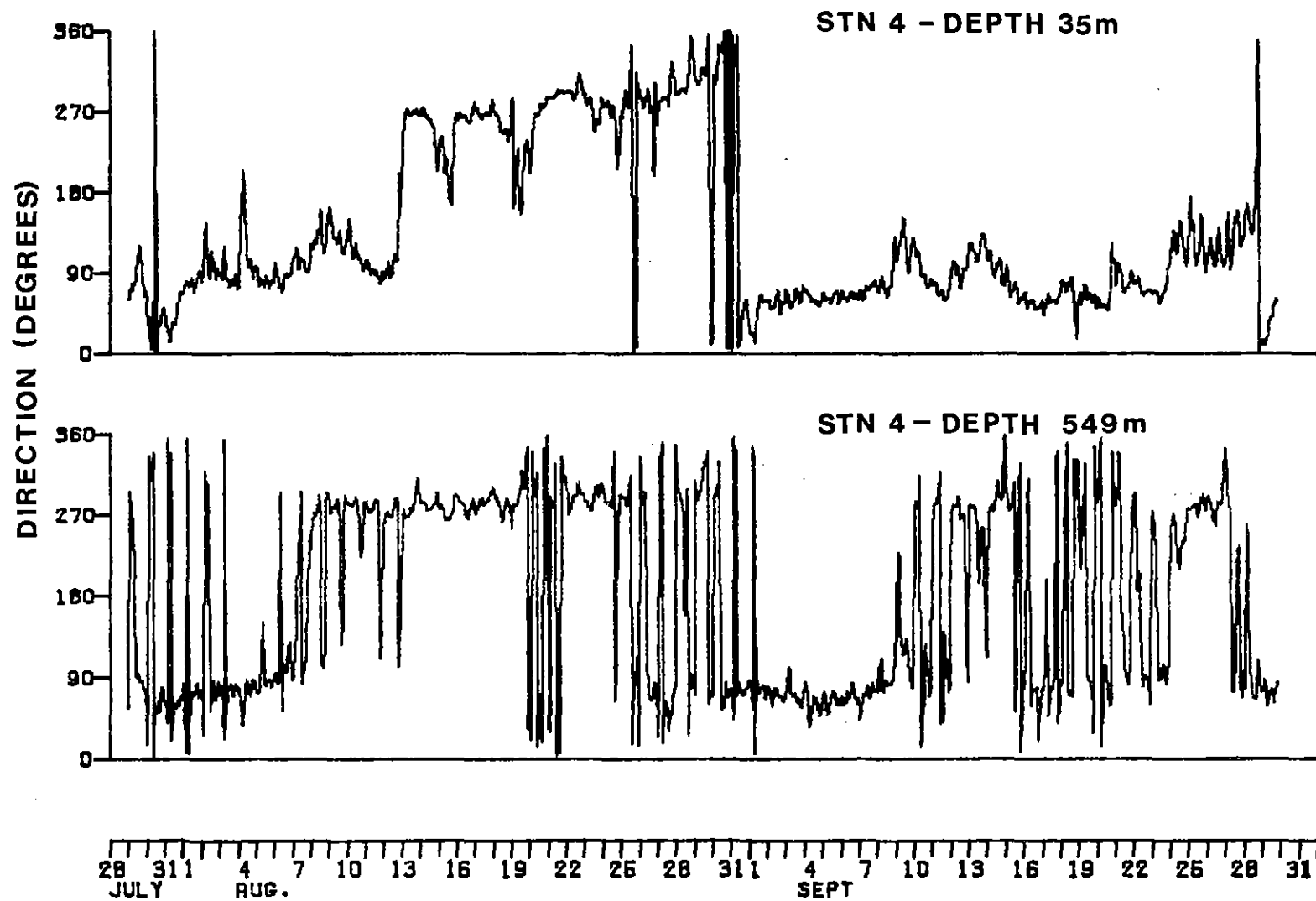


Figure 11c: Time series plots of the direction measurements at station 4.

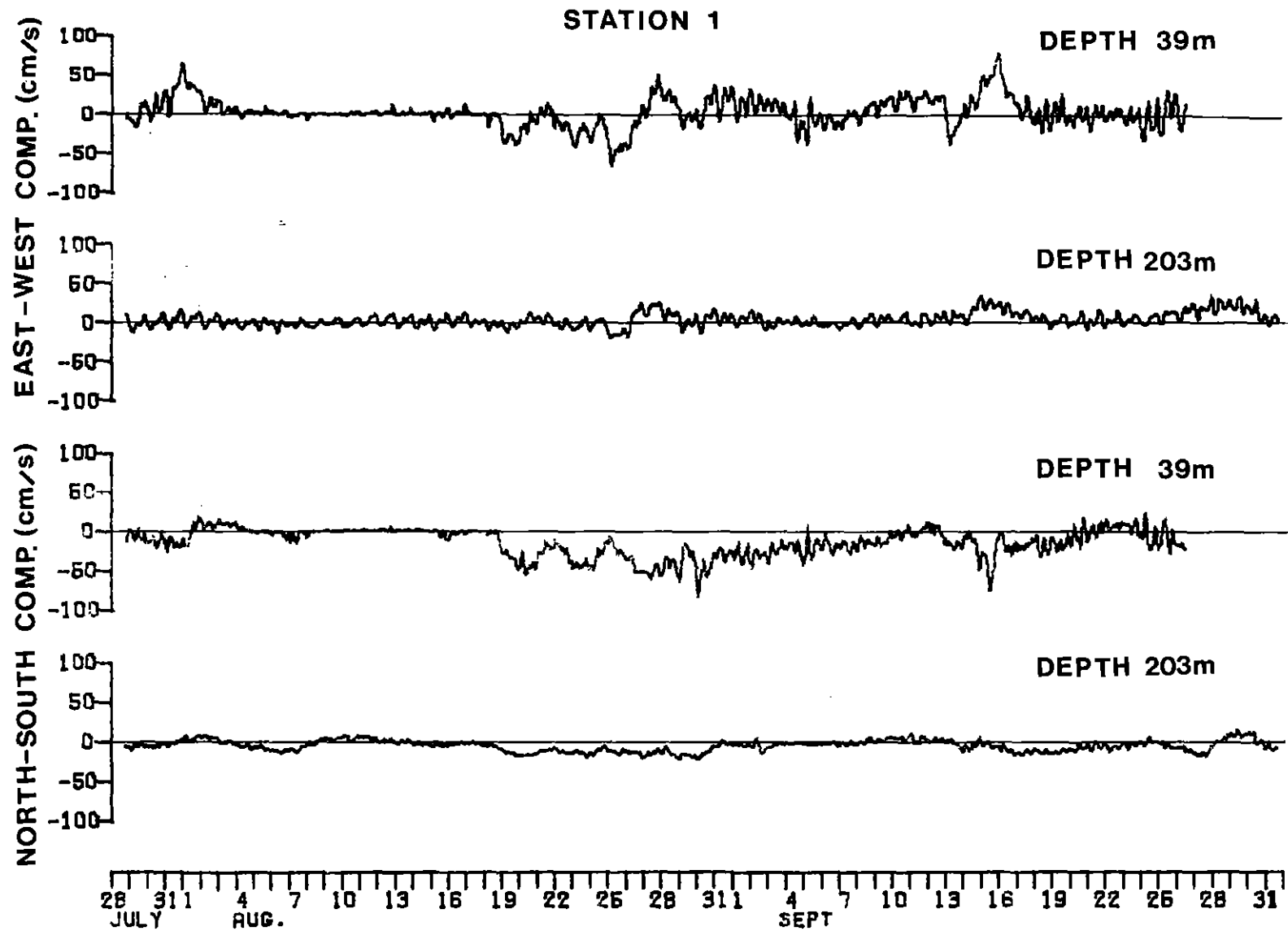


Figure 12a: Time series plots of the easterly and northerly current components at station 1.

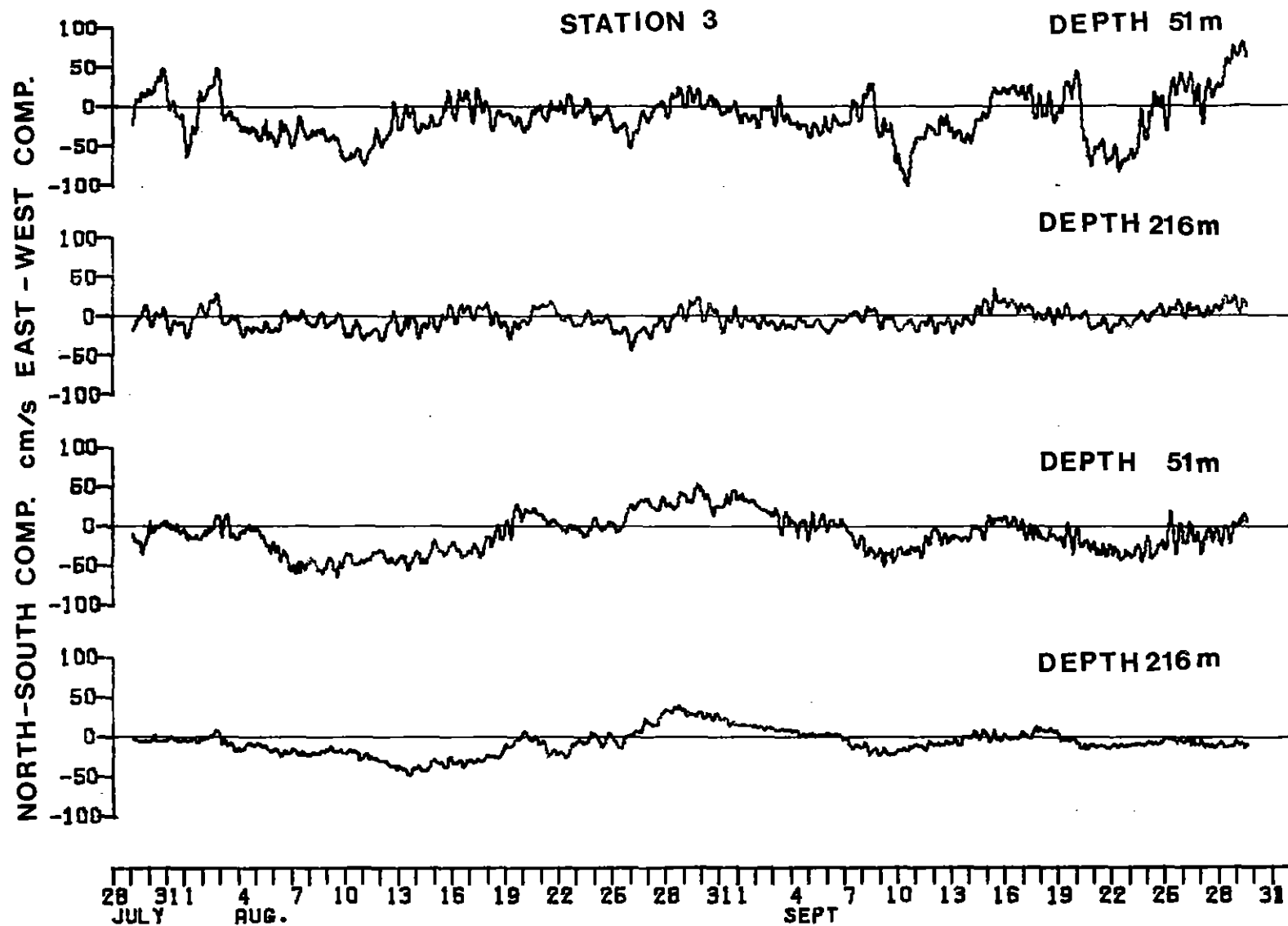


Figure 12b: Time series plots of the easterly and northerly current components at station 3.

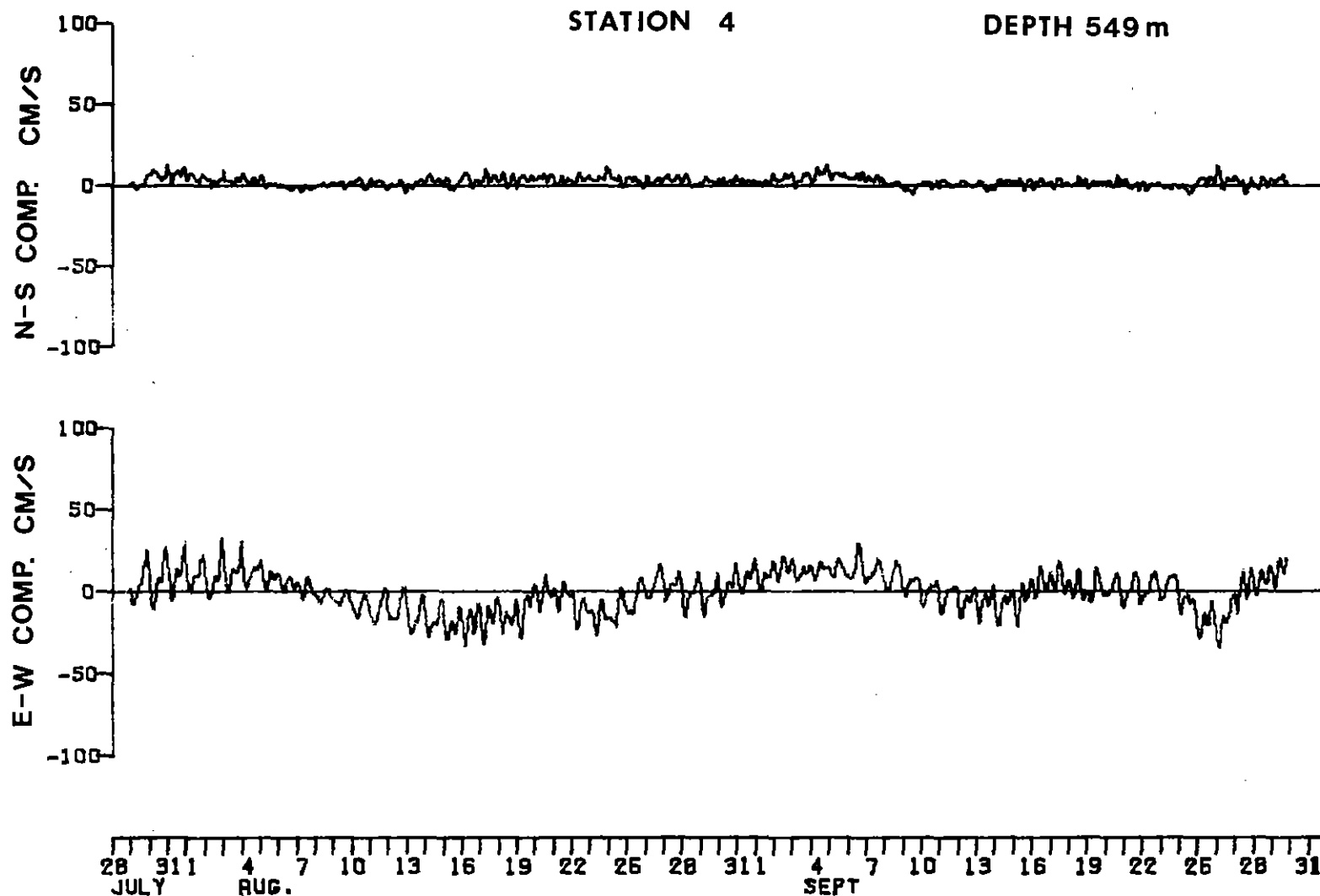


Figure 12c: Time series plots of the easterly and northerly current components at station 4.

are presented in Table 5 . The speeds decrease markedly with increasing depth; for example, at station 3, the speeds decrease from 37.4 ± 20.0 cm/s (mean \pm standard deviation) at 51 m depth to 20.1 ± 10.0 cm/s at 216 m depth to 7.4 cm/s ± 3.3 at 550 m depth. In addition the spectral character of the speeds recorded by the upper and mid-depth current meters the time series plots indicate large variations at periods of several days or longer, while in the 550 m currents the shorter period variations are more important; these shorter period variations are in large part due to diurnal and semi-diurnal tidal currents. Further discussion is left to section 4.2.2 where the results of harmonic and spectral analyses are presented.

Another interesting aspect of the speed data is the reduced average speeds measured at station 1 in comparison with those of station 3 for both the upper and middle current meters. While both stations are located in the middle of the sound, the more easterly station 1, has a mean speed of 24.3 cm/s at 39 m depth and 12.0 cm/s at 203m depth in comparison to mean speeds of 37.4 cm/s at 51m depth and 20.1 cm/s at 216m depth found at station 3. The histograms of the speed measurements, shown in Figure 13, reflect this difference as the histograms for station 3 show a greater range of recorded speeds than the histograms at station 1 at the level of the upper and middle current meters. The speeds measured by the deepest current meters (550m) have nearly identical average values and frequency distributions at stations 1 and 3 but are significantly larger at station 4, on the south side of the Sound.

The current directions appear to differ markedly according to the distance offshore. From the histograms of direction (figure 14) for the centre stations, the most common direction is southerly (station 2) and south-westerly (station 3) at the upper and middle current meters while the direction measurements at station 4 show a bimodal frequency distribution, being predominately easterly or westerly. At station 4, the upper current meter (depth 35m) has twice as many occurrences of easterly flow as those of westerly flow while at the deepest current meter (549m), the number of recordings of easterly and westerly currents are very nearly equal.

These observed current directions are in good agreement with the current patterns expected from earlier studies (section 2). The predominately southerly currents measured in the centre of the Sound are consistent with the hypothesis of the anti-clockwise gyre extending into eastern Lancaster Sound from Baffin Bay while the bimodal easterly and westerly current direction distribution at station 4 reflects the influence of the east-west orientation of Lancaster Sound on the currents near the side of the Sound. The fact that twice as many occurrences of easterly over westerly directions at the upper current meter were measured at station 4 suggests that a net eastward flow occurs here although this cannot be confirmed since no simultaneous speed measurements were obtained.

The histogram of the directions measured at station 1 at a depth of 203m, shows no measurements at directions between 250 degrees and 300 degrees. This is likely due to a faulty compass potentiometer in the instrument. Because of this, currents with directions in the range

Table 5a

The basic data statistics for station 1.

STATISTICS FOR STATION: LA1 INSTRUMENT 340/16 WITH 8006 RECORDS
 TIME OF FIRST RECORD: 18:50 28 JULY 1977 LAST RECORD: 13:00 26 SEPT 1977 GMT
 SAMPLING INTERVAL: 10 MINUTES LATITUDE: 74 05 30 LONGITUDE 81 11 00
 NOMINAL DEPTH: 39.0M

QUANTITY	UNITS	MEAN	STD.DEV.	MAXIMUM	MINIMUM
TEMPERATURE	DEG C	1.90	1.78	5.90	-1.54
SPEED	CM/S	24.33	18.87	95.39	1.50
N-S COMPONENT	CM/S	-16.20	18.19	26.23	-68.09
E-W COMPONENT	CM/S	.89	18.81	79.10	-71.50

STATISTICS FOR STATION: LA1 INSTRUMENT 360/5 WITH 9353 RECORDS
 TIME OF FIRST RECORD: 18:40 28 JULY 1977 LAST RECORD: 17:30 1 OCT. 1977 GMT
 SAMPLING INTERVAL: 10 MINUTES LATITUDE: 74 05 30 LONGITUDE 81 11 00
 NOMINAL DEPTH: 203.0M

QUANTITY	UNITS	MEAN	STD.DEV.	MAXIMUM	MINIMUM
TEMPERATURE	DEG C	-1.12	.37	.46	-1.58
SPEED	CM/S	11.96	6.97	38.40	1.50
N-S COMPONENT	CM/S	-7.04	7.31	14.08	-27.23
E-W COMPONENT	CM/S	2.51	9.08	37.42	-22.06

STATISTICS FOR STATION: LA1 INSTRUMENT 361/10 WITH 9353 RECORDS
 TIME OF FIRST RECORD: 18:40 28 JULY 1977 LAST RECORD: 17:30 1 OCT. 1977 GMT
 SAMPLING INTERVAL: 10 MINUTES LATITUDE: 74 05 30 LONGITUDE 81 11 00
 NOMINAL DEPTH: 554.0M

QUANTITY	UNITS	MEAN	STD.DEV.	MAXIMUM	MINIMUM
TEMPERATURE	DEG C	.97	.22	1.61	.07
SPEED	CM/S	7.29	4.22	23.23	1.50

Table 5b

The basic data statistics for station 3.

STATISTICS FOR STATION: LA3 INSTRUMENT 2697/1 WITH 9019 RECORDS
 TIME OF FIRST RECORD: 01:10 29 JULY 1977 LAST RECORD: 16:10 29 SEPT 1977 GMT
 SAMPLING INTERVAL: 10 MINUTES LATITUDE: 74 07 24 LONGITUDE 82 13 00
 NOMINAL DEPTH: 51.0M

QUANTITY	UNITS	MEAN	STD.DEV.	MAXIMUM	MINIMUM
TEMPERATURE	DEG C	1.59	1.33	5.28	-1.59
CONDUCTIVITY	MMHO/CM	28.15	1.16	31.96	25.42
SPEED	CM/S	37.41	19.97	111.54	1.50
N-S COMPONENT	CM/S	-12.93	24.27	51.33	-70.05
E-W COMPONENT	CM/S	-13.90	29.13	83.93	-105.46
SALINITY	MILLE	32.08	.42	33.39	31.01
SIGMA-T		25.68	.33	27.54	24.01

STATISTICS FOR STATION: LA3 INSTRUMENT 2700/1 WITH 9019 RECORDS
 TIME OF FIRST RECORD: 01:10 29 JULY 1977 LAST RECORD: 16:10 29 SEPT 1977 GMT
 SAMPLING INTERVAL: 10 MINUTES LATITUDE: 74 07 24 LONGITUDE 82 13 00
 NOMINAL DEPTH: 216.0M

QUANTITY	UNITS	MEAN	STD.DEV.	MAXIMUM	MINIMUM
TEMPERATURE	DEG C	-1.35	.18	-5.58	-1.65
CONDUCTIVITY	MMHO/CM	26.94	.21	27.84	26.49
SPEED	CM/S	20.14	10.00	51.90	1.50
N-S COMPONENT	CM/S	-9.15	15.69	38.87	-50.56
E-W COMPONENT	CM/S	-4.85	12.34	35.37	-46.24
SALINITY	MILLE	33.56	.21	33.96	33.23
SIGMA-T		27.02	.17	27.50	26.67

STATISTICS FOR STATION: LA3 INSTRUMENT 2703/1 WITH 9019 RECORDS
 TIME OF FIRST RECORD: 01:10 29 JULY 1977 LAST RECORD: 16:10 29 SEPT 1977 GMT
 SAMPLING INTERVAL: 10 MINUTES LATITUDE: 74 07 24 LONGITUDE 82 13 00
 NOMINAL DEPTH: 550.0M

QUANTITY	UNITS	MEAN	STD.DEV.	MAXIMUM	MINIMUM
TEMPERATURE	DEG C	.99	.23	1.82	.15
CONDUCTIVITY	MMHO/CM	29.65	.21	30.35	28.80
SPEED	CM/S	7.43	3.29	19.14	1.50
SALINITY	MILLE	34.36	.06	34.57	34.11
SIGMA-T		27.56	.05	27.73	27.35

Table 5c

The basic data statistics for station 4.

STATISTICS FOR STATION: LA4 INSTRUMENT 2698/1 WITH 9076 RECORDS
 TIME OF FIRST RECORD: 22:00 28 JULY 1977 LAST RECORD: 22:40 29 SEPT 1977 GMT
 SAMPLING INTERVAL: 10 MINUTES LATITUDE: 73 51 00 LONGITUDE 62 13 00
 NOMINAL DEPTH: 35.0M

QUANTITY	UNITS	MEAN	STD.DEV.	MAXIMUM	MINIMUM
TEMPERATURE	DEG C	.65	1.51	5.59	-1.61
CONDUCTIVITY	MMHO/CM	27.46	1.33	32.10	24.95
SALINITY	MILLE	32.19	.46	33.57	30.83
SIGMA-T		25.81	.36	29.43	23.19

STATISTICS FOR STATION: LA4 INSTRUMENT 2701/1 WITH 9076 RECORDS
 TIME OF FIRST RECORD: 22:00 28 JULY 1977 LAST RECORD: 22:40 29 SEPT 1977 GMT
 SAMPLING INTERVAL: 10 MINUTES LATITUDE: 73 51 00 LONGITUDE 62 13 00
 NOMINAL DEPTH: 200.0M

QUANTITY	UNITS	MEAN	STD.DEV.	MAXIMUM	MINIMUM
TEMPERATURE	DEG C	-1.35	.20	.22	-1.62
CONDUCTIVITY	MMHO/CM	27.17	.14	28.28	26.31
SALINITY	MILLE	33.88	.14	34.16	33.43
SIGMA-T		27.28	.12	28.60	26.30

STATISTICS FOR STATION: LA4 INSTRUMENT 2704/1 WITH 9075 RECORDS
 TIME OF FIRST RECORD: 22:20 28 JULY 1977 LAST RECORD: 22:40 29 SEPT 1977 GMT
 SAMPLING INTERVAL: 10 MINUTES LATITUDE: 73 51 00 LONGITUDE 62 13 00
 NOMINAL DEPTH: 549.0M

QUANTITY	UNITS	MEAN	STD.DEV.	MAXIMUM	MINIMUM
TEMPERATURE	DEG C	.93	.21	1.60	.34
CONDUCTIVITY	MMHO/CM	29.63	.19	30.44	29.05
SPEED	CM/S	10.50	7.17	37.34	1.50
N-S COMPONENT	CM/S	2.27	3.06	16.08	-6.63
E-W COMPONENT	CM/S	-5.53	12.12	36.48	-36.36
SALINITY	MILLE	34.40	.04	34.48	34.27
SIGMA-T		27.59	.03	27.67	27.37

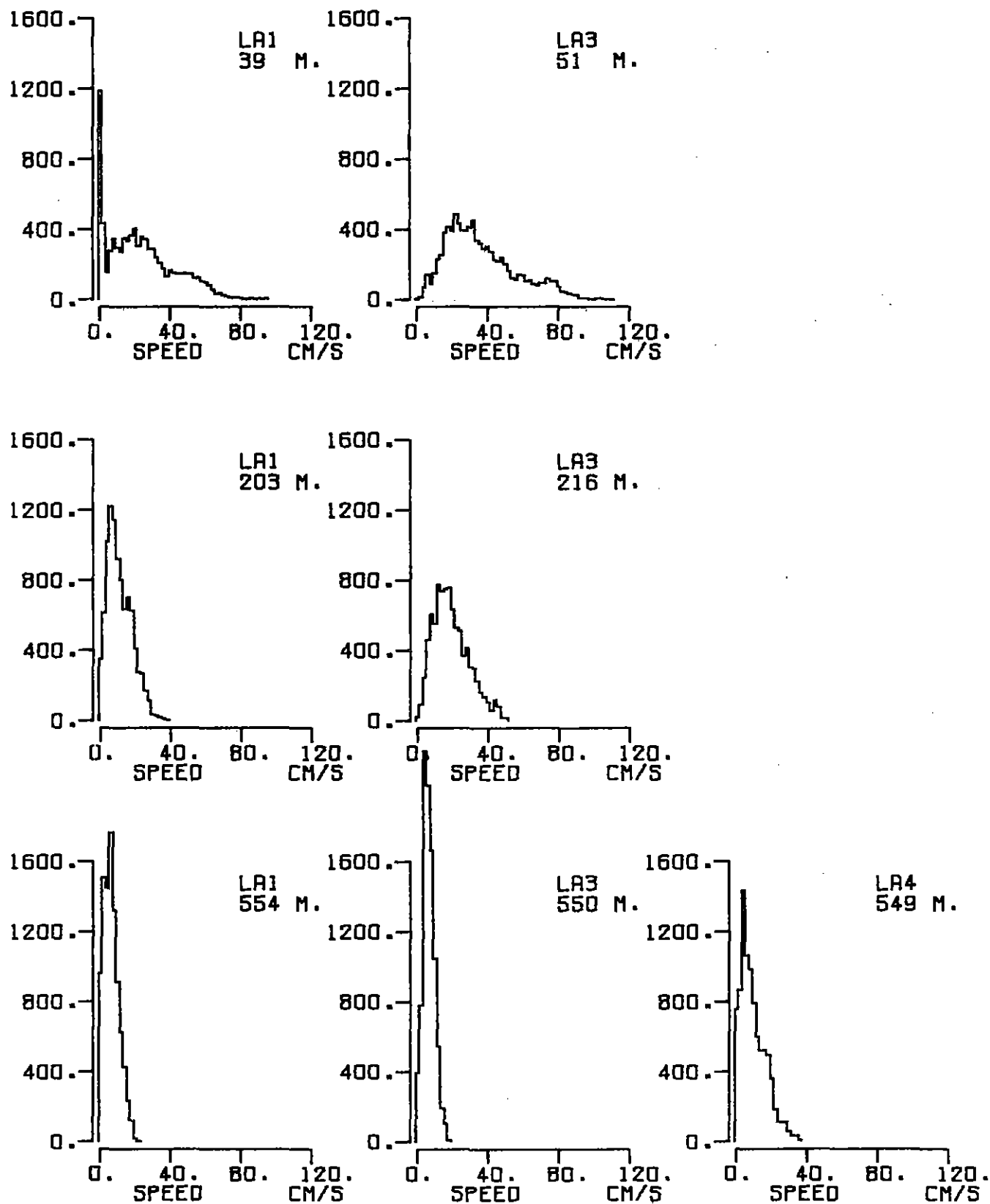


Figure 13: Histograms of the current speeds.

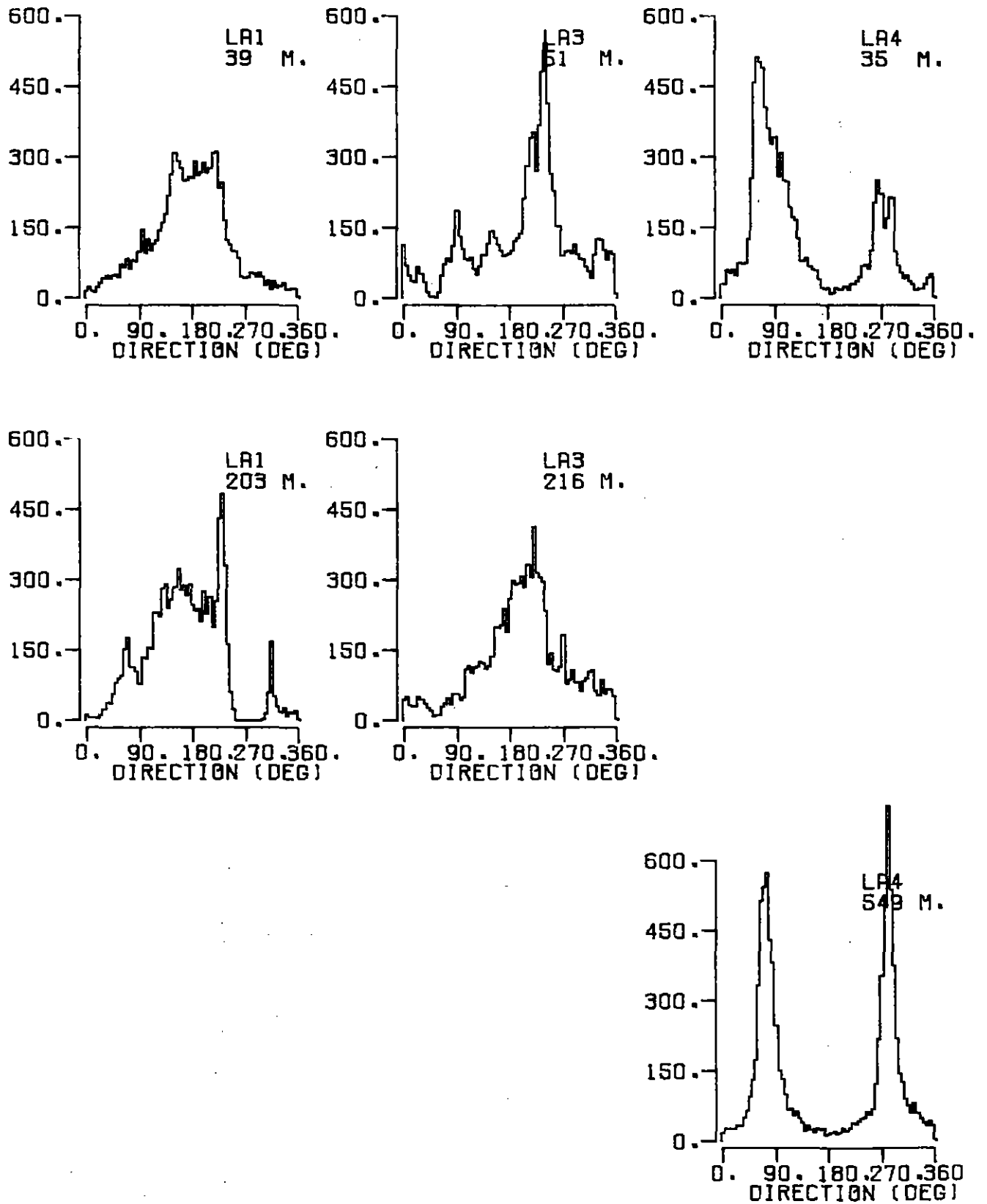


Figure 14: Histograms of the current direction.

of 250 to 300 degrees were recorded as approximately 240 degrees or 315 degrees. In discussing the results for this current meter, this probable error should be borne in mind.

A striking feature of the direction measurements is the similarity in the time variations of the current directions between the upper and middle level current meters, particularly at station 3 (see Figure 11.) At this station, the directions at 51 m and 216m change in a very similar fashion, particularly in those long period variations which dominate the time series record. At station 1, the agreement is not as good, partly because of the compass error of the current meter at 216 m depth. Apparently this similarity in the directions does not extend to deeper water since little agreement is found at station 4 between the direction measurements at 35m and 549m.

The progressive vector diagrams for each current meter that measured both speed and direction are shown in Figure 15. These diagrams indicate that the currents at station 1 set southerly with no significant reversals of the flow. However at station 3, while the current was southwesterly most of the time, it showed more variability. In particular from Aug.25 (day of the year 237) to Sept 4 (day of the year 247), the current was generally northerly at 51m and 216 m depth. The station 4 currents at a depth of 549m show large variations in the east-west component with much smaller north-south variations. Over the entire record, the east-west component has a standard deviation of 12.1 cm/s as compared to a standard deviation of 3.1 cm/s in the north-south component. The east-west flow appears to be oscillatory on both diurnal and semi-diurnal time scales and over longer periods with the result that the average east-west component was only -0.5 cm/s. However, in the component of the current perpendicular to the shoreline, a weak but persistent northerly flow with an average speed of 2.3 cm/s was measured.

4.2.2 Spectral and Harmonic Analysis

In this section, we examine the variations of the currents using the results of spectral and harmonic analyses. The spectral analysis was computed from the currents recorded between 0000 July 30 and 2300 Sept. 25 1977, a period of 58 days. The power spectral densities of the current components (Figure 16) and the speeds (Figure 17) are computed with 10 degrees of freedom to improve statistical reliability and are corrected for the losses due to the application of a filter used to decimate the data from 10 minute to hourly samples.

The power spectra of all of the speed and current component time series have the same prominent features; the largest spectral levels occurring at the lowest frequencies and the presence of peaks in the spectrum at the diurnal and semi-diurnal frequency bands. At frequencies greater than 2 cycles per day, the spectral levels decrease as the frequency increases with the result that contributions to the total variance from frequencies greater than 5 cycles per day are negligible. Because of this, we limit the spectral plots to frequencies less than 5 cycles per day.

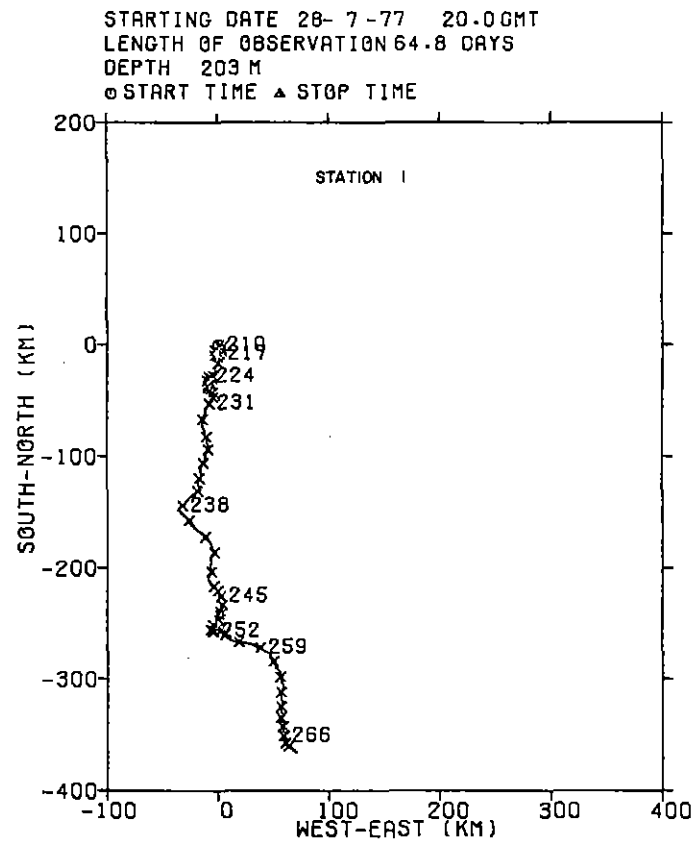
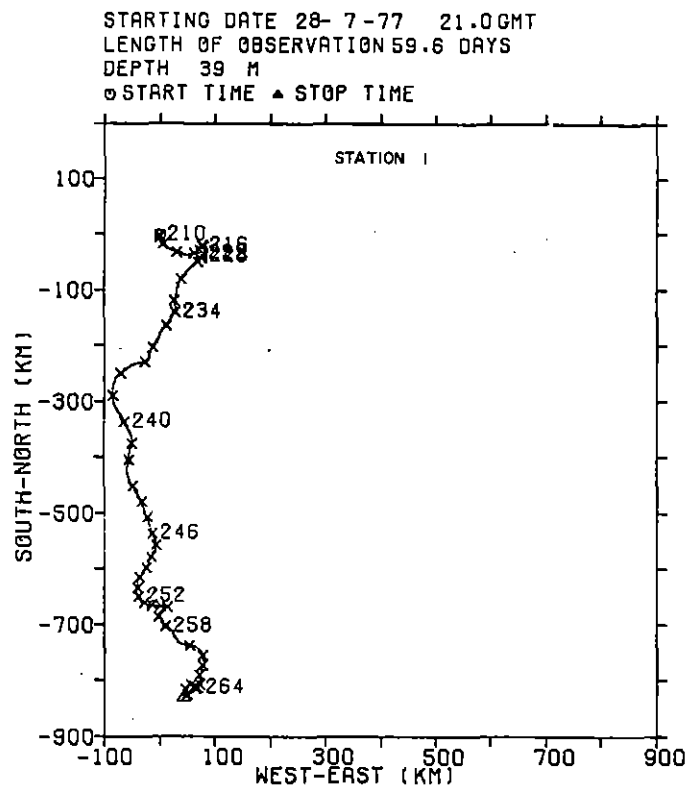


Figure 15a: Progressive vector diagrams of the currents at station I.

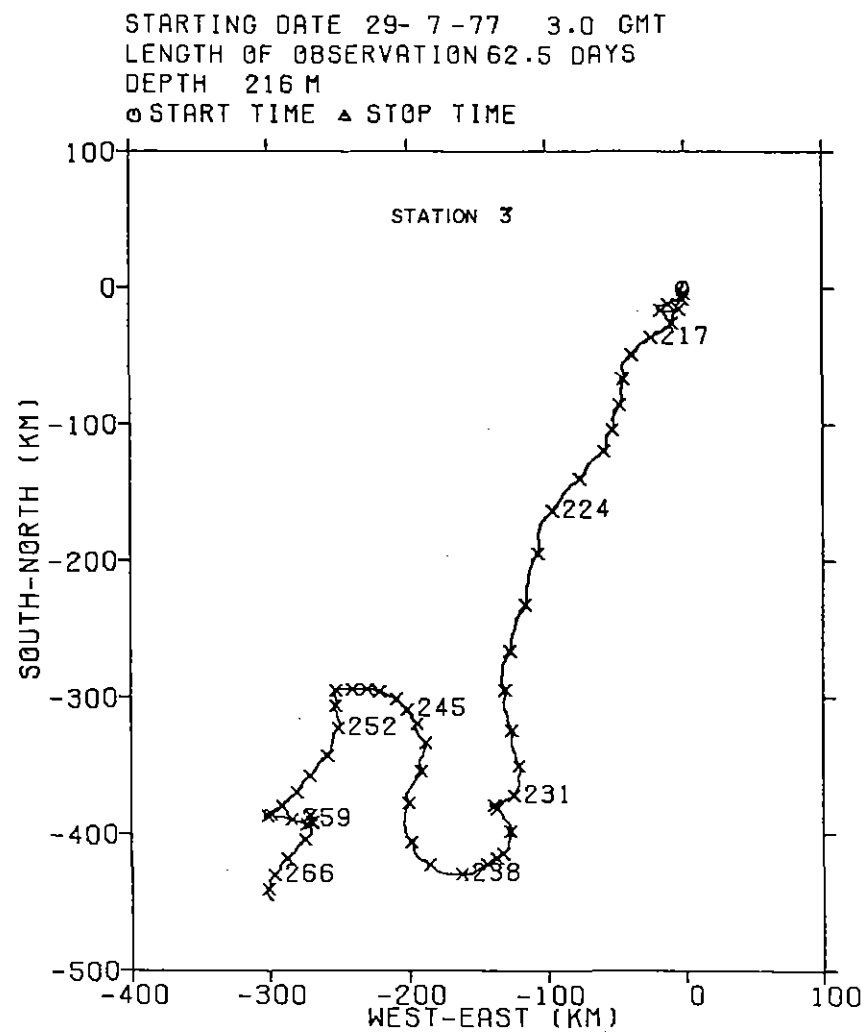
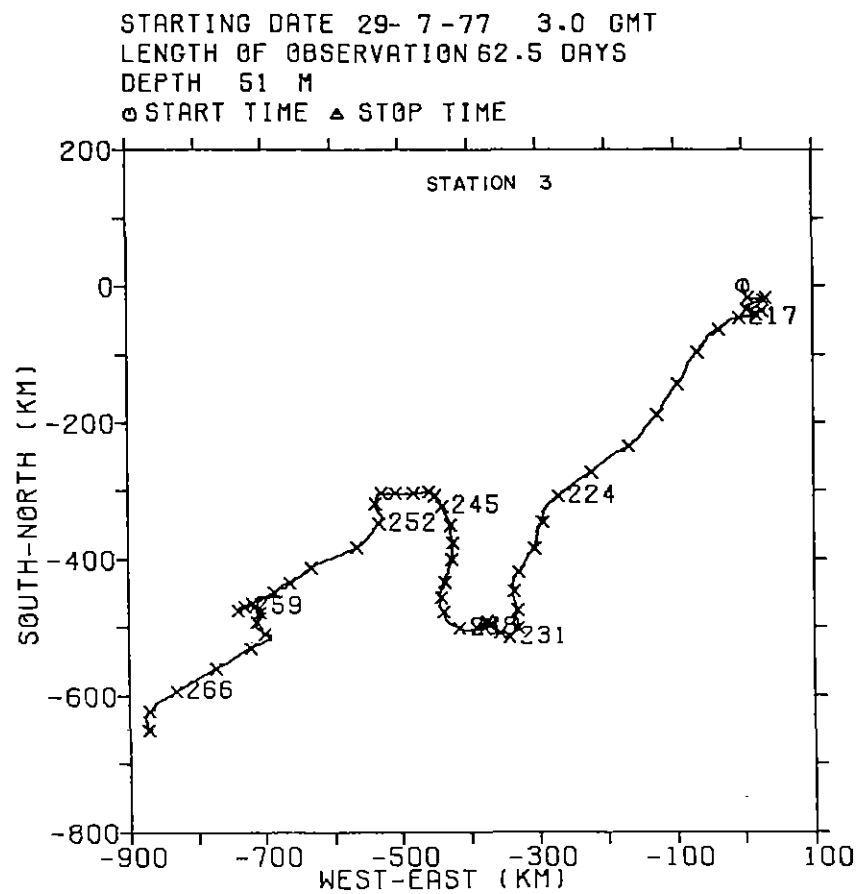


Figure 15b: Progressive vector diagrams of the currents at station 3.

STARTING DATE 29- 7 -77 0.0 GMT
 LENGTH OF OBSERVATION 62.9 DAYS
 DEPTH 549 M
 ○ START TIME ▲ STOP TIME

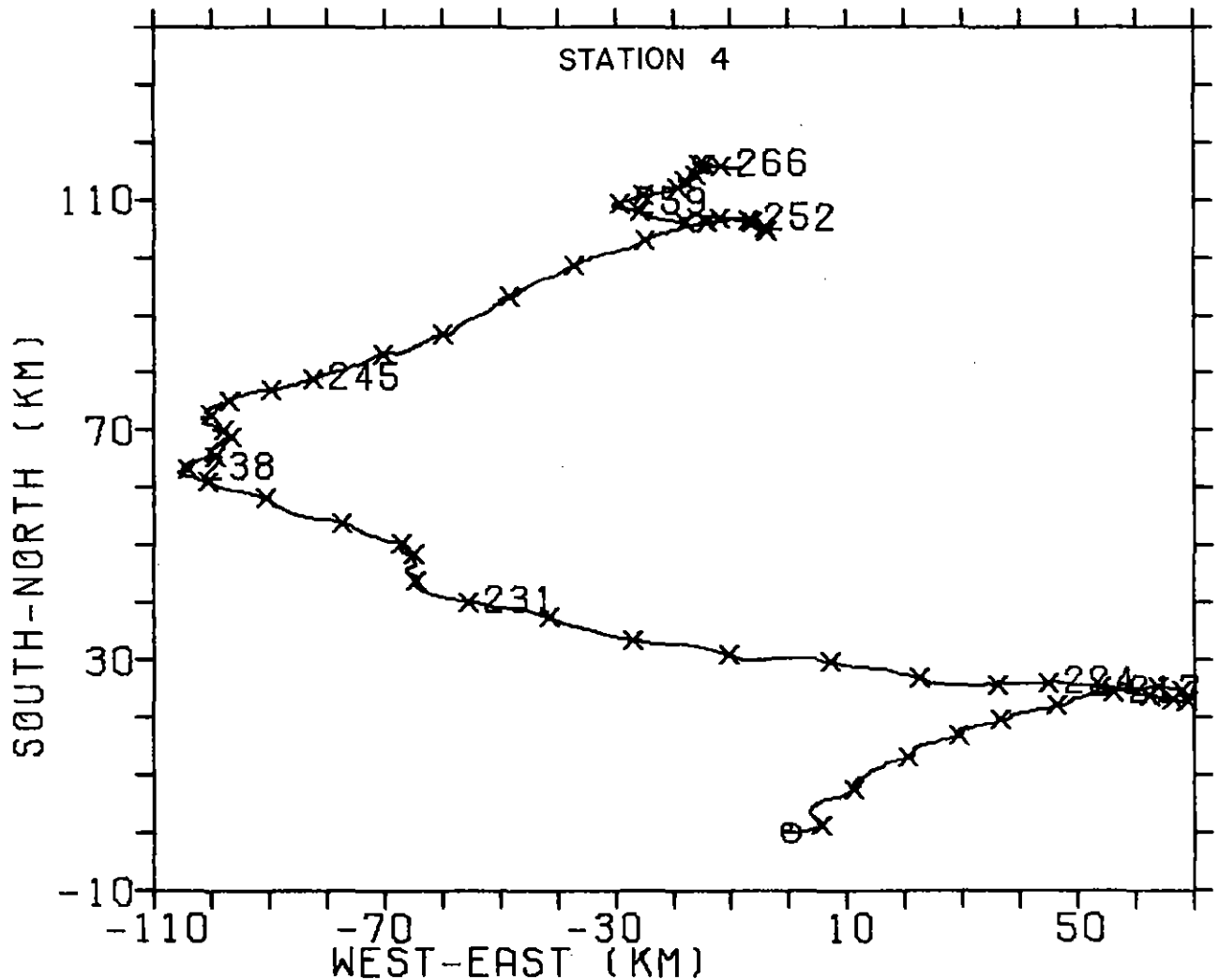


Figure 15c: Progressive vector diagram of the current at station 4 - 549 m depth.

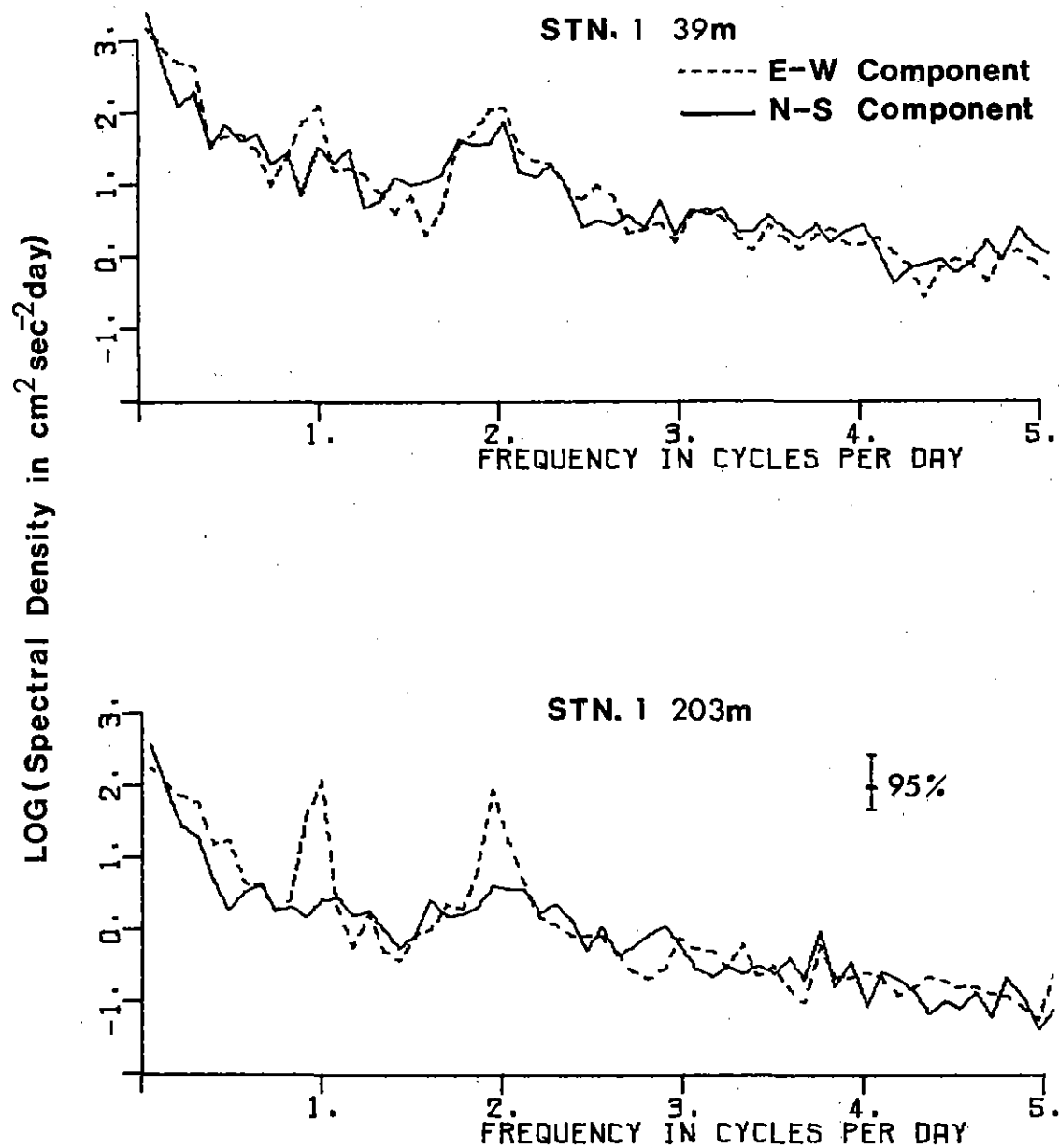


Figure 16a: Power spectral densities of the easterly and northerly current components at station 1.

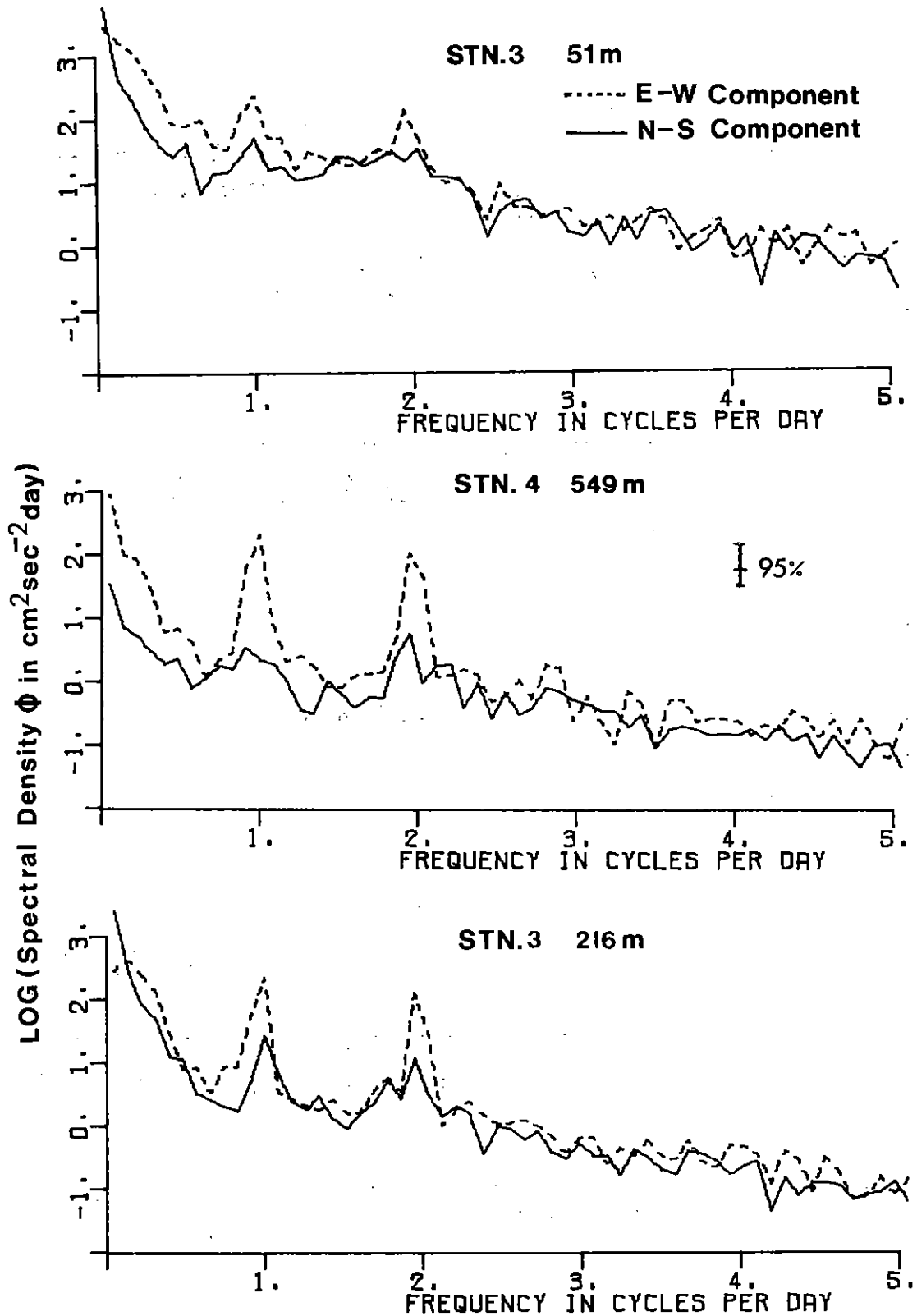


Figure 16b: Power spectral densities of the easterly and northerly current components at station 3.

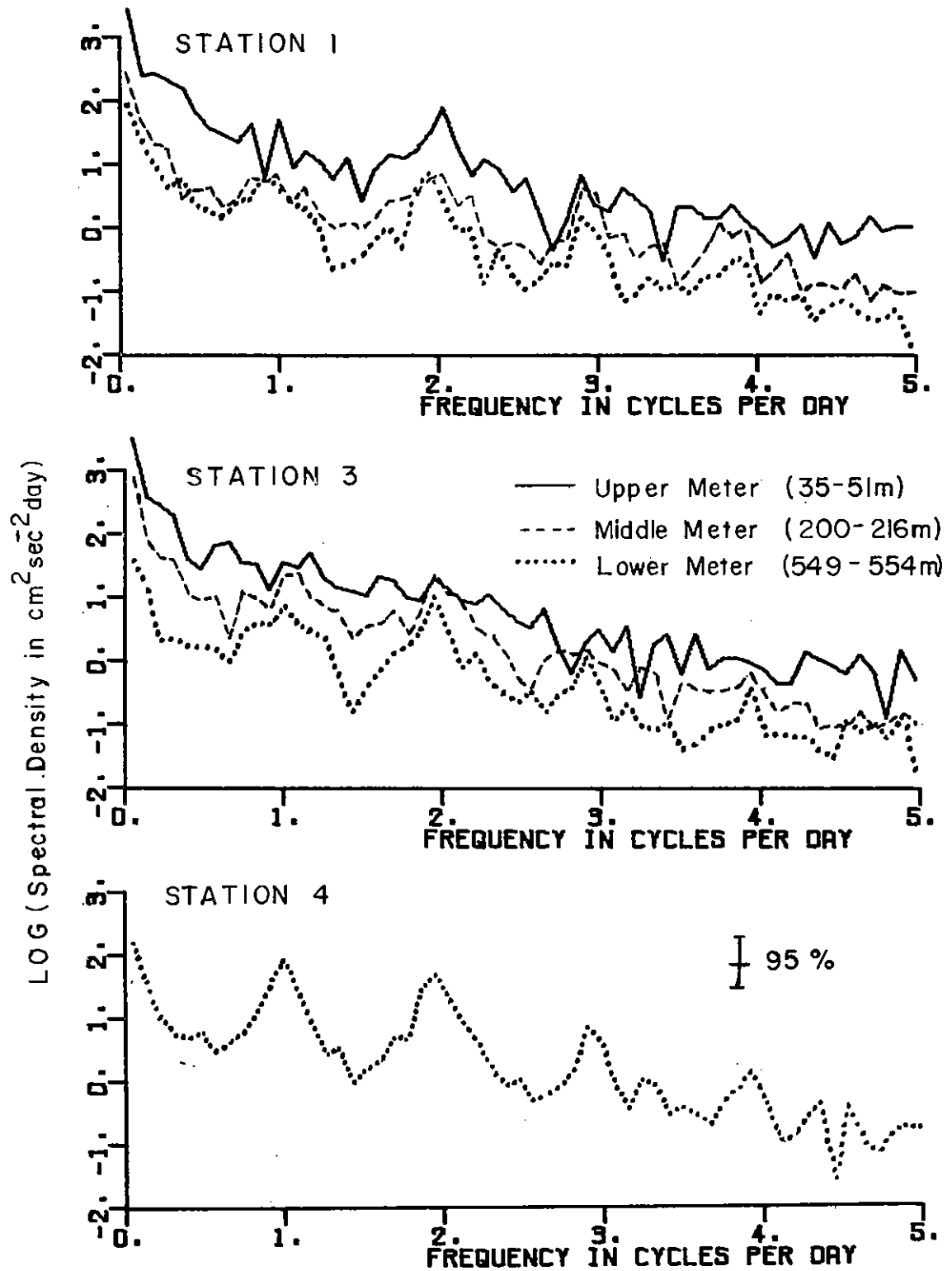


Figure 17: Power spectral densities of the current speeds.

Table 6

Harmonic analysis results for currents at station 1 - 39 m depth over the period 0300 July 29 to 1500 Sept. 25 GMT. The speed (frequency) of each constituent is given in cycles per hour while the lengths of the semi-minor axes of the current ellipse are in cm/s.

NAME	SPEED	MAJOR	MINOR	INC	G	G+	G-
1 Z0	.00000000	15.811	.001	93.9	180.0	86.1	273.9
2 MM	.00151215	8.054	3.090	80.1	195.4	135.4	255.5
3 MSF	.00282193	12.317	-1.094	174.7	212.6	37.9	27.3
4 ALP1	.03439657	1.953	.098	92.8	257.8	165.0	350.6
5 ZQ1	.03570635	2.089	.492	34.4	122.0	87.6	156.4
6 Q1	.03721850	.039	.171	25.0	124.4	99.4	149.3
7 Q1	.03873065	3.687	-.071	1.4	48.5	47.1	49.9
8 M01	.04026859	1.565	-1.018	171.4	249.7	78.3	61.1
9 K1	.04178075	5.050	-.065	169.0	313.5	144.6	122.5
10 J1	.04329290	1.731	.476	37.7	173.6	135.8	211.3
11 O01	.04483084	2.135	-.790	115.9	36.3	280.4	152.2
12 UPS1	.04634299	2.013	1.275	50.6	333.0	282.4	23.6
13 EPS2	.07617732	.819	-.071	76.5	155.2	78.7	231.8
14 M02	.07768947	.575	-.314	155.9	141.8	345.9	297.7
15 N2	.07899925	2.079	-1.275	174.5	111.0	296.5	285.4
16 M2	.08051140	3.506	-.261	16.8	310.0	293.2	326.9
17 L2	.08202355	1.518	-1.060	40.9	149.6	108.6	190.5
18 S2	.08333333	3.891	-2.447	144.9	140.6	355.8	285.5
19 L1A2	.08507364	4.703	-3.531	30.1	26.9	356.8	57.0
20 M03	.11924206	.875	.035	91.8	59.1	327.3	151.0
21 M3	.12076710	.521	.036	71.2	193.8	122.6	265.0
22 MK3	.12229215	.585	-.239	43.9	320.6	276.6	4.5
23 SK3	.12511408	.312	.057	80.4	163.9	103.5	224.4
24 MN4	.15951065	.461	-.102	16.8	242.7	223.9	261.5
25 M4	.16102280	.366	-.174	95.6	319.9	224.3	55.5
26 SN4	.16235258	.305	-.121	39.1	101.1	21.0	181.2
27 MS4	.16384473	.224	-.102	19.7	219.6	199.9	239.2
28 S4	.16666667	.480	-.351	40.7	76.3	36.1	117.6
29 ZMK5	.20280355	.188	.037	24.4	186.1	161.7	219.4
30 ZSK5	.20844741	.312	-.025	180.5	225.1	64.6	25.6
31 ZMK6	.24002205	.212	-.045	100.7	90.9	350.2	191.6
32 M6	.24153420	.253	-.115	42.2	220.7	178.5	262.9
33 ZMS6	.24435613	.270	-.115	34.7	42.6	7.9	77.4
34 ZSM6	.24717807	.342	.067	30.6	312.2	231.6	32.7
35 SMK7	.28331495	.170	-.014	110.7	354.3	243.6	105.1
36 M6	.32204560	.198	.007	64.1	132.5	68.4	196.5

Table 7

Harmonic analysis results for currents at station 1 - 203 m depth over the period 1500 July 29 to 0300 Sept. 29 GMT. The speed (frequency) of each constituent is given in cycles per hour while the lengths of the semi-major and semi-minor axes of the current ellipse are in cm/s.

NAME	SPEED	MAJOR	MINOR	LNC	G	G+	G-
1 ZU	.00000000	7.371	.000	105.8	130.0	74.2	285.8
2 MM	.00151215	5.715	.233	101.0	198.5	97.5	299.5
3 MSF	.00262193	4.976	-1.206	21.0	8.5	347.4	29.5
4 ALP1	.03439657	.496	-.275	35.8	265.5	229.8	301.3
5 ZU1	.03570635	.606	-.033	160.5	357.2	196.7	157.6
6 J1	.03721850	.413	-.056	169.4	141.7	332.3	311.2
7 O1	.03873065	2.879	.092	3.0	55.5	52.5	58.5
8 NO1	.04026859	.627	.059	4.1	55.5	51.4	59.6
9 K1	.04178075	4.756	.143	1.4	132.7	131.3	134.1
10 J1	.04329296	.585	-.001	24.7	53.7	29.0	78.4
11 O01	.04483084	1.410	-.115	104.3	43.2	296.9	147.6
12 UPS1	.04634299	.504	-.333	5.6	231.5	225.7	237.3
13 EPS2	.07617732	.437	-.340	5.5	308.0	302.5	313.5
14 MU2	.07768947	.154	-.091	94.0	149.8	55.7	243.8
15 N2	.07899925	.648	-.194	157.3	69.6	272.3	226.9
16 M2	.08051140	3.977	-.206	4.6	280.1	275.5	284.6
17 L2	.08202355	.310	.094	66.5	350.3	261.9	78.8
18 S2	.08353333	1.734	-.111	5.3	332.7	327.4	337.9
19 ETA2	.08567364	1.105	-.735	59.9	82.4	51.5	113.3
20 MO3	.11924206	.146	-.103	142.8	265.4	122.7	48.2
21 M3	.12076710	.288	-.123	62.5	295.9	233.3	353.4
22 MK3	.12229215	.243	-.105	67.3	149.3	62.0	236.7
23 SK3	.12511408	.206	-.147	42.4	359.7	317.3	42.1
24 MN4	.15951065	.061	-.031	25.6	2.5	336.7	28.3
25 M4	.16102280	.083	-.031	171.3	131.8	320.6	303.1
26 SN4	.16233258	.125	.041	126.1	256.8	130.7	22.8
27 MS4	.16384473	.214	-.057	107.1	152.0	44.9	259.1
28 S4	.16666667	.138	-.013	2.9	82.7	79.8	85.6
29 ZMK5	.20280355	.158	-.072	69.8	50.3	340.5	120.2
30 ZSK5	.20844741	.054	.022	73.9	355.4	281.5	69.3
31 ZMNO	.24002205	.047	-.017	111.1	346.6	235.5	97.6
32 MO	.24153420	.105	-.029	36.4	99.9	63.5	136.4
33 ZMS6	.24435613	.053	.037	153.9	36.3	242.5	190.2
34 ZSM6	.24717807	.095	.037	99.9	2.5	262.6	102.4
35 ZMK7	.28331495	.122	-.026	40.7	105.6	64.9	146.3
36 M8	.32204560	.051	-.003	15.7	36.2	20.5	52.0

Table 8

Harmonic analysis results for currents at station 3-51 m depth over the period 1500 July 29 to 0300 Sept. 29 GMT. The speed (frequency) of each constituent is given in cycles per hour while the lengths of the semi-major and semi-minor axes of the current ellipse are in cm/s.

NAME	SPEED	MAJOR	MINOR	INC	G	G+	G-
1 Z0	.000000000	21.534	.000	42.1	180.0	137.9	222.1
2 MM	.00151215	18.737	1.661	52.7	52.7	.0	105.4
3 MSF	.00282193	21.739	3.570	37.0	55.4	18.4	92.3
4 ALP1	.03439657	1.683	-.543	34.8	257.1	222.4	291.9
5 2Q1	.03570635	1.276	-.126	72.0	304.5	232.4	16.5
6 Q1	.03721850	2.442	-1.405	41.4	247.6	206.2	289.1
7 O1	.03873065	4.034	.563	151.7	215.5	63.7	7.2
8 NO1	.04026859	.484	.141	86.8	109.8	22.9	196.6
9 K1	.04178075	6.675	1.529	165.0	301.5	136.5	106.5
10 J1	.04329290	1.407	-.422	122.6	144.1	21.5	266.7
11 OO1	.04483084	3.605	-.734	28.0	166.6	138.6	194.5
12 UPS1	.04634299	2.155	.232	50.4	179.0	128.6	229.3
13 EPS2	.07617732	.633	-.225	166.4	317.5	151.1	123.9
14 MU2	.07768947	1.364	-.639	131.5	197.5	66.0	329.1
15 N2	.07899925	1.849	-.903	24.2	291.9	267.7	316.1
16 M2	.08051140	4.340	.629	10.2	284.3	274.2	294.5
17 L2	.08202355	.747	-.078	56.6	128.9	72.2	185.5
18 S2	.08333333	2.516	.449	6.6	327.2	320.6	333.8
19 ETA2	.08507364	3.593	-2.036	72.2	12.3	300.1	84.5
20 MO3	.11924206	.471	.224	22.9	355.6	332.7	13.5
21 M3	.12076710	.553	-.090	141.4	175.3	33.9	316.7
22 MK3	.12229215	.545	-.093	69.6	14.2	304.6	83.9
23 SK3	.12511408	.442	.310	13.5	37.6	24.2	51.1
24 MN4	.15951065	.269	-.010	10.6	180.4	169.8	191.0
25 M4	.16102280	.229	.058	74.5	169.0	94.4	243.5
26 SN4	.16233258	.512	-.102	151.7	114.0	322.2	265.7
27 MS4	.16384475	.261	.034	111.1	263.0	151.9	14.0
28 S4	.16666667	.256	-.103	171.0	314.3	143.2	125.3
29 2MK5	.20280355	.154	-.040	41.4	34.3	352.9	75.7
30 2SK5	.20844741	.194	.033	77.0	261.3	184.3	338.3
31 2MN6	.24002205	.233	.032	118.9	144.6	25.7	263.5
32 M6	.24153420	.199	-.011	162.3	321.5	159.3	123.8
33 2MS6	.24435613	.306	.121	59.8	177.5	117.7	237.3
34 2SM6	.24717807	.157	.045	16.3	130.2	113.8	146.5
35 3MK7	.28331495	.199	-.013	46.8	187.0	140.2	233.8
36 M8	.32204560	.156	.017	108.2	5.1	257.0	113.3

Table 9

Harmonic analysis results for currents at station 3-216 m depth over the period 1500 July 29 to 0300 Sept. 29 GMT. The speed (frequency) of each constituent is given in cycles per hour while the lengths of the semi-major and semi-minor axes of the current ellipse are in cm/s.

NAME	SPEED	MAJOR	MINOR	INC	G	G+	G-
1 ZU	.00000000	11.480	.000	63.6	180.0	116.4	243.6
2 MM	.00151215	12.265	2.583	82.4	69.5	347.1	152.0
3 MSF	.00282193	7.350	.496	42.5	64.7	22.1	107.2
4 ALP1	.03439657	1.121	.219	1.0	206.8	205.8	207.7
5 2Q1	.03570635	.579	.198	3.1	164.8	161.7	167.9
6 Q1	.03721850	.554	-.253	71.6	221.6	150.0	293.2
7 O1	.03873065	3.570	.211	170.3	230.8	60.4	41.1
8 NO1	.04026859	.566	-.372	131.8	209.2	77.5	341.0
9 K1	.04178075	6.654	1.427	172.4	309.9	137.5	122.3
10 J1	.04329290	1.431	-.004	91.0	202.3	111.3	293.2
11 OQ1	.04483084	.651	.071	104.7	52.1	247.4	216.7
12 UPS1	.04634299	.956	-.440	11.4	117.3	105.9	128.7
13 EPS2	.07617732	.290	-.227	109.5	260.3	150.8	9.7
14 MU2	.07768947	.413	-.201	146.1	138.6	352.5	284.6
15 NZ	.07899925	.660	.241	124.2	21.1	256.8	145.3
16 M2	.08051140	4.674	-.261	13.3	286.1	272.8	299.4
17 L2	.08202355	.382	-.191	15.2	42.9	27.7	58.1
18 S2	.08333333	2.039	-.045	176.6	148.5	331.9	325.1
19 E1A2	.08507364	.296	.046	102.7	59.0	256.3	221.7
20 M03	.11924206	.219	.071	12.7	246.8	234.1	259.5
21 M3	.12076710	.109	.008	49.1	327.5	278.4	16.6
22 MK3	.12229215	.210	-.061	168.7	192.4	23.7	1.0
23 SK3	.12511408	.109	-.015	169.4	236.7	67.3	46.1
24 MN4	.15951065	.159	.008	133.2	43.6	270.4	176.8
25 M4	.16102280	.122	.039	51.9	151.0	99.2	202.9
26 SN4	.16233258	.253	-.035	2.5	139.3	136.8	141.7
27 MS4	.16384473	.158	-.065	143.5	176.1	32.5	319.6
28 S4	.16666667	.154	-.030	96.6	357.9	261.3	94.5
29 2MK5	.20280355	.086	-.020	102.6	198.3	95.7	301.0
30 2SK5	.20844741	.134	-.066	147.8	281.2	133.4	69.1
31 2MNO	.24002205	.087	-.013	136.4	261.4	131.0	31.8
32 M6	.24153420	.087	-.051	149.9	275.9	126.0	65.8
33 2MS6	.24435613	.074	.035	87.2	318.1	230.9	45.2
34 2SM6	.24717807	.060	-.009	105.5	68.5	323.0	173.9
35 3MK7	.28331495	.087	-.057	140.3	311.1	164.8	97.5
36 M6	.32204560	.018	.017	59.5	335.2	275.7	34.6

Table 10

Harmonic analysis results for currents at station 4-549 m depth over the period 1500 July 29 to 0300 Sept, 29 GMT. The speed (frequency) of each constituent is given in cycles per hour while the lengths of the semi-major and semi-minor axes of the current ellipse are in cm/s.

NAME	SPEED	MAJOR	MINOR	INC	G	G+	G-
1 ZU	.00000000	2.519	.000	116.5	360.0	243.5	116.5
2 MM	.00151215	7.634	-.428	1.8	121.9	120.1	123.7
3 MSF	.00282193	5.515	-.548	7.8	130.1	122.3	137.8
4 ALP1	.03439657	.464	.098	168.7	214.3	45.6	23.0
5 2G1	.03570635	.347	-.242	125.6	266.1	140.5	31.6
6 G1	.03721850	.627	-.439	177.2	116.4	299.2	293.6
7 O1	.03873065	3.527	.566	179.9	250.4	70.5	70.3
8 NO1	.04026859	.416	.065	22.8	94.7	71.9	117.4
9 K1	.04178075	6.877	.340	178.9	331.0	152.1	149.9
10 J1	.04329290	.586	-.132	124.4	279.5	155.1	43.8
11 O01	.04483084	1.174	-.598	108.4	237.7	129.3	346.1
12 UPS1	.04634299	.426	.072	2.4	81.8	79.3	84.2
13 EPS2	.07617732	.252	-.015	114.5	143.5	29.0	258.0
14 MU2	.07768947	.434	-.216	154.3	174.8	20.0	329.6
15 N2	.07899925	.818	-.442	179.0	87.2	268.2	266.2
16 M2	.08051140	4.436	-.274	174.0	96.5	282.5	270.4
17 L2	.08202355	.415	-.073	156.1	210.9	54.8	7.0
18 S2	.08333333	2.879	-.106	179.4	156.6	337.1	336.0
19 ETA2	.08507364	.562	-.067	124.6	72.8	308.2	197.4
20 MU3	.11924206	.384	-.014	32.0	298.7	266.7	330.7
21 M3	.12076710	.316	.027	26.3	158.8	132.5	185.1
22 MK3	.12229215	.259	-.139	100.7	54.9	314.2	155.6
23 SK3	.12511408	.229	-.043	66.4	84.7	18.3	151.1
24 MN4	.15951065	.103	-.038	21.0	118.4	97.4	139.4
25 M4	.16102280	.163	.017	73.6	223.8	150.2	297.4
26 SN4	.16233258	.152	.015	167.8	281.9	114.1	89.7
27 MS4	.16384473	.070	-.011	64.7	262.2	197.5	326.9
28 S4	.16666667	.096	.026	6.1	30.4	24.4	36.5
29 2MK5	.20280355	.101	-.083	15.2	71.9	56.6	87.1
30 2SK5	.20844741	.118	-.053	60.4	52.0	351.6	112.4
31 2MNO	.24002205	.074	.026	33.3	40.4	7.1	73.7
32 M6	.24153426	.136	-.010	57.4	197.3	139.9	254.7
33 2MS6	.24435613	.035	-.003	172.5	314.7	142.1	127.2
34 2SM6	.24717807	.074	-.011	25.3	113.0	87.7	138.3
35 3MK7	.28331495	.119	-.009	177.0	201.1	24.1	18.0
36 M8	.32204560	.068	-.016	16.3	131.2	114.9	147.5

The low frequency spectral levels show a marked decrease with increasing depth. For the current components, the ratio of power spectral levels at 200m to those at 35m varies from 0.16 to 0.4 with similar reductions with depth found in the low frequency speed spectra. Thus, the low frequency variations which dominate the spectra of currents are baroclinic in nature. In contrast, the spectral levels of the east-west component at the diurnal and semi-diurnal frequency bands remain relatively constant (to within a factor of 2) with depth, indicating that these variations are largely due to barotropic tidal streams.

At stations 1 and 3, the low frequency variations of the east-west and north-south components differ significantly. While the largest spectral levels of both components almost always occur in the lowest frequency band, the spectrum of the north-south components falls off very rapidly with increasing frequency, approximately as f^{-2} , while the east-west spectrum shows a less precipitous decline, decreasing approximately as $f^{-0.6}$ at frequencies less than 0.3 day^{-1} . For the north-south component, the lowest frequency band, centred at 0.052 day^{-1} or a period of 19 days, accounts for well over half of the total variance ranging from 62% at station 1, 39m depth to 84% at station 3, depth 216 m. In contrast, the spectra of the east-west components shows larger contributions to the total variance from the second, third and fourth frequency bands (extending to frequencies of $0.3 \text{ cycles day}^{-1}$) in addition to the important contribution from the lowest frequency band. Thus, the low frequency variations in the north-south component are longer in period and more concentrated in frequency space than those of the east-west component at the two stations in the centre of the Sound. This difference in the low frequency characteristics of each current component may be related to a difference in the dynamical origin of each component. As noted previously, the anti-clockwise gyre extending into eastern Lancaster Sound from northwestern Baffin Bay will result in strong southerly flows at the centre of the sound, consistent with the observations of this study. On the other hand, this large scale gyre should have only a small direct contribution to the east-west component of the current at these locations. The results of the spectral analysis suggest, then, that a considerable portion of the long period activity of typically 20 days period, is associated with the intruding anti-clockwise gyre in eastern Lancaster Sound while the direct east-west motions in the centre of the Sound vary over somewhat shorter periods.

Given the large long period variations of the currents, it may be possible to anticipate the mean daily current over the next several days at one site on the basis of the present and previous measurements at the same site, particularly at the near surface levels of the upper current meters used in this study. At the surface, currents will be influenced more by direct forcing by the wind so that allowance for wind driven currents could be important.

The diurnal and semi-diurnal peaks are prominent in the spectra of east-west current components and much less evident in the spectra of north-south current components. This result is consistent with the notion of tidal currents flowing in alignment with the east-west orientation of the Sound. Diurnal and semi-diurnal peaks are found

in the spectra of the speed, but these peaks are not statistically significant in the records from the upper current meters, presumably because of the higher background levels of the spectral density estimates through these frequency bands. The speed spectra from the middle and deep current meters have more prominent tidal peaks, with the spectral levels for the deepest meter (549m) at station 4, being significantly larger (by a factor of 6 to 11) than the equivalent spectral peaks for the mid channel currents at similar depths.

The results of a harmonic analysis of the vector current time series (see Tables 6 - 10) provides more detailed information on the diurnal and semi-diurnal variations of the currents. Variation at these frequencies may be due to phenomena of other than tidal origin. The inertial frequency at the latitudes of the study area is 1.927 cycles per day or 0.0803 cycles per hour which is very close to the frequency of the M_2 tidal constituent of 0.0805 cycles per hour. Thus oceanic responses at the inertial frequency would be expected to increase the size of the M_2 constituent. However this effect would diminish with the length of the record analysed since inertial responses to individual events, such as strong winds, are expected to be approximately random in phase and therefore more likely to cancel one another with longer records. A possible source of variation at diurnal frequencies is the observed daily fluctuation of the geomagnetic field direction as discussed in section 3. A rough estimate of the average expected direction error due to geomagnetic variations is ± 3 degrees in the current directions; this amounts to a daily amplitude variation of 1.9 cm/s for the mean speed at the 51 m depth level of station 3, with the variation directed perpendicular to the geomagnetic field direction (i.e. orientated about 15 degrees clockwise to true north). As the nearest resolvable diurnal constituent to the daily frequency is the K_1 constituent with a frequency of 0.0418 cycles per hour, the effect of diurnal geomagnetic variations would be to increase the size of the K_1 constituent. Because this geomagnetic variation of the apparent current is directed almost north-south and the major axis of the tidal ellipses are directed east-west, the effect will be to increase the size of the minor axis of the ellipse. From the harmonic analysis results, there is no evidence for excessively large minor axes of the K_1 tidal ellipses; therefore, the effect of the geomagnetic direction variations appears to be unimportant.

The large amplitudes of the monthly (MM) and the fortnightly (MSF) constituents are fictitious. The variations found at these constituents are due to the non-tidal low frequency variations discussed above in the spectral analysis results rather than being of tidal origin, which accounts for the large differences in the amplitude and phase of these constituents among the different records analysed.

Of the diurnal constituents, the K_1 and O_1 are consistently the largest in amplitude while the largest semi-diurnal constituents are the M_2 and S_2 . Each of these constituents has the major axis of the tidal ellipses aligned within 35 degrees of the east-west orientation, parallel to the bathymetry of Lancaster Sound. The tidal ellipses of the major constituents are generally narrow, with the cross-channel

amplitude always less than one-fifth of the along-channel amplitude. The along-channel root-mean-square current amplitude computed from the K_1 , O_1 , M_2 , and S_2 constituents ranges from 7.3 to 9.4 cm/s depending on location and depth.

For the currents, the sum of the two diurnal constituents (K_1 and O_1) are consistently larger than the sum of the two major semi-diurnal constituents by a factor ranging from 1.17 to 1.57. In contrast, a harmonic analysis of 29 day water level records at Dundas Harbour and other nearby locations, show that the semi-diurnal water level variations are larger than those of the diurnal variations in this region (unpublished data of the Marine Environmental Data Service, Dept. of Fisheries and the Environment). Similar differences in the diurnal to semi-diurnal ratios for currents and water levels have been found in Crozier Strait and Byam and Austin Channels within the Canadian Arctic Islands (P. Greisman, personal communication) so this difference may reflect a large scale feature of tidal currents in this region.

4.2.3 Correlation and Cross-Spectral Analysis of Currents

To examine spatial variations, both in the horizontal and the vertical, the current measurements were subjected to a linear regression and cross-spectral analysis. Significant correlations at the 95% level are found between the upper and 200 m level currents at both stations 1 and 3 for the easterly and northerly current components. The correlation coefficients, given in Table 11, range from 0.59 to 0.79 while the cross-spectral analysis results indicate that significant coherence levels at the lowest frequencies are present for both components. Not surprisingly, the easterly component shows high levels (0.90 to 0.98) of coherence at the diurnal and semi-diurnal frequencies. The speeds appear to have less correlation than the components; at station 1, the correlation coefficients are 0.63 and 0.62 for upper-middle and middle-lower meter combinations while at station 3 the correlation coefficients are only 0.37 and 0.21, respectively. Given the larger correlation among current components, this finding reflects the well correlated current directions with depth, remarked upon previously.

In the horizontal, the north-south components are significantly correlated but out of phase; the correlation coefficient between the northerly currents at stations 1 and 3 is -0.67 at the level of the upper current meters decreasing to -0.40 at the 200 m level. The cross-spectra between the north-south components shows a coherence of 0.88 in the lowest frequency band with a phase of 172 degrees for the near surface currents. For the east-west component, the correlation coefficient is only 0.18 at the level of the upper current meters but has a statistically significant value of 0.59 at the 200 m level. Low correlation coefficients are noted for the components measured at 550 m and both near surface and 200 m currents at station 3.

The opposite phase determined between the near surface north-south current component at stations 1 and 3 suggests that the southerly current which dominates the flow at stations 1 and 3 has the same origin; both may be due to the southerly current which shifts

Table 11

Results of the linear regression analysis between time series of currents of the form: $x_1 = a + b \cdot x_2$ with correlation coefficient r

where x_1 is the predictand time series of N hourly points

where x_2 is the predictor time series of N hourly points

Both time series begin at 0300 July 29 GMT.

Easterly Component

x_1 Stn. Depth (m)	x_2 Stn. Depth (m)	a (cm/s)	b	r	N
1- 39	1-203	-23.7	2.31	0.62	1423
3- 51	3-216	- 2.5	2.36	0.68	1500
1- 39	3- 51	12.6	0.71	0.18	1423
1-203	3-216	5.8	0.73	0.59	1500
3- 51	4-549	-12.4	2.41	0.14	1500
3-216	4-549	- 4.2	1.02	0.21	1500

Northerly Component

1- 39	1-203	2.3	2.57	0.57	1423
3- 51	3-216	1.1	1.54	0.79	1500
1- 39	3- 51	- 6.7	0.73	-0.67	1423
1-203	3-216	- 3.0	0.46	-0.40	1500
3- 51	4-549	-31.5	8.20	0.37	1500
3-216	4-549	-21.2	5.32	0.21	1500

Speed

1- 39	1-203	-8.7	2.93	0.63	1423
1- 39	1-554	-8.1	4.57	0.21	1423
1-203	1-554	-0.1	1.66	0.61	1549
3- 51	3-216	-2.9	2.00	0.34	1500
3- 51	3-550	-8.6	6.19	0.18	1500
3-216	3-550	-2.9	3.09	0.21	1500
1- 39	3-651	-10.7	0.95	-0.46	1423
1-203	3-216	-2.0	0.69	-0.08	1500
1-554	3-550	-2.4	1.30	0.16	1500
1-554	4-549	1.0	0.59	-0.29	1500
3-550	4-549	2.6	0.46	-0.13	1500

in its position within the Sound, resulting in the opposite phase of the north-south current components. While this hypothesis is no doubt over simplified, (for example, a strong southerly flow from August 18 to September 2 at station 1 is accompanied by a northerly flow at station 3 over the same period), it does present some interesting possibilities. The southerly current, which presumably extends into Lancaster Sound from Baffin Bay, may be steady in time over periods that are longer than the low frequency temporal variations observed at stations 1 and 3. The observed temporal variations could be due to a change in the extent of the current's intrusion into Lancaster Sound rather than a change in the magnitude of the current.

4.3 Temperatures and Salinities

The time series of temperature and salinity, plotted in Figures 18 and 19, represents the longest such record made in eastern Parry Channel to this time. A comparison between the mean temperature and salinity values (Tables 5a - 5c) of this study and previous temperature and salinity profiles in the same general area, using Marine Environmental Data Services records, is shown in Figure 20; the comparison indicates good overall agreement between the present and earlier data sets.

From histograms of temperature and salinity (Figure 21), it is noted that lower temperatures at the level of the uppermost current meter occur more frequently at station 4 on the southern side of the Sound than at stations 1 and 3 located at the centre of the Sound. This difference, which is also reflected in the lower average temperature of 0.65°C at station 4 in comparison to 1.59°C at station 3 and 1.90°C at station 1, is consistent with the north-south temperature gradient at 20 m depth described by Collin (1962) to extend over the length of Lancaster Sound and Barrow Strait in September, 1957. The lower temperatures observed on the southern side of Lancaster Sound likely result from the anti-clockwise circulation within eastern Lancaster Sound, described previously, which carries the warmer upper layer water of Baffin Bay into the northern side of Lancaster Sound and confines the eastward flowing colder water of Parry Channel to the southern side of the Sound.

At the 200 m level, no difference in average temperatures was observed across the strait, but a significantly larger standard deviation was found at station 1 than at the other two stations. This difference is largely due to an intrusion of warm water of up to 0°C between August 6-12 at station 1 which did not occur at the other locations. At this level, significantly larger salinities were measured at station 4 (mean value \pm standard deviation of $33.88 \pm .14^{\circ}/\text{oo}$) than at station 3 (mean value \pm standard deviation of $33.56 \pm .21^{\circ}/\text{oo}$).

At the 550 m level, the average values of both salinity and temperature differ little with location. However, large instantaneous differences do occur, particularly in the temperature. Temperature differences of 0.5°C at different locations are common with temperature differences as large as 1.0°C being observed (Figure 18c).

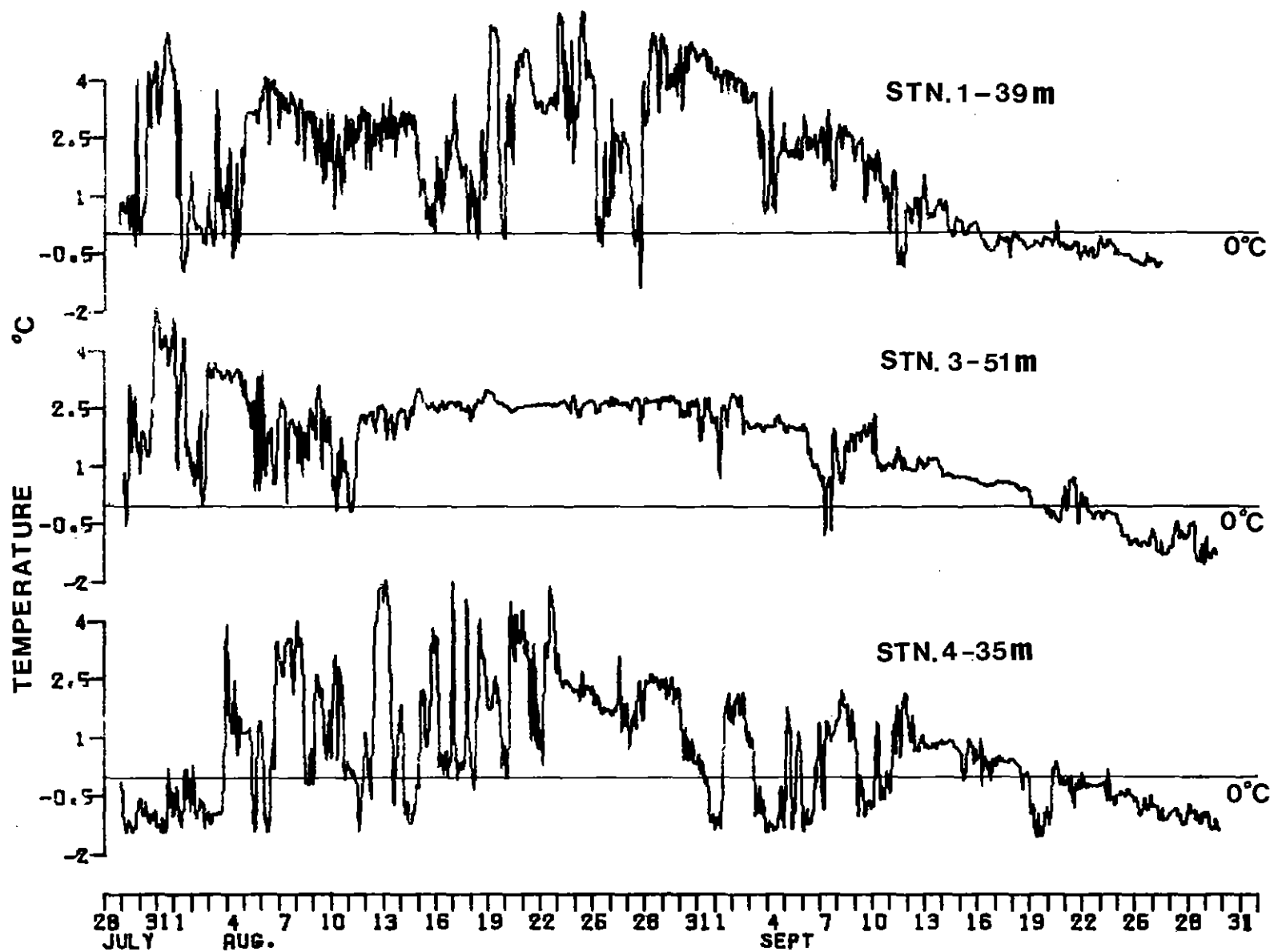


Figure 18a: Time series plots of temperature recorded at the upper current meter level on each mooring.

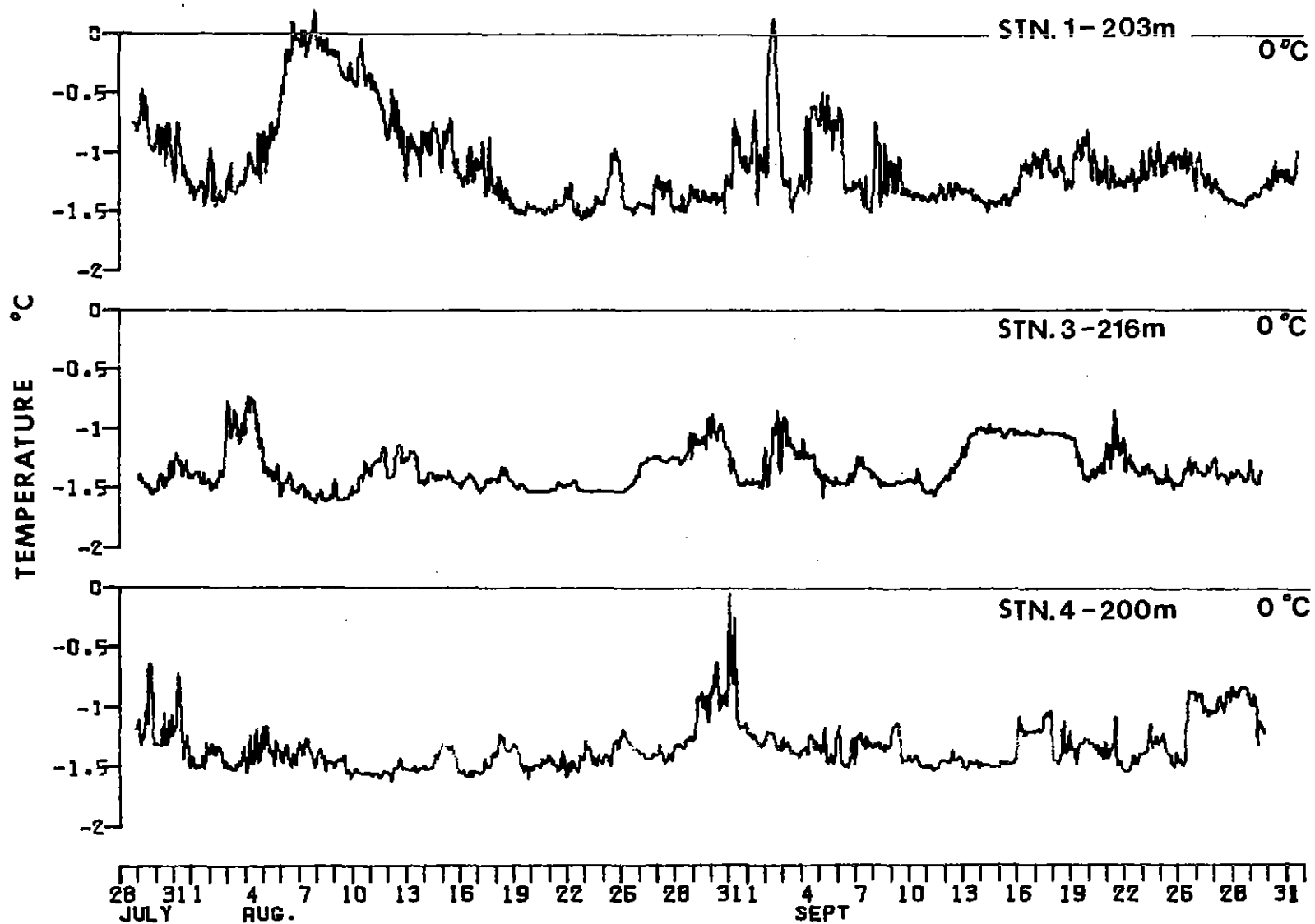


Figure 18b: Time series plots of temperature recorded at the 200m level on each mooring.

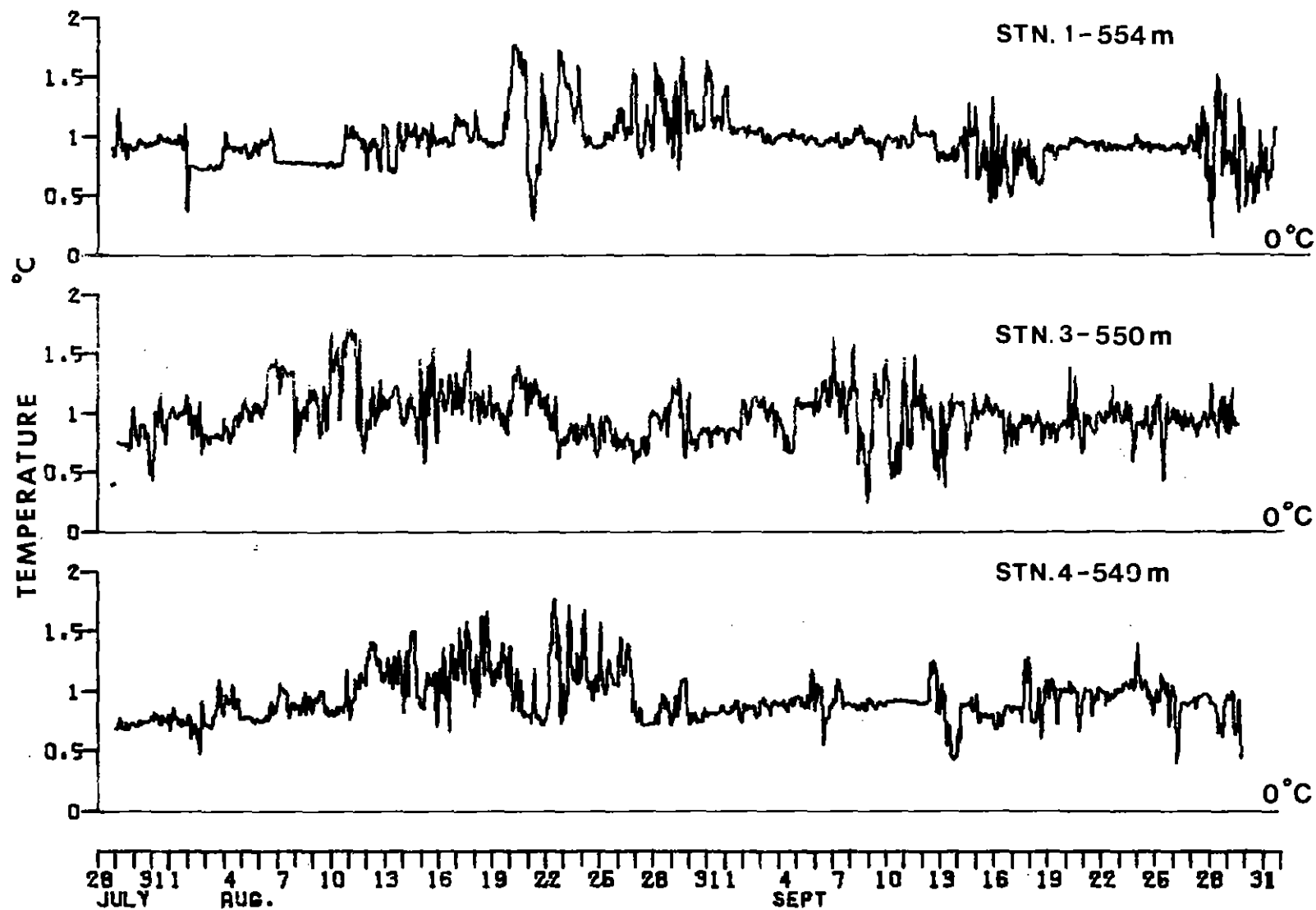


Figure 18c: Time series plots of temperature recorded at the 550m level on each mooring.

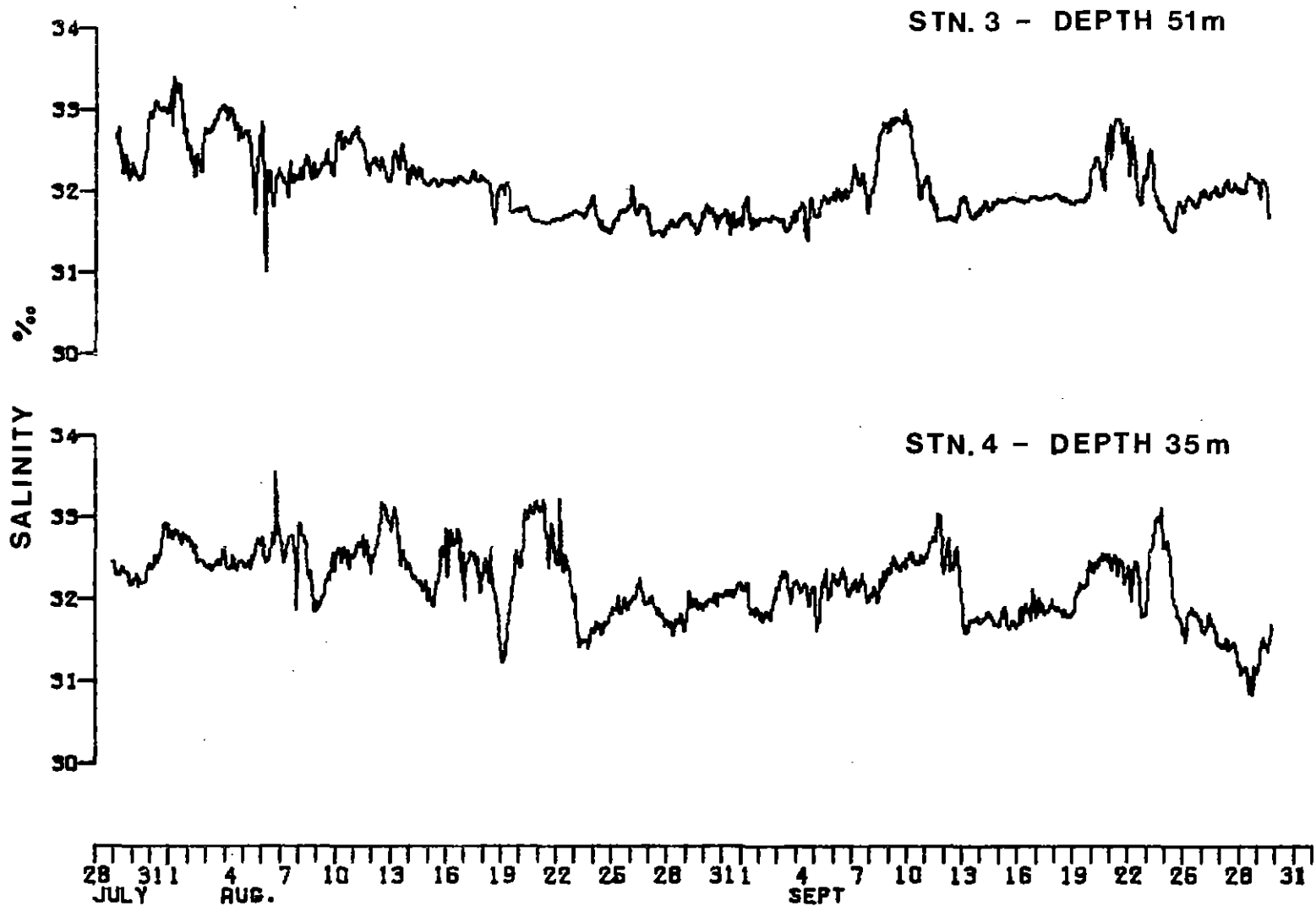


Figure 19a: Time series plots of salinity recorded at the upper current meter level on each mooring.

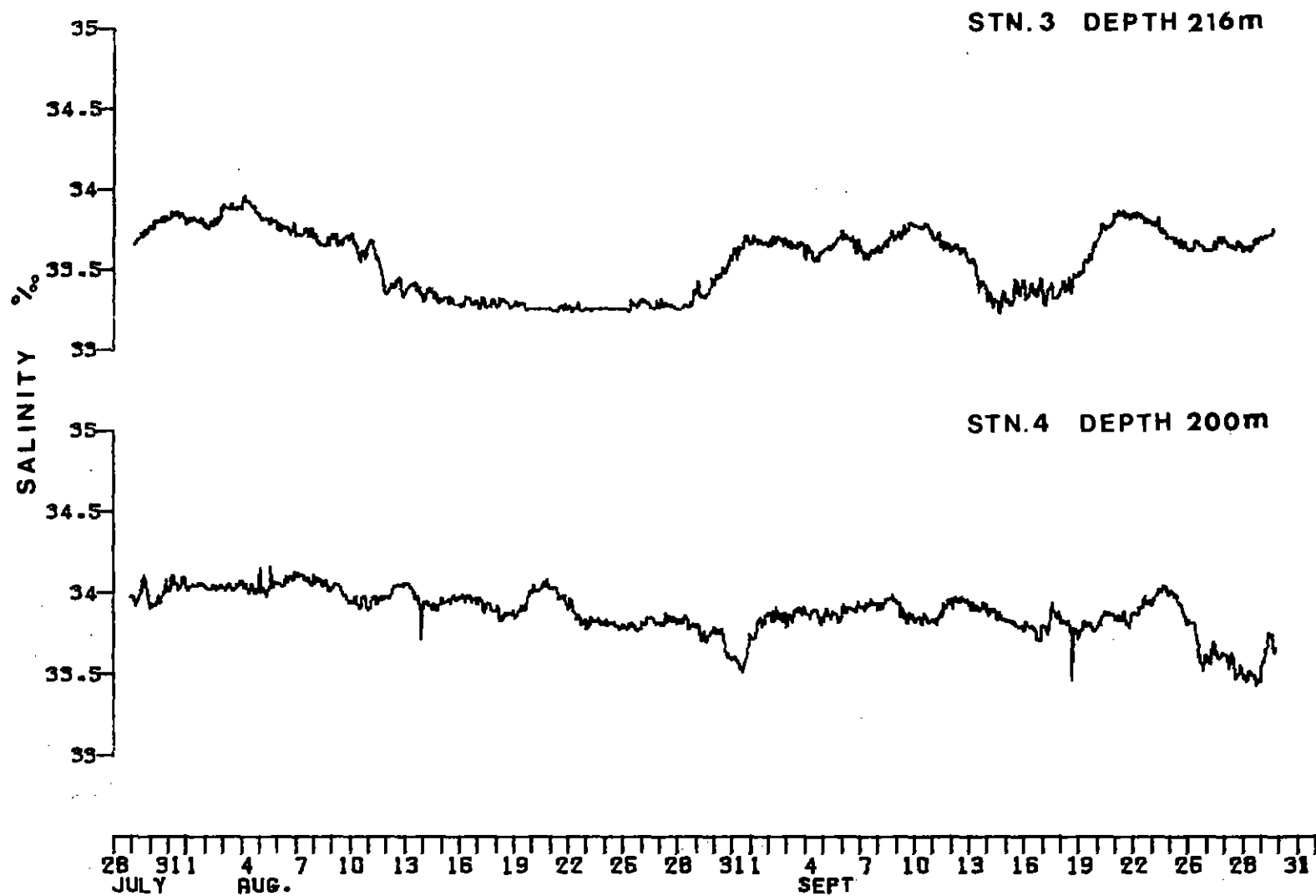


Figure 19b: Time series plots of salinity recorded at the 200m level on each mooring.

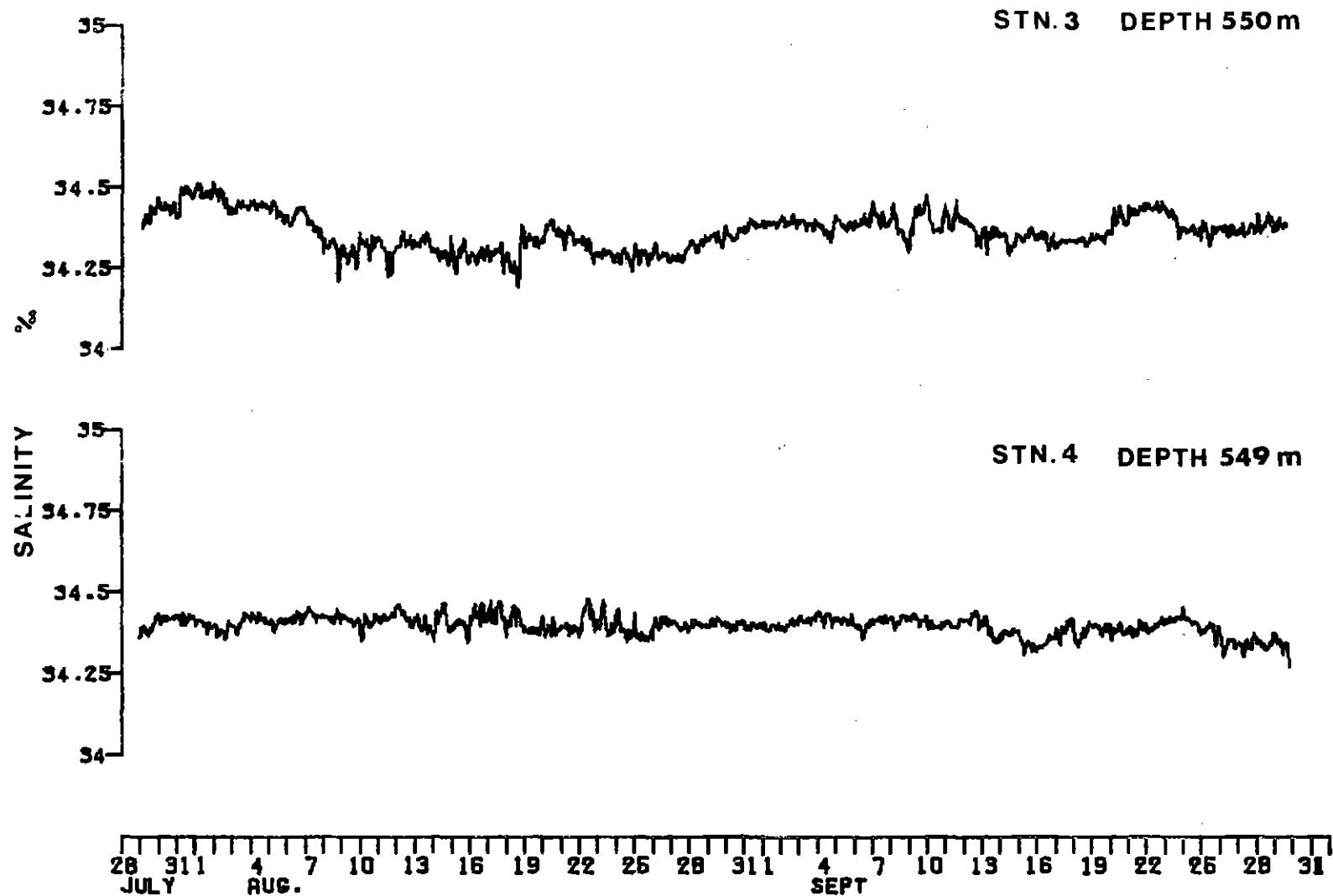


Figure 19c: Time series plots of salinity recorded at the 550m level on each mooring.

Figure 20: Temperature and salinity profiles taken from the files of the Marine Environmental Data Service, Ottawa together with the average and range of temperatures and salinities observed at stations 1,3 and 4.

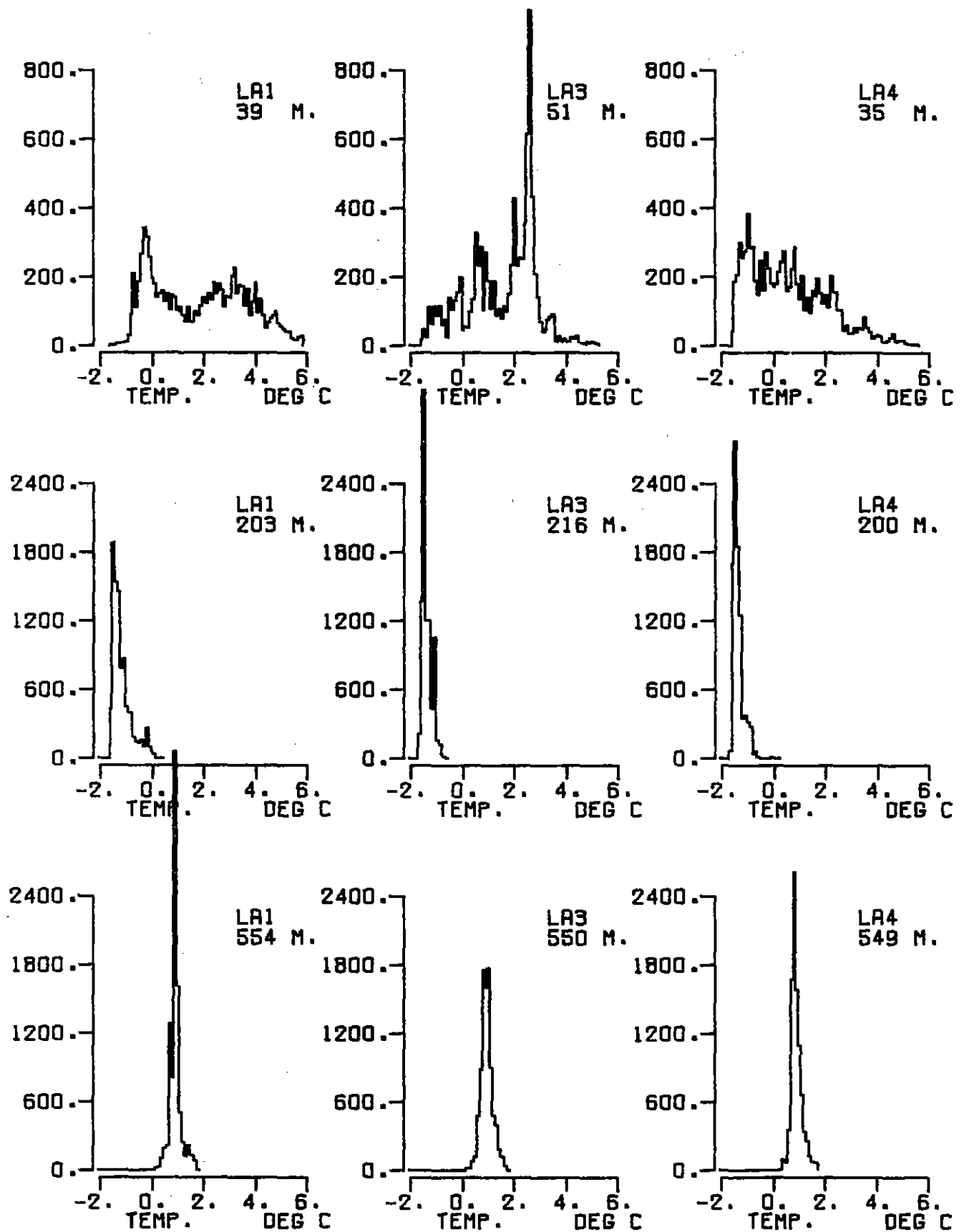


Figure 21a: Histograms of the temperatures.

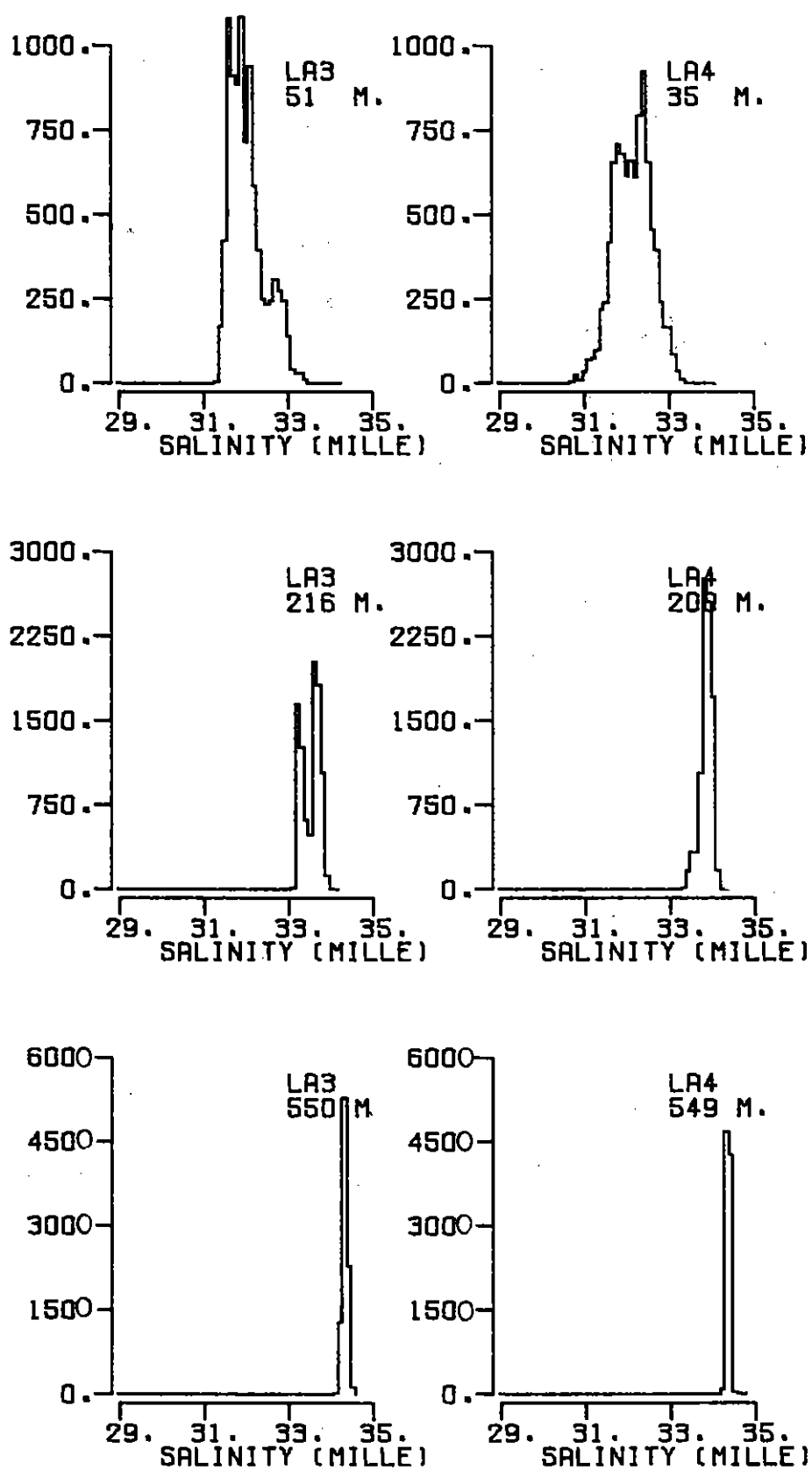


Figure 21b: Histograms of the salinities.

The largest temporal variations are found, not surprisingly, in the temperature and salinity records of the uppermost current meter where the effects of surface heat and mass exchanges are important. A distinct seasonal cycle is evident in the near surface temperature records amid higher frequency variations; the warmest temperatures occur in mid-August with the onset of rapid cooling beginning in early September. As the water cools, the variability of the temperatures decrease markedly as well, suggesting that the large vertical temperature gradients of the upper layer are being eroded through surface heat losses with the result that internal wave disturbances and vertical mixing processes result in smaller temperature changes. The upper layer salinities show a gradual decline of approximately $0.5^{\circ}/\text{oo}$ over the sixty days of observations. This decline may reflect the cumulative ice melt and river runoff sources of freshwater which are mixed within the upper layer through wind action.

Some of the temperature and salinity variations are undoubtedly fictitious; due to the vertical excursions of the current meter moorings discussed in section 4.1. For example the increases in salinity of $1^{\circ}/\text{oo}$ on September 10 and September 21 are likely related to the strong currents recorded on those days. For the temperature and salinity measurements at 200 and 550 m, this effect will be much smaller because the vertical excursions are smaller and the vertical gradients are weaker.

The observed salinity variations decrease significantly as a function of depth; the standard deviation of salinity at station 3 drops from $0.42^{\circ}/\text{oo}$ at 51 m to $0.21^{\circ}/\text{oo}$ at 216 m to $0.06^{\circ}/\text{oo}$ at 550 m. The temperature variations, though much reduced at 200 m depth in comparison with those of the upper layer, are found to increase with depth being larger at 550 m than at 200 m for two of the three stations.

One curious feature of the temperatures observed at 550 m depth is the burst of high frequency variations which last several days and then diminish. These variations with amplitudes of approximately 0.3°C and periods of less than one day, are apparent at station 1 and to a lesser extent at station 4 (see Figure 18c). From examination of the speed and direction measurements, there are no simultaneous occurrences of unusual activity in the velocity field.

The power spectra of the temperature (Figure 22) and salinity (Figure 23) all show the same general features: the largest spectral levels occur at the lowest frequencies with a general decrease but no statistically significant peaks being found with increasing frequency. From the spectra of salinity, the low frequency variations account for a very large proportion of the total variance. The temperature spectra are dominated less by low frequency variations, particularly at 550 m depth.

The results of a cross-spectral analysis between pairs of temperatures or salinities measured at the same level but different

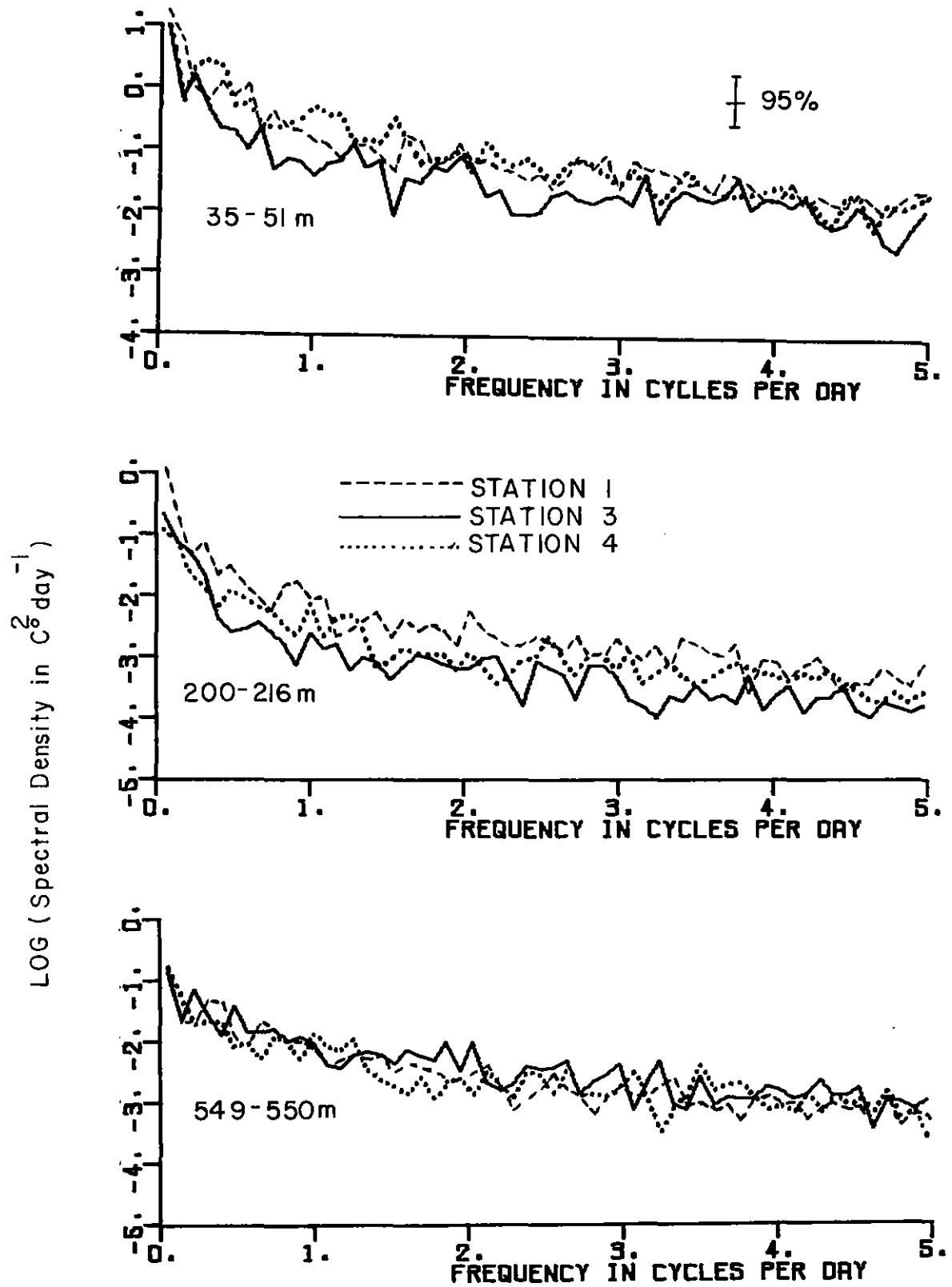


Figure 22: Power spectral densities of the temperature data.

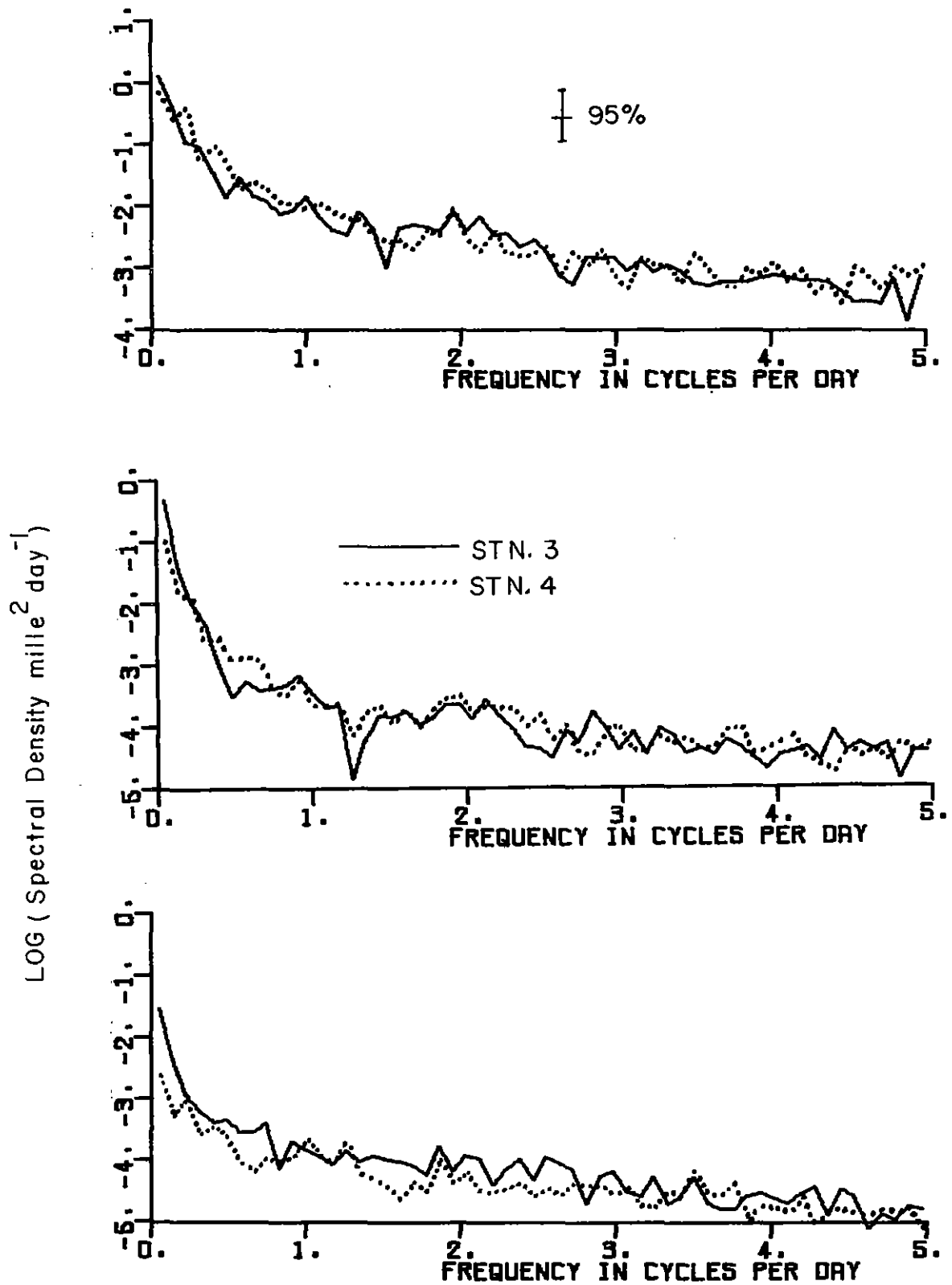


Figure 23: Power spectral densities of the salinity data.

stations shows generally low coherence levels below the 95% significance levels. The only statistically significant coherences are found in the lowest frequency band for some cross-spectra, reflecting the similarity due to seasonal cooling and freshening of the near surface water. The general lack of coherence of temperature (and salinity) at different locations can be attributed to the spatial variations in the flow field, discussed in section 4.2, as well as the importance of local processes.

4.4 The Local Wind and Near Surface Currents

The local wind was measured from a shore Station located at Cape Charles Yorke on Baffin Island, immediately to the south of the current meter stations. From the time series plots of the weather data shown in Figure 24, the wind is characterised by large easterly and westerly components, indicating that the wind is aligned with Lancaster Sound; this feature of the wind field may be somewhat enhanced by the topographic effect of the Baffin Island mountains. A definite change in the wind regime occurred in late August, when the predominant direction reversed from easterly winds to westerly winds.

The results of the linear regression analysis indicate low correlation between the wind components and the upper level current components at both stations 1 and 3. For all pairs of wind and current components, the regression correlation coefficient was not statistically significant. These results suggest that the local wind has little influence in directly generating currents at the depths of the upper current meters (39 m and 51 m for stations 1 and 3, respectively). This lack of correlation is not unexpected in view of the density stratification of the near surface layer above the level of the upper current meters.

Nearer the surface, the wind generated currents will increase. Using the usual rule of thumb that the directly wind driven surface currents amount to 3 % of the wind speed, the surface currents due to the local wind were 15 cm/s on average with a maximum value of 36 cm/s based on the Cape Charles Yorke wind data. In comparison, the current speeds measured at the upper level current meters at stations 1 (and 3) were 24 cm/s (37cm/s) on average, with maximum currents of 95 cm/s (112 cm/s). As discussed previously these currents appear to be related to the large scale circulation of Lancaster Sound and Baffin Bay and are expected to extend upward to the surface.

Based on the relative magnitudes at the surface, the effect of the wind driven currents on surface movements will be less than the effect of the large scale current patterns but still significant, particularly when the large scale currents wane.

An occurrence of surface currents flowing against the wind was observed aboard the ship on the night of Sept. 29-30 while drifting near station 3. In easterly winds of 5 to 7 m/sec, the ship was drifting eastward at an average rate of 50 cm/s. For this time period, easterly currents of 70 cm/s were recorded at 51m depth at station 3.

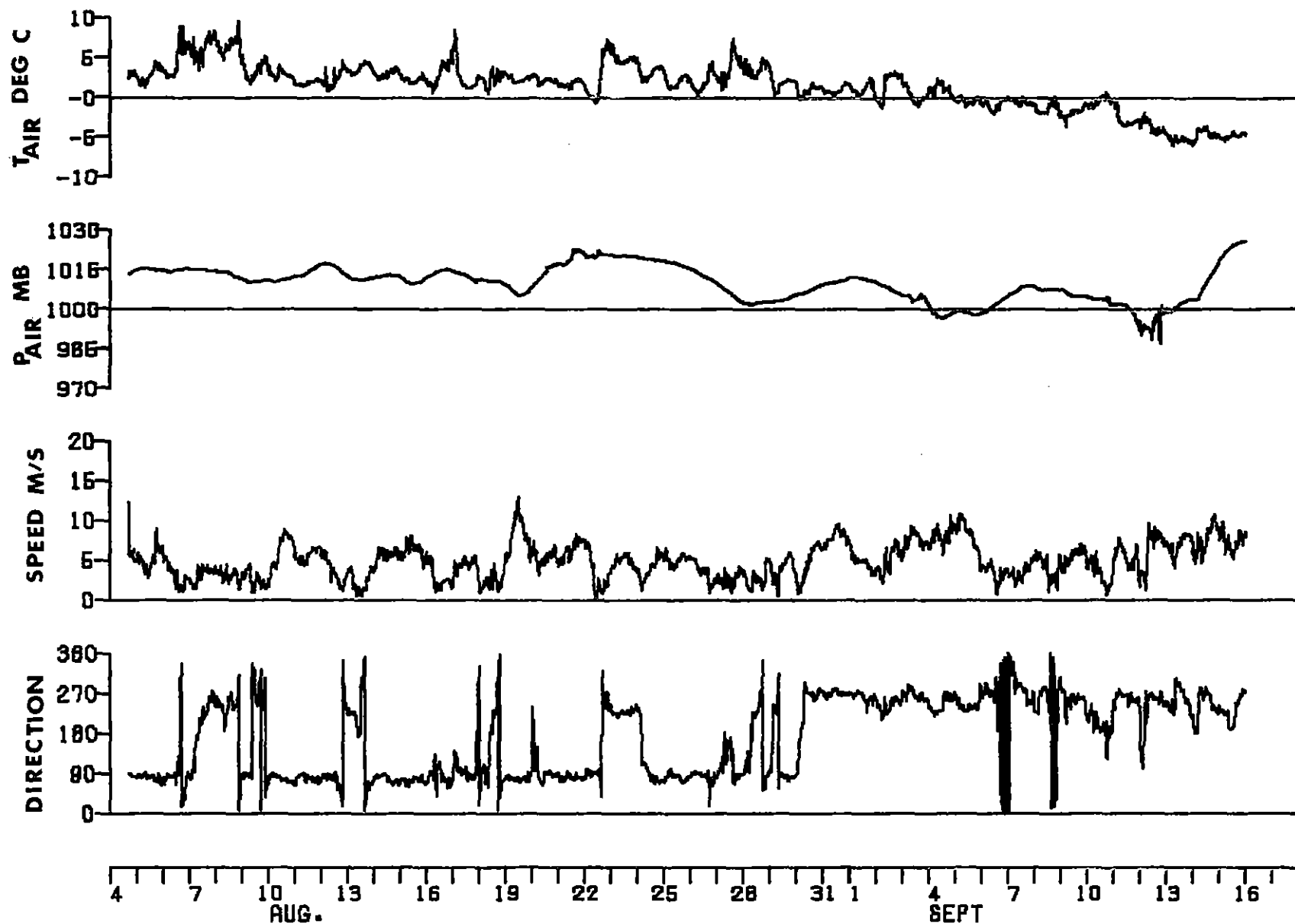


Figure 24a: The air pressure, air temperature, wind speed and direction measured at Cape Charles Yorke. The wind direction gives the direction that the wind blows from.

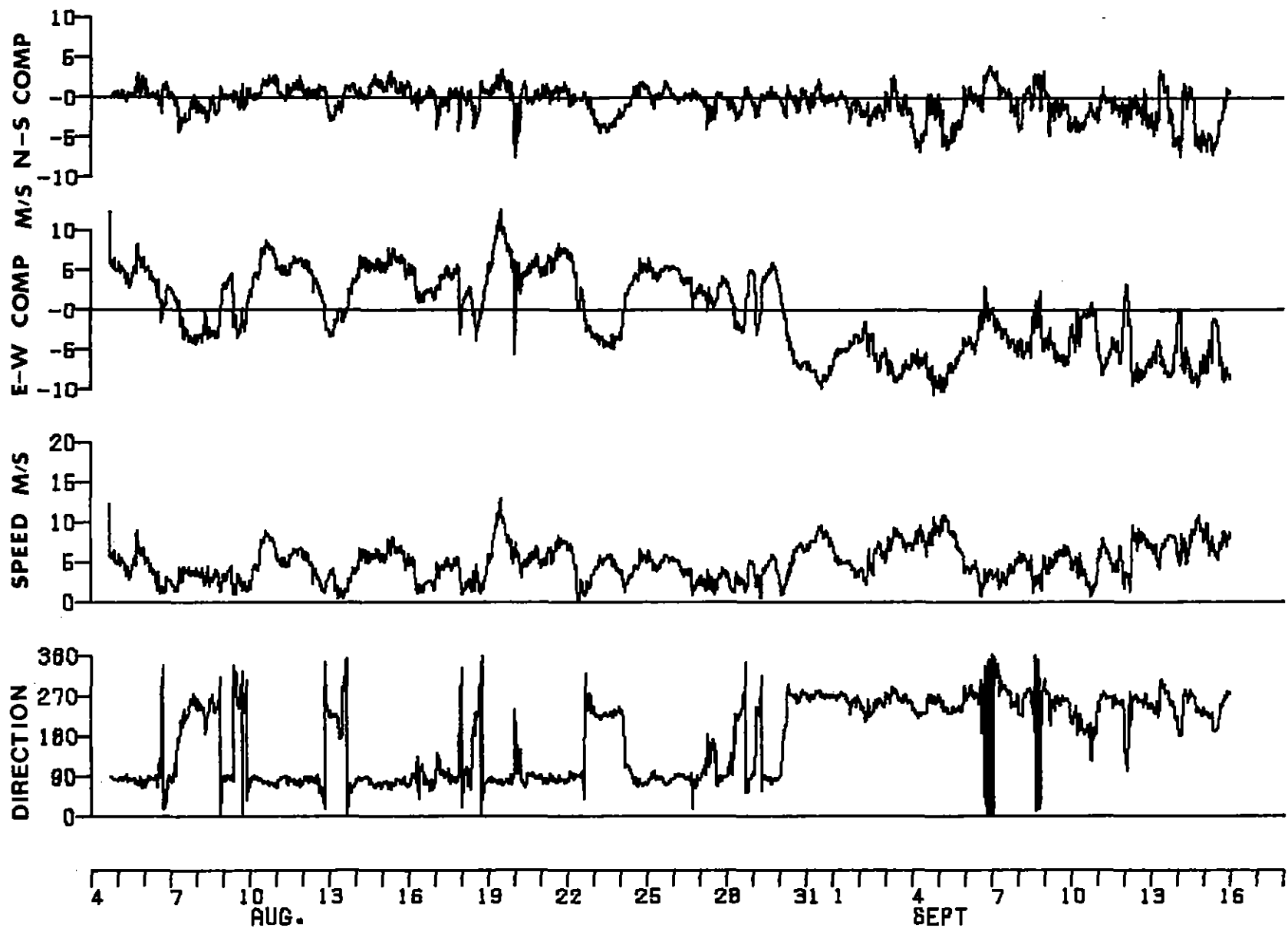


Figure 24b: The wind components, speed and direction. The wind direction indicates the direction from which the wind blows.

5. Summary and Conclusions

From three current moorings located in eastern Lancaster Sound in August and September 1977, time series measurements of current speed and direction, temperature and conductivity were obtained at three levels at each site: near surface (35 to 51 m depth), approximately 200 m and approximately 550 m depth. In this report, we present a description and preliminary analysis of the data.

The mean circulation is characterised by strong southerly flows in the centre of the Sound and easterly flows along the southern side at the near surface and 200 m levels; this circulation pattern is consistent with the existence of an anti-clockwise gyre extending into eastern Lancaster Sound from northwestern Baffin Bay as described by Muench (1971) and others. In the centre of the Sound, the near-surface currents can reach speeds of up to 112 cm/s with an average magnitude of 30 cm/s. Based on wind measurements taken at a shore station on the south coast, surface movements expected from the large scale circulation pattern were generally larger than those movements expected from directly generated wind driven currents.

The temporal variations of the currents at all depths vary over relatively long periods; the power spectra of the currents showed that the largest spectral levels occurred in the lowest frequency band centred on a frequency of 0.052 cycles per day or a period of 19 days. For the north-south component of the current at the near surface and 200 m levels of the two stations located in the centre of the Sound, the low frequency variations were particularly important with the lowest frequency spectral band accounting for 62 to 84 % of the total variance.

The southerly current measured in the centre of the Sound is baroclinic in nature; the low frequency variations, though significantly correlated, are reduced in amplitude by a factor of about 2 at the 200 m level in comparison with the near surface variations.

The near surface north-south component variations at the two centre stations, separated by 30 km, are essentially opposite in phase. This is interpreted as evidence of a shift in the extent of the intrusion of the anti-clockwise gyre within eastern Lancaster Sound.

Tidal currents are generally small in comparison with the low frequency currents at the near surface and 200 m levels. From a harmonic analysis of the current data, the diurnal and semi-diurnal tidal ellipses are found to be oriented along the east-west axis of the sound with typical amplitudes of 7 to 10 cm/s. At the 550 m level, the tidal currents are relatively more important, accounting for roughly one-half of the total variance, largely because the lower frequency

variations are significantly reduced in amplitude at this depth.

In comparison with previous measurements in eastern Lancaster Sound, the mean temperature and salinity values are in good agreement. Variations of both the temperature and salinity decrease markedly from the near surface level to 200 m depth. The variations of salinity are further reduced at 550 m but the temperature variations at 200 m and 550 m are comparable in magnitude. The correlation among both the temperature and salinity variations at the same level but at different locations is poor, apparently due to variability in the currents as well as to the effect of local processes at each location.

6. References

- Bailey, W.B. (1957). Oceanographic features of the Canadian Archipelago
J. Fish. Res. Bd. Canada, 14 (5): 731-769
- Barber, F.G. (1977). Lancaster Sound some 1960 data. Unpublished
manuscript, Marine Sciences Directorate, Ottawa: 177p.
- Barfoot, B.L. (1972). Current meter direction detection as a function
of magnetic field intensity. Canada Centre for Inland Waters,
Environment Canada, Burlington, Ontario. 34p.
- Bell, W.H. (1977). Static analysis of single-point moorings.
Pacific Marine Science Report 77-12, Institute of Ocean
Sciences, Patricia Bay. (Unpublished manuscript). 61 p.
- Bennett, A.S. (1976). Conversion of in situ measurements of conductivity
to salinity. Deep-Sea Research, 23: 157-165.
- Collin, A.S. (1958). An oceanographic study of Prince Regent Inlet,
the Gulf of Botha and adjacent waters. Fisheries Research
Board of Canada, Oceanographic and Limnological Manuscript
Report Series No. 13.
- Collin, A.E. (1962). On the oceanography of Lancaster Sound.
Ph.D. Thesis, McGill University, Montreal. 204 p.
- Collin, A.E. (1963). The waters of the Canadian Arctic Archipelago.
Proc. Arctic Basin Symp., Arctic Institute of North America,
Washington: 128-136.
- Fenco. (1974). An environmental study related to offshore operations
with emphasis in Lancaster Sound. Foundation of Canada
Engineering Corporation Ltd., Calgary.
- Fissel, D.B. (1976). Pressure differences as a measure of currents
in Juan de Fuca Strait. Pacific Marine Science Report 76-17,
Institute of Ocean Sciences, Patricia Bay. (Unpublished
Manuscript). 63 p.
- Fissel, D.B. (1978). Measurements of the direction sensitivity of
three current meters a function of magnetic field intensity.
Contractor Report Series, 78-1, Institute of Ocean Sciences,
Patricia Bay. (Unpublished Manuscript).
- Fissel, D.B. and J.R. Marko (1978). A surface current study of eastern
Parry Channel, N.W.T. - Summer, 1977. Contractor Report
Series, Institute of Ocean Sciences, Patricia Bay. (in preparation)
- Fofonoff, N.P. (1962). Physical properties of sea water. The Sea,
Vol. 1. ed. M.N. Hill, Interscience Publishers, New York: 3-28.

- Foreman, M.G.G. (1978). Manual for tidal currents analysis and prediction. Pacific Marine Science Report 78-6, Institute of Ocean Sciences, Patricia Bay. (Unpublished manuscript). 70 p.
- Godin, G.G. (1972). The analysis of tides. University of Toronto Press. 264 p.
- Hill, S.H., D.B. Fissel and H.V. Serson. (1978). Wind and air pressure measurements in eastern Parry Channel - Summer, 1977. Pacific Marine Science Report, Institute of Ocean Sciences, Patricia Bay. (in preparation).
- Keenan, P.V. (1976). Sources of compass error with the Aanderaa recording current meter. Bedford Institute of Oceanography Report Series BI-R-76-2. Dartmouth, N.S. 30 p.
- Killerich, A. (1939). The "Godthaab" expedition, 1928. A theoretical treatment of the hydrographical observation material. Medd. am Grohl. 78(5):1-49.
- Lea, B.N. (1977). Calibration, testing and installation of a recording meteorological station at Cape Charles Yorke, Baffin Island, N.W.T. Dobrochy Seatech, Ltd., Victoria. 15 p. (Unpublished manuscript).
- Marko, J.R. (1977). A satellite-based study of sea ice dynamics in the central Canadian Arctic archipelago. Contractor Report Series 77-4, Institute of Ocean Sciences, Patricia Bay: 106 p.
- Muench, R.D. (1971). The physical oceanography of the northern Baffin Bay region. Baffin Bay-Northwater Project Scientific Report No. 1. The Arctic Institute of North America, Washington. 150 p.
- Milne, A.R. and B.D. Smiley (1978). Offshore drilling in Lancaster Sound. Institute of Ocean Sciences, Patricia Bay. 95 p.
- Panofsky, H.A. and G.W. Brier (1958). Some applications of statistics to meteorology. Pennsylvania State University, College of Mineral Industries, University Park, Pa. 224 p.
- Singleton, R.C. (1969). An algorithm for computing the mixed radix fast Fouries transforms. IEEE Transactions on Audio and Electroacoustics, 17(2): 93103.
- Witham, K. and F. Anderson (1962). The anomaly in geomagnetic variations at Alert in the Arctic archipelago of Canada. Quaterly J. Roy. Astr. Soc. 7:220-243.

